



Validating age-determination of anglerfish and hake

FINAL REPORT

October 2019

EUROPEAN COMMISSION

Executive Agency for Small and Medium-sized Enterprises (EASME)
Unit A.3 — European Maritime and Fisheries Fund (EMFF)

E-mail: EASME-EMFF@ec.europa.eu

*European Commission
B-1049 Brussels*



Validating age-determination of anglerfish and hake

EASME/EMFF/2016/1.3.2.7/SI2.762036

Final Report

Europe Direct is a service to help you find answers to your questions about the European Union.

Freephone number (*):

00 800 6 7 8 9 10 11

(*) The information given is free, as are most calls (though some operators, phone boxes or hotels may charge you).

LEGAL NOTICE

This document has been prepared for the European Commission however it reflects the views only of the authors, and the Commission cannot be held responsible for any use which may be made of the information contained therein.

More information on the European Union is available on the Internet (<http://www.europa.eu>).

Luxembourg: Publications Office of the European Union, 2020

ISBN 978-92-9460-203-9

doi: 10.2826/748632

© **EUROPEAN UNION, 2020**

Table of Contents

1	EXECUTIVE SUMMARY	12
2	OVERVIEW	13
	Background	13
	2.1.1 Age information in stock assessment	13
	2.1.2 Hake age determination	14
	2.1.3 Hake stock assessment	14
	2.1.4 Anglerfish age determination	14
	2.1.5 Anglerfish stock assessment	15
	2.1.6 Microchemistry in age determination.....	15
	Objectives	16
	Consortium.....	16
3	METHODOLOGY	16
	Approach to sampling design and analyses	16
	TASK 1 SAMPLE AND DATA GATHERING	17
	3.1.1 Hake: Collation of data for reanalysis.....	17
	3.1.2 Hake: Sourcing of chemically tagged hake otoliths	17
	3.1.3 Anglerfish (L. piscatorius): sampling	18
	TASK 2 SAMPLE PROCESSING.....	18
	3.1.4 Sample preparation – Hake otoliths	18
	3.1.5 Sample preparation – Anglerfish otoliths and illicia	18
	3.1.6 Imaging and measurement of anglerfish ageing structures	19
	3.1.7 Analysis of tagged hake otoliths using Laser ICPMS	19
	3.1.8 Analysis of anglerfish otoliths and illicia using Laser ICPMS.....	20
	3.1.9 Stable isotope analysis.....	20
	TASK 3 DEVELOPMENT OF AN OBJECTIVE METHOD TO INTERPRET THE OBSERVED PATTERNS	21
	3.1.10 Underlying assumptions	21
	3.1.11 Reanalysis of hake data	21
	3.1.12 Seasonal microchemistry patterns in tagged hake otoliths	22
	3.1.13 Seasonal variation in edge chemistry of anglerfish otoliths and illicia.....	22
	3.1.14 Comparison of methods for detecting cycles in microchemistry data	22
	TASK 4 COMPARISON OF RESULTS FROM DIFFERENT STRUCTURES IN ANGLERFISH.....	24
	TASK 5 Development of growth models.....	24
	3.1.15 Estimating age of chemically tagged hake using the modified Lomb Scargle periodogram.....	25
	3.1.16 Estimation of anglerfish age using the modified Lomb Scargle periodogram	25
	3.1.17 Back-calculation of individual growth curves for anglerfish.....	25
	3.1.18 Comparison of microchemistry based anglerfish age estimates with mixture model estimates	26
4	RESULTS	26
	Pilot phase: elements and isotopes in hake otoliths and in anglerfish otoliths and illicia.....	26
	4.1.1 Reanalysis of previously collected hake data	26
	4.1.2 Optimising methodologies for analysing trace elemental profiles in hake otoliths.....	26
	4.1.3 Trace element analysis of anglerfish otoliths and illicia using Laser ICPMS.....	27
	4.1.4 Anglerfish: stable isotope analysis using IRMS	28

	Main phase: seasonal trends in elements and isotopes	29
4.1.5	Investigation of periodic signals in trace element profiles from chemically tagged hake.....	29
4.1.6	Analysis of oxygen stable isotope profiles from hake otoliths.....	29
4.1.7	Seasonal variation in trace elements at the edge of anglerfish otoliths	29
4.1.8	Stable isotope profiles in otoliths and illicia of anglerfish.....	30
	Comparison of peak detection approaches	30
4.1.9	Simulation outputs	31
4.1.10	Application to data from independently aged cod (<i>Gadus morhua</i>).....	31
4.1.11	Lomb Scargle age estimation	31
4.1.12	Estimation using the chirp function	31
4.1.13	Age estimation of chemically tagged hake otoliths from phosphorous profiles.....	31
4.1.14	Age estimation of anglerfish otoliths from strontium profiles	32
4.1.15	Hake: accuracy and precision of microchemistry based age determination	32
5	DISCUSSION AND CONCLUSIONS	34
	The optimal approach to measuring annual cycles	34
	Evidence for age related microchemistry trends.....	34
	The optimal approach to detecting annual cycles	35
	Insights into age and growth of hake and anglerfish	35
	Conclusions and extent to which project objectives have been addressed	37
	Annex 1: Map of ICES area boundaries in the Northeast Atlantic	95
6	ANNEX 2: LIST OF PROJECT PARTICIPANTS	96
7	ANNEX 3: GLOSSARY OF ABBREVIATIONS AND ACRONYMS USED IN TEXT.....	97
8	ANNEX 4: PROTOCOL FOR THE ANALYSIS OF ANGLERFISH ILLICIA AND OTOLITHS.....	99
9	REFERENCES	1

List of Tables

Table 1: Summary of the numbers of individuals, for hake and anglerfish, analysed in both pilot and main phase.

Table 2: Origin of hake otoliths used for the trace element analysis. Slide reference indicates that otolith had been prepared prior to the current project (see text). New preparations were made to complete the samples. Two otoliths (8493 and 7521) did not show an OTC mark and date or length at recapture appeared to be misreported at the time of collection. For otolith 5154 the difference in size between the release and recapture dates indicated that the date of recapture had been misreported. These samples were excluded from further analysis

Table 3: Tagged hake otoliths samples analysed with ion probe-SIMS. Four previously prepared samples were discarded because of the lack of the OTC mark making them useless for the study. Instead, the most valuable samples were analysed from the core to edge (Core) rather than from c.a. the OTC tag to the edge (OTC). TL total length.

Table 4: Sample size used in the pilot phase (PP) and main phase (MP) of the anglerfish analysis. Sample number refers to number of individuals sampled by size category and quarter. In the pilot phase otoliths and illicia from each individual were analysed using LA ICPMS and IRMS. In the main phase the otoliths were analysed using LA-ICPMS and a subsample were analysed using SIMS. In the main phase Illicia were imaged and ages were estimated by expert readers.

Table 5: Numbers of anglerfish otoliths in each category included in the final analysis of the LA ICPMS data from the main phase after exclusion on unreliable data.

Table 6: Summary of the results of $\delta^{18}\text{O}$ measured in otoliths of tagged hakes. Mean values represent the mean of all measurements obtained in each otolith. SD standard deviation. $\pm \%$: averaged precision i.e averaged the overall one sigma uncertainty on an analysis, which includes the within run uncertainty (std. error of the mean) and the standard deviation on the standards, propagated together. Note that this statistics come from data that still need to be validated.

Table 7: Age and growth estimates for chemically tagged hake, derived from otolith phosphorous profiles

Table 8: Growth rates for chemically tagged hake calculated from measured body size at the time of tagging and recapture and estimated from the individual growth curves derived from otolith phosphorous signals.

Table 9: Mean length at each age as estimated by back-calculation using peaks identified from strontium profiles in anglerfish otoliths compared to mean lengths at age estimated using two published growth models

List of Figures

Figure 1: Images of sectioned otoliths from collections of chemically tagged hake held by IFREMER. a) Fluorescence microscope image with the position of the chemical (OTC) mark indicated by a red arrow. b) Image showing the four growth transects along which otolith growth was measured (OTC mark to otolith edge).

Figure 2: Image of an illicium (left) and an otolith (right) showing the axis that were measured for the construction of back calculation equations.

Figure 3: A vonBertalanffy chirp function with the phase given by the reverse von Bertalanffy function with ($L_{\infty} = 100, K = 0.2, t_0 = 0, \phi_0 = -\pi/2$). X-axis is back-calculated fish length putative annual signal extracted by the model overlaid (black line). The bottom panels show the periodogram with the period of the putative annual cycle indicated by the vertical line. The dashed horizontal line shows the threshold for statistical significance. In the example on the left one clear signal dominates the series and is easily isolated. In the middle plot the period of the selected signal does not coincide with a peak in the periodogram. The routine is repeated with a different range of parameters for the grid search. The results of this iteration are shown on the right; now the extracted signal aligns with the peak and the result is accepted. In this example (MP-Q2-9) there is a visible peak at the beginning of the time series and another just before estimated age 2; these features are not consistent with the constraints of the Von Bertalanffy growth function that are incorporated into the signal detection process and are therefore not detected as part of the annual signal.

Figure 5: Plots of the linear relationships between otolith and illicia radii and fish length for anglerfish

Figure 6: Strontium profiles from hake otoliths collected as part of previous projects OTOMIC FAIR CT98-4365; IBACS QLRT-2001-01610, IDEADOS CTM2008-0489-CO3; EU DGXIV-96-075). Blue shaded areas indicate the locations of translucent areas on the otolith transects.

Figure 7: Sodium profiles from hake otoliths collected as part of previous projects (OTOMIC FAIR CT98-4365; IBACS QLRT-2001-01610, IDEADOS CTM2008-0489-CO3; EU DGXIV-96-075). Blue shaded areas indicate the locations of translucent areas on the otolith transects

Figure 8: Results from a Lomb Scargle analysis of otolith chemistry profiles from a 70cm hake. The peak with annual periodicity is indicated with the vertical black line in the bottom panel; the normalised power falls below the significance threshold (horizontal dashed line). The detected signals are therefore not significant and not considered to be indicative of age.

Figure 9: 2D mapping of ^{24}Mg and ^{26}Mg and the resulting isotopic ratio $^{24/26}\text{Mg}$

Figure 10: 2D mapping of $^{25}\text{Mg}/\text{Ca}$ (left) and $^{55}\text{Mn}/\text{Ca}$ (right) on M5-M123 otolith showing that concentrations of these two elements are much lower on the proximal side (sulcus) than on the distal side (anti sulcus)

Figure 11: 2D mapping of $^{31}\text{P}/\text{Ca}$ (left) and $^{39}\text{K}/\text{Ca}$ (right) on M5-M123 otolith showing that concentrations of these two elements are much higher on the proximal side (sulcus) than on the distal side (anti sulcus)

Figure 12: 2D mapping of $^{88}\text{Sr}/\text{Ca}$ (left) and $^{138}\text{Ba}/\text{Ca}$ (right) on M5-M123 otolith showing that concentrations of these two elements do not show any asymmetry.

Figure 13: Plot showing relationships between zinc and opacity profiles in anglerfish illicia.

Figure 14: Boxplots showing the distribution of $\delta^{13}\text{C}$ (a and c) and $\delta^{18}\text{O}$ (b and d) concentrations at edge of anglerfish otoliths. Data for males and females are compared in plots a) and b) (quarter 1 data only). Data from fish collected in quarter 1 and quarter 2 are compared in plots b) and c). Medians are indicated by the dark line, the upper

and lower edges of the boxes represent the 75th and 25th percentiles respectively, whiskers represent the data extremes.

Figure 15: Example plots showing concentrations of $\delta^{13}\text{C}$ (left) and $\delta^{18}\text{O}$ (right) along anglerfish otolith transects. Data shown in the upper plot is from a fish collected in quarter 3 2017, data shown in the lower plot is from a fish collected in quarter 1 2018

Figure 16: Concentration of Mn/Ca on M5M123 otolith. Transect extracted on the proximal side, OTC at 1576 μm (top left), transect extracted on the distal side, OTC at 1892 μm (top right), corresponding chemical image (bottom left).

Figure 17: Example outputs from the Lomb Scargle analysis of oxygen stable isotope profiles from chemically tagged hake otoliths. The top panels show the detrended oxygen isotope data (blue points) with the dominant signal extracted by the model overlaid (black line). The point on the otolith corresponding to the time of tagging (OTC mark) is indicated with a vertical blue line. The time of recapture (otolith edge) is indicated with a vertical red line. The dates beside each line refer to the time of release and capture. The bottom panels show the periodogram with the period of the putative annual cycle indicated by the vertical line. The dashed horizontal line shows the threshold for statistical significance. In plot (a) almost three full cycles are completed within a period of just over 1 year while in plot (b) 1.5 cycles are completed within the 474 days of liberty. This shows that the fluctuations in oxygen stable isotopes do not show a regular seasonal or annual pattern. The detected signals are not statistically significant.

Figure 18: Plots displaying how concentrations of ^{23}Na and ^{88}Sr vary between quarters, length classes and ICES divisions. The regional comparison is based on samples collected in quarter 2 only.

Figure 19: Plot showing how detrended ^{88}Sr concentrations at the otolith edge (40 μm) vary across samples collected in different months. Measurements are shown as black dots. The blue line is a loess smooth used to highlight broad trends in the data.

Figure 20: Relative $\delta^{18}\text{O}$ values across edge to core transects on individual anglerfish otoliths. Colours indicate the time of year (quarter) when the fish was collected.

Figure 21: Boxplots showing the distribution of $\delta^{18}\text{O}$ concentrations at the edge of anglerfish illicia collected in each quarter. Medians are indicated by the dashed line, the upper and lower edges of the boxes represent the 75th and 25th percentiles respectively, whiskers represent the data extremes. There was no significant difference between quarters ($p=0.37$)

Figure 22: Relative $\delta^{18}\text{O}$ values across edge to core transects on individual anglerfish illicia. Colours indicate the time of year (quarter) when the fish was collected.

Figure 23: Example simulations of random peak detection. Simulated true series are shown as black lines, observations with error from the simulated series are shown in grey, true peaks are denoted with a vertical dashed line. Points denote peaks detected using: fixed window of eight observations (red triangles); fixed window of 20 observations (red crosses, mostly covered by decreasing window peaks); decreasing window (blue crosses); adaptive smoother and automatic peak detection algorithm (green x).

Figure 24: Scatterplots summarising the results of the method comparison based on simulated data. The true number of peaks are shown on the x axis and the number detected by each method are shown on the y axes. n_op1_w8: fixed window of eight observations; n_op1_w20: fixed window of twenty observations; n_op2: decreasing window; n_gam_ampd: adaptive smoother and automatic peak detection algorithm). Rows denote the length of the time series (T) and scale the height of the peaks. 1:1 line shown for reference.

Figure 25: Plots showing the occurrence of peaks in Phosphorous (^{31}P) profiles from otoliths of 6 year old cod (*Gadus morhua*). Grey points indicate the observations. The black line is a loess smoother with a span equal to 100 divided by the time series length. The beginning and end of each translucent band on the otolith is indicated by the dashed

vertical lines. The red dots indicate local maxima identified by the argmax peak detection algorithm.

Figure 26: The annual signal extracted from ^{31}P profiles in 6 year old cod otoliths using the modified Lomb Scargle approach (black line) overlaid on the detrended ^{31}P measurements.

Figure 27: Chirp function fits to ^{31}P profiles in otoliths from 6 year old cod

Figure 28: Example outputs from the modified Lomb Scargle method applied to 2D image LA ICPMS data from chemically tagged hake otoliths. The top panels show the detrended elemental data (blue points) with the putative annual signal extracted by the model overlaid (black line). The point on the otolith corresponding to the time of tagging (OTC mark) is indicated with a vertical blue line. The time of recapture (otolith edge) is indicated with a vertical red line. The dates beside each line refer to the time of release and capture. The bottom panels show the periodogram with the period of the putative annual cycle indicated by the vertical line. The dashed horizontal line shows the threshold for statistical significance. In example (a) the annual signal extracted by the Lomb Scargle method fits to the general visual trend in the data, other fluctuations occur at high frequencies. In example (b) in the middle there are two prominent sub-annual peaks in the middle of the time series; these features are not consistent with the constraints of the Von Bertalanffy growth function that are incorporated into the signal detection process and are therefore not detected as part of the annual signal. (b) and (c) show data from two transects taken from the same otolith. The peaks in phosphorus concentration are more pronounced on the proximal transect (b) compared to the distal transect (c), although both show similar trends.

Figure 29: Example plots from an individual anglerfish for which annual cycles in strontium profiles are difficult to isolate using the Lomb Scargle approach.

Figure 30: Strontium profile for one individual (blue points in left panel) overlaid with the annual signal extracted by the modified Lomb Scargle algorithm (black line in left panel) showed alongside an otolith (centre) and illicium (right) from the same individual. The red dots on the otolith and illicium images mark the position on the transects that correspond to the end of each year in the annual cycle (the minima). The ages estimated by expert readers for this individual were 4 and 5 (two otolith readings) and 3, 3 and 5 (three illicia readings).

Figure 31: Plots showing the correspondence between age estimates derived from the strontium profiles and those provided by three expert readers based on visual examination of otolith and illicium images. The blue points are individual age estimates, the grey line shows a 1:1 relationship (perfect agreement).

Figure 32: Frequency distribution of the back-calculated lengths from individual growth curves for the anglerfish samples in this study overlaid on the frequency distribution of lengths from the Irish groundfish survey.

Figure 33: Boxplot showing the distribution of lengths of fish assigned to each age class using the mixture mode (orange) and the microchemistry method (green).

Figure 34: Mean probabilities of mixture model assignments to pseudo age cohorts for each age group as estimated using microchemistry

Figure 35: (a) Back-calculated growth histories, reconstructed using the age estimates from the strontium profiles (grey lines), with the best fitting Von Bertalanffy growth curve shown in red and 95% confidence limits shown in grey (bootstrap estimates) and cyan (delta estimates). (b) From the subset of the sample for which sex information was available: back-calculated growth histories for the females (green) and the males (purple)

1 EXECUTIVE SUMMARY

Reliable measures of fish length-at-age are needed to estimate the biological reference points used in fish stock assessment. These data are usually obtained by counting and measuring seasonal growth marks in otoliths or other calcified structures for a representative sample of the population. For anglerfish (*Lophius* spp.) and hake (*Merluccius merluccius*) in the Northeast Atlantic, traditional age-estimation methods are unreliable. The assessments for these stocks are based on survey indices or are length-based and require accurate information on length-at-age. Without this information, accurate assessments and the estimation of MSY reference points are problematic.

For some other species, objective methods of age-determination have been developed using seasonal patterns in chemical composition across otolith transects. This project (**A**ge validation of **H**ake and **A**nglerfish: AHA project) investigated the feasibility of using this approach in age determination for selected stocks of anglerfish and hake with a view to improving the growth models used in stock assessment. Validation of the annual periodicity of chemical signals was conducted using existing collections of chemically tagged hake (from ICES divisions 7 and 8a, and from 8c and 9a), and through analysis of edge chemistry in otoliths and illicia of white anglerfish (*Lophius piscatorius*) (from ICES Divisions 7b-k and 8a,b,d). A comprehensive assessment of a range of approaches was carried out to establish the optimal methods for sample preparation, microchemical analysis and data analysis.

The most effective approach to detecting annual signals was high resolution profiling of trace elements (elements present in minute amounts) across otolith growth transects using laser ablation inductively coupled plasma mass spectrometry (LA ICPMS). This technique collects data by ablating the otolith surface with a laser and passing it to a mass spectrometer where the quantity of elements in the ablated material is determined. As the laser moves across the otolith from the core to the edge, changes in otolith elemental concentrations from hatching until capture are recorded. These patterns reflect fluctuations in the environment or the fish's internal state and may display annual cycles. By collecting data continuously (within the limits of machine speed), the LA ICPMS approach ensures that peaks are recorded at a sufficiently high resolution to be detected.

Concentrations of strontium and sodium at the edge of anglerfish otoliths showed small but significant levels of seasonal variation that could provide an indicator of age. Variability was also detected between size groups and areas, which could make annual signals more difficult to detect. Here, statistical treatment of the data (detrending using a general additive model smoother) helped to elucidate age related patterns. Microchemistry analysis of chemically tagged hake otoliths revealed pronounced fluctuations in phosphorous concentrations. When these patterns were examined in relation to the chemical tag in the otolith (known time point on the otolith growth transect) they appeared to have an annual periodicity in some fish. However, there was a lot of variability between fish and sub-annual fluctuations also occurred in the profiles.

A novel method was developed for detecting annual cycles in microchemistry data, which incorporates properties of Von Bertalanffy growth. This approach performed well relative to other methods when applied to simulated and real microchemistry data. The technique was used to estimate age of anglerfish and hake from strontium and phosphorous profiles respectively.

The mean estimated growth rate of 14 chemically tagged hake was $0.38\text{mm}^{-1}\text{day}$ compared to an actual mean growth rates of $0.42\text{mm}^{-1}\text{day}$. The absolute mean percentage error rate was 23%. Estimated back calculated lengths at age across the growth transect were reasonably consistent with the current growth model used in the stock assessment and corroborate existing evidence that the previous international ageing criteria underestimated growth rates. The microchemistry based age estimates of length at age 3 were lower than the growth model predictions, however this comparison is based on a small sample size ($N=13$). Although the accuracy of microchemistry based age estimation of hake is moderate, the technique could be useful

for investigating growth rate variability between sexes and across years, thus improving the accuracy of the stock estimates and reference points. Future work should focus on applying the approach to a larger sample size that is more representative of the population size structure to enable robust comparison of the current growth model and microchemistry based age estimates.

For anglerfish, age estimates derived from the analysis of otolith microchemistry profiles tended to be higher than ages estimated from counts of growth marks on illicia. The microchemistry method also produced lower estimates of growth than the method that is used to split survey length frequency data into pseudo age classes prior to stock assessment; the mean difference in the age assignments was 0.42 years (± 0.09 95% confidence interval). The microchemistry based method for age determination of anglerfish may overestimate age; further work is needed to assess accuracy. This could be achieved using daily increment analysis (to confirm the timing of the first microchemistry cycle) and chemical tagging (which could be incorporated into planned international tagging programmes for anglerfish). The length splitting approach supports an age structured assessment for white anglerfish and is more robust than direct ageing methods. Nonetheless, given the discrepancy between the microchemistry based age determination method and the cohort splitting approach, it is recommended that implications of growth overestimation are evaluated within a management strategy evaluation framework.

For black anglerfish (*Lophius budegassa*) and for other stocks of white anglerfish which do not have an age structured assessment, microchemistry based age estimation, in combination with other direct ageing methods could be used to estimate growth parameters and to evaluate the accuracy of stock estimates and reference points. Given their biological similarity, it is likely that the microchemistry patterns observed in white anglerfish will be detectable in otoliths from black anglerfish and other stocks of white anglerfish. Microchemistry based age estimation could be applied to these stocks using the methodologies developed here.

The AHA project has demonstrated for the first time that otolith composition of anglerfish and hake varies seasonally and has identified the optimal methods for measuring age related microchemistry patterns in these stocks. A novel statistical technique has been developed to process these time series while incorporating their biological properties. The patterns identified in the otolith elemental profiles show promise as indicators of age and provide some insight that can inform the assessment of the stocks. The application of microchemistry techniques to age determination is a relatively new technique; as these methods develop, rigorous testing and refinement are required and sources of error should be quantified. The microchemistry based age determination methods presented here are resource intensive and are unlikely to provide a routine method of age estimation. Nonetheless, they have practical application for corroborating other sources of data describing age and growth and for investigating variability in growth rates. It is recommended that the methods presented here be applied within a large sampling program that ensures full representation of size structure, maturity stages and sexes in the stocks of interest and that incorporates tag recapture. This would facilitate a comprehensive evaluation of growth rate variability, information that is currently lacking from the stock assessment

2 OVERVIEW

Background

2.1.1 Age information in stock assessment

The estimation of the biological reference points used in fish stock assessment requires reliable length-at-age information, which is usually obtained by counting and measuring seasonal growth marks in otoliths for a representative sample of the population. Otoliths and other calcified structures such as bones and scales register the life history of

individual fish; daily and seasonal growth patterns are reflected in the relative opacity of the structure. However, for some stocks, clearly defined growth marks do not occur, hampering age estimation and age-based assessment and challenging the implementation of MSY-based management, as required under the common fisheries policy (CFP) (Maunder and Piner 2014). Length-structured models provide an alternative means to estimate growth parameters and support stock assessment (Hampton and Fournier 2001). The length-composition of the stock from survey and catch data can be used to identify length cohorts and follow their progression over time, allowing for the generation of a growth model (Drouineau et al. 2010b). For the stocks of anglerfish (*Lophius piscatorius*) and hake (*Merluccius merluccius*) that are the focus of this study, the reliability of available age-estimation methods is low and analysis of length data form the basis of the stock assessments.

2.1.2 Hake age determination

Prior to 2010 stock assessments for both the northern and southern stocks of hake relied on age estimates from otolith readings. Tagging studies from across the range of the species distribution in the Atlantic and Mediterranean showed that the internationally agreed ageing method substantially overestimated age and produced growth estimates that were biased by a factor of ~ 2 (de Pontual et al., 2006; Piñeiro et al., 2007; Mellon-Duval et al., 2010; de Pontual et al., 2013). International otolith exchanges and workshops also showed that the interpretation of growth structures in hake otoliths is highly problematic and is neither accurate nor precise (Piñeiro et al. 2009; ICES, 2010). This prompted the development of a new assessment model for northern and southern hake. However, these models still require accurate growth parameters, and there is a need to develop a validated growth model for the species or to integrate age reading errors into the stock assessment (ICES 2010).

2.1.3 Hake stock assessment

Northern hake are assessed using a forward simulating age structured model (Stock Synthesis 3; (Methot and Wetzal, 2013)). In 2018, the incorporation of an egg survey index into the assessment was investigated. The index was not accepted for inclusion in the stock assessment but was recommended as an external indicator of stock size (ICES, 2019). Southern hake are assessed using a length-age based model (GADGET). For both stocks growth is described using a Von Bertalanffy curve and lengths at each age are assumed to follow a normal distribution. Asymptotic size is assumed to be constant ($L_{inf}=130\text{cm}$). For southern hake, the growth parameter k is estimated from the progression of length cohorts through the year. The northern hake growth parameters were fixed in 2013 as the model could no longer estimate them. For both stocks, the accuracy of the growth parameters is considered crucial. The species is known to be strongly sexually dimorphic and the exploration of sex-specific assessment models is recommended for both stocks (ICES, 2014). A better understanding of growth rates and how they vary between the sexes and over time is needed to reduce uncertainty and increase the robustness of the stock assessment

2.1.4 Anglerfish age determination

For anglerfish, the occurrence of secondary structures in otoliths makes age estimation using otoliths difficult (Crozier 1989; Woodroffe et al. 2003). Therefore, illicia (modification of the first dorsal-fin spine that is located on the tip of the snout and functions as a luring apparatus) are the preferred structure for routine age estimation in most European countries (Landa et al. 2008; ICES 2011).

The periodicity of growth marks in illicia has been indirectly validated using length cohort analysis (Landa et al. 2013). Uncertainties remain however, regarding interpretation of growth marks in both ageing structures for anglerfish (Wright et al. 2002; Velasco et al. 2008). There are large inconsistencies between age estimates obtained from otoliths and illicia and considerable disagreement between readers interpreting the same structures (Illicia % agreement: 49%; Otoliths % agreement: 18-25%; agreement between structures 5-16%, Woodroffe et al. 2003; ICES 2011). Anglerfish migrate to deep waters at older ages (Laurenson et al 2005) where seasonal temperature

fluctuations are low; this may prevent the formation of clear seasonal growth marks in their calcified structures.

2.1.5 Anglerfish stock assessment

For all anglerfish stocks direct estimates of age are considered unreliable and are not used in stock assessment. The anglerfish stock that is the focus of this study (*Lophius piscatorius* in ICES area 7b-k and 8a,b,d) is a category 1 stock with a quantitative stock assessment. A mixture model is used to split the survey length frequency data into cohorts (Batts et al., 2019) and the pseudo-age structured data are fed into an age-based stock assessment using the a4a package (Jardim et al., 2014). This assessment model approach is considered sufficiently reliable and robust to provide a basis for harvest advice for this stock. However, the MSY reference points are sensitive to the assumed growth parameters. Additionally, considerable sexual dimorphism is known to exist in the growth of anglerfish and this is currently not accounted for the mixture model.

For the black bellied anglerfish (*Lophius budegassa*) stock in the same area, indices at age derived using the length frequency splitting approach do not align well with the progression of cohorts across years in the fishery or survey data and assessment model outputs are highly sensitive to the growth estimates used. The stock is therefore not assessed using this approach and remains a category 3 stock that is assessed based on a combined Irish-French survey index (ICES, 2018). The other four anglerfish stocks in the Northeast Atlantic are assessed using either production models or survey indices. In general, across all stocks uncertainties around growth remain. A reliable method of age determination would help to address these issues and could improve the accuracy of assessments and estimation of MSY reference points.

2.1.6 Microchemistry in age determination

Chemical elements from the surrounding water enter the blood plasma of fish via the gills and are incorporated into calcified structures (as for example otoliths and illicia) in trace amounts as they grow (trace elements); rates of uptake vary depending on the element and are influenced by the fish's physiology. For some elements (e.g. oxygen and strontium) the relative concentrations of the different isotopic forms of that element (stable isotopes) reflect their relative concentrations in the ambient environment while for other stable isotopes (e.g. carbon) their incorporation is under metabolic control (Campana, 1999). Seasonal changes in temperature and physiology can produce periodic patterns in the chemical composition of otoliths (Seyama et al. 1991). Across several species, clearly defined minima and maxima in the concentrations of some elements and isotopes in otoliths have been shown to correspond to age (Hüssy et al. 2015; Siskey et al. 2016; Kastle et al. 2017). ~~The anglerfish illicium is a modification of the first dorsal fin spine which is located on the tip of the snout and functions as a luring apparatus.~~ Fin rays have also been used as valid structures to provide seasonal growth marks, fin ray chemistry has been shown to correlate with water chemistry (Clarke et al. 2007) and age-related trends have been observed (Luque et al. 2017).

For species that are difficult to age from visual examination of their growth structures, microchemistry based age determination methods offer great promise for objectively estimating age and corroborating other methods of age estimation. For anglerfish and hake, a microchemistry based age determination method could be used to validate the growth models currently used in the stock assessments and to further investigate variation in growth parameters over time and between the sexes. However, the incorporation of elements and isotopes into calcified structures is a complex process that can vary between species habitats and life history stages. Before applying the method to new species the seasonal nature of microchemistry patterns must be thoroughly validated and potential sources of variability investigated.

Otolith chemistry is influenced by various interacting endogenous (e.g. genetics, metabolism, maturity) and exogenous factors (e.g. water chemistry, temperature, salinity) (Campana 1999; de Pontual and Geffen 2002; Elsdon et al. 2008; Loewen et al. 2016). Seasonal patterns may be overlaid by geographic and ontogenetic variation

(Morales-Nin et al. 2005; Tomas et al. 2006) making their detection and interpretation difficult.

Teleost fin rays and spines are composed of dermal bone, consisting primarily of calcium phosphate (Findeis, 1997), unlike otoliths which are predominately composed of calcium carbonate. Fin rays differ from otoliths in their composition of hydroxyapatite, the presence of osteoclasts, the remobilization of their constituents, and the processes linked to calcification (Loewen et al, 2016). Remodelling and resorption of illicia constituents (de Pontual and Geffen 2002) may confound the use of microchemical analysis of illicia for age determination. Differences in structure and composition between illicia and otoliths will affect the manner in which elements and isotopes are incorporated and has consequences for the analytical protocols used to analyse illicia (e.g. choice of method and standards, limits of detection, range of elements/isotopes analysed).

Before microchemical analysis can be used to assist age determination of anglerfish or hake it is necessary to 1) determine which elements can be reliably detected in each growth structure; 2) confirm the seasonality of any observed trends in microchemistry; and 3) examine correspondence between seasonal patterns in microchemistry, visual growth marks and length distributions.

Objectives

The primary objectives of the study were to:

1. Analyse microchemistry patterns in otoliths and illicia of hake and anglerfish
2. Develop statistical approach for detecting seasonal patterns in microchemistry
3. Relate detected seasonal trends to visual growth marks and length distributions
4. Use available information to refine growth models for associated stocks

These aims were addressed by combining the reanalysis of previously collected microchemistry data with additional analyses of existing and newly collected material and an analysis of length distributions from available survey data. For hake, seasonal microchemistry patterns could be directly validated using existing collections of chemically tagged otoliths. The study focused on hake from ICES Divisions 7 and 8a (northern stock) and from ICES Division 8c/7a (southern stock). For anglerfish, the seasonality of microchemistry patterns was tested by comparing otolith edge chemistry in fish collected in different seasons (quarter1-4). The study focussed on white anglerfish (*Lophius piscatorius*) from ICES Divisions 7b-k and 8a,b,d (see map of ICES areas in Annex 1)

Consortium

The AHA consortium (**A**ge validation of **H**ake and **A**nglerfish: AHA project) brought together scientists from the:

- Galway Mayo Institute of Technology (GMIT), in Ireland;
- Marine Institute, in Ireland;
- Mediterranean Institute for Advanced Studies (IMEDEA), in Spain;
- University of Bergen (UiB), in Norway;
- Institut Français de Recherche pour l'Exploitation de la Mer (IFREMER), in France and
- National Institute of Aquatic Resources (DTU Aqua), in Denmark.

See Annex 2 for a list of all participants.

3 METHODOLOGY

Approach to sampling design and analyses

The use of microchemistry patterns in age determination is an emerging technique and its broad applicability is yet to be demonstrated. This study was designed to comprehensively test a range of analytical approaches in order to identify the optimal methods for detecting and analysing age related microchemistry patterns in otoliths (hake and anglerfish) and illicia (anglerfish). The study was divided into a pilot phase and a main phase. During the pilot phase a number of analytical techniques were compared, statistical tools were developed and the elements or isotopes most likely to display annual signals were identified. In the main phase the analytical approaches that were identified as optimal in the pilot phase were applied to a larger sample size and the extent to which putative annual microchemistry signals represents growth was evaluated.

For hake, the seasonality of microchemistry patterns was tested using otoliths from hake that had been chemically tagged using Oxytetracycline (OTC), which leaves a fluorescent mark in the otolith corresponding to the time of release (de Pontual et al. 2006; de Pontual et al. 2013). In addition, Microchemical data collected as part of previous projects¹ were reanalysed to determine if seasonal patterns occurred. For anglerfish, otoliths and illicia from tagged or known age individuals were not available. Therefore, seasonality was investigated by comparing chemical composition at the edge of the structure between samples collected at different times of year. The numbers of samples analysed in each phase are detailed in Table 1.

Trace elements (elements present in minute amounts within the calcified structure) were analysed using laser ablation inductively coupled plasma mass spectrometry (LA ICPMS). Stable isotopes of carbon ($\delta^{13}\text{C}$) and oxygen ($\delta^{18}\text{O}$) were analysed using Isotope Ratio Mass Spectrometry (IRMS); $\delta^{18}\text{O}$ was also analysed using secondary ionisation mass spectrometry (SIMS). These methods are fully described in section 3.3.

Microchemistry patterns were analysed with reference to interpretations of visual growth marks by expert readers through an ageing exchange conducted via ICES SmartDots² and in collaboration with the ICES working group on biological parameters (WGBIOP). Linkages with the TABACOD³ project led by DTU Aqua enabled the testing of methods on known age cod that displayed clear annual microchemistry signals in their otoliths. Finally, the results are evaluated in the context of a parallel analysis of length distributions from survey data (Batts et al., 2019).

TASK 1 SAMPLE AND DATA GATHERING

3.1.1 Hake: Collation of data for reanalysis

Detailed high resolution microchemical data, collected as part of previous projects (OTOMIC FAIR CT**98**-4365; IBACS QLRT-**2001**-01610, IDEADOS CTM**2008**-0489-CO3; EU DGXIV-**96**-075; year of project initiation highlighted in bold) (Morales-Nin et al. 2005; Tomas et al. 2006) were collated and formatted for use in the project (Table 1).

3.1.2 Hake: Sourcing of chemically tagged hake otoliths

Otoliths from chemically tagged hake were sourced from collections held by IFREMER. These samples were obtained from their tagging program that ran from 2002-2007 (de Pontual et al. 2006; de Pontual et al. 2013). Twenty one fish that were recaptured after at least one year were selected. When both otoliths were available, the left was used for the analysis of trace element concentrations and the right for oxygen stable isotope ($\delta^{18}\text{O}$) analysis. A total of 14 otoliths were analysed for trace elements using LA-ICPMS

¹ OTOMIC FAIR CT**98**-4365; IBACS QLRT-**2001**-01610, IDEADOS CTM**2008**-0489-CO3; EU DGXIV-**96**-075; year of project initiation highlighted in bold

² <https://www.ices.dk/marine-data/tools/Pages/smartdots.aspx>

³ <http://www.tabacod.dtu.dk/polski/about>

during the pilot phase (Table 2) and 16 were analysed for stable isotopes using SIMS in the main phase (Table 3).

*3.1.3 Anglerfish (*L. piscatorius*): sampling*

Samples for the pilot phase of the analysis were collected from ICES Division 7 in quarter 3, 2017 and quarter 1, 2018. The main phase of the analysis used anglerfish collected from ICES Division 7 collected in quarter 4, 2017 and quarters 1-3, 2018. The objective within each phase was to investigate seasonal changes in edge chemistry at different time points within an annual cycle, inter-annual variation was not investigated and data from each phase were analysed separately. In the pilot phase, broad changes from quarter 3, 2017 to quarter 1, 2018 were examined. In the main phase changes were investigated at a finer temporal resolution, from quarter 4, 2017 through quarters 1 and 2, 2018 and to quarter 3, 2018. This sampling design ensured that a complete annual cycle could be investigated within the time that was available to complete the project.

The original sample size target for the main phase was 120 anglerfish: 10 individuals from three size categories at four time points. Based on feedback received from the ICES stock assessment working group and with reference to length cohorts identified by Batts et al (2019). The sampling design was modified to include large fish (>52 cm) as well as the most abundant length cohorts (<31cm, 31-41 cm and 42-52 cm). A total of 159 fish were obtained for inclusion in the analyses (Table 4). The largest fish were rare in survey and commercial samples so the target of 10 individuals was not met for this category. The sourcing of small fish (<31 cm) from commercial samples proved difficult and the target of 10 fish was not met for this category in quarter 3. Nonetheless the sample size was deemed sufficient to address the main hypotheses; this was subsequently confirmed by the analysis which had sufficient statistical power to detect significant variation in elemental concentrations between length groups and quarters.

Quarter 1 samples were collected during the Marine Institute anglerfish survey. Samples from quarter's 2, 3 and 4 were obtained from port samples by the Marine Institute and IFREMER. IFREMER secured an official exemption to capture small (<500 g limit) white anglerfishes in area 7e.

TASK 2 SAMPLE PROCESSING

3.1.4 Sample preparation – Hake otoliths

Fifteen hake otoliths had been previously prepared for use in an ICES workshop on age estimation of European hake (ICES, 2010). An additional six were prepared in the same manner by embedding in epoxy resin (Buehler EpoThin, 2), sectioning on the transverse plane through the core region (to reveal a growth history for the entire life of the individual) and sequentially grinding and polishing. For the purpose of standardisation, left otoliths were systematically used for the analysis of trace element concentrations and right otoliths for oxygen stable isotope ($\delta^{18}O$) analysis. All otolith sections were imaged using fluorescent microscopy to record the position of the oxytetracycline mark (OTC, indicating the otolith edge at time of tagging; Figure 1). Otolith growth measurements were obtained along four transects from the OTC mark (time of release) to the edge (time of recapture). Inspection under fluorescence showed that in two otoliths the OTC mark was no longer visible. These sections were excluded from further analysis. Sufficiently detailed data were obtained from the remaining sections (average time at liberty 507 days, range: 279-1555) to investigate seasonal cycles.

3.1.5 Sample preparation – Anglerfish otoliths and illicia

Otoliths and illicia were soaked in deionised water for 5-10 minutes to remove any biological tissue. Otoliths were mounted in epoxy resin (Buehler EpoThin), and ground on the sagittal plane (sulcus side) with P320 grit silicon carbide paper to expose the otolith surface and then sanded with silicon carbide paper ranging from P1500 to P4000 grit to produce a flat longitudinal section. Final polishing was conducted using diamond suspensions (9 μ m, 3 μ m and 1 μ m) and sections were glued to sample holders

appropriate to each analytical method. Otolith sections were imaged before and after analysis.

Illicia were mounted in polyester resin (Crystic R115PAV01) and sectioned transversally according to the protocol described by Duarte et al (2002). Three sections of between 0.3 and 0.5mm thickness were taken from the base of each illicium. Sections were ground with P2500 to P4000 and polished using diamond suspensions (3µm and 1µm). Illicium sections were imaged for subsequent analysis of visual growth marks and glued to sample holders appropriate to each analytical method.

3.1.6 *Imaging and measurement of anglerfish ageing structures*

All of the anglerfish structures used in the analyses were photographed under reflected light on a stereomicroscope. Images of each structure were used to measure the radius from core to edge along the longest axis on the illicia and across three axes of each otolith (Figure 2). Opacity was measured by extracting pixel values along a core to edge transect. Measurements were made using the ImageJ software. Images were shared with three readers with expertise in the anglerfish age estimation. Images were read by each reader independently and the three age estimates for each structure were compared to age estimates obtained using microchemistry. The ICES SmartDots⁴ platform was used to coordinate the ageing exchange.

3.1.7 *Analysis of tagged hake otoliths using Laser ICPMS*

The elemental composition of OTC marked hake otoliths was quantified using a UV high-repetition-rate femtosecond laser ablation (fs-LA) system (Lambda III, Nexeya SA/Amplitude Systèmes, Canejan, France) coupled to a High Resolution Inductively Coupled Plasma Sector Field Mass Spectrometer (HR-ICP-SFMS, XR, Thermo Scientific, USA) at the IPREM (Institute of Analytical Sciences and Physico-Chemistry for Environment and Materials, Pau, France).

Otolith elemental composition can vary spatially within an otolith (Payan et al., 1999; Limburg and Elfman, 2017; Pracheil et al., 2019) and microchemistry profiles can differ depending on the transect that is analysed. If not accounted for this variation could result in non-detection of annual cycles or inconsistencies between individuals. This question was addressed in this study by adopting a two dimensional elemental mapping to investigate the distribution of the elements in the otolith. With this approach, the whole surface of the otolith is ablated through a series of successive single scans producing an elemental image of each transverse section. The ablation was performed at 200 Hz with a 13 µm beam diameter.

We tested different laser plating speeds to optimize the spatial resolution given by the final pixel size : 13 individuals were analysed with a 18 µm.s⁻¹ speed resulting in a 40 µm² pixel, 6 otoliths with a 10 µm.s⁻¹ speed (20 µm² pixel) and one with a 15 µm.s⁻¹ speed (30 µm² pixel). The surface of each section was cleaned prior to the analysis using a 9KHz and 5 mm.s⁻¹ ablation. The analysis of two certified reference glasses NIST612 and NIST610 (National Institute of Standards and Technology, USA) ensured accurate analysis. Calcium was used as an internal standard to account for any variation in the amount of ablated material and laser energy in the ablation yield. Analytical accuracy was measured with the fish certified otolith reference material FEBS-1 (National Research Council Canada, Canada). Ten isotopes, that are known to be detectable in otoliths and that have been reported to show seasonal trends or be under physiological control, were selected for analysis (⁷Li, ²³Na, ²⁵Mg, ³¹P, ³⁹K, ⁵⁵Mn, ⁶³Cu, ⁸⁵Rb, ⁸⁸Sr, ¹³⁸Ba, ⁴³Ca; see Annex 3 for glossary of isotope names). The distribution of ⁶⁶Zn, ⁸⁹Y and ¹³⁹La was examined in at least one individual but as these three isotopes were below the detection limits, they were not analysed in the remaining samples. The average detection limits were calculated on three standard deviations of the blank gas: ⁷Li: 48.7 ng.g⁻¹, ²³Na: 2826.6 ng.g⁻¹, ²⁵Mg: 23.7 ng.g⁻¹, ³¹P: 502.7 ng.g⁻¹, ³⁹K: 160.2

⁴ <https://www.ices.dk/marine-data/tools/Pages/smartdots.aspx>

ng.g⁻¹, ⁵⁵Mn: 25.9 ng.g⁻¹, ⁶³Cu: 21.5 ng.g⁻¹, ⁸⁵Rb: 14.1 ng.g⁻¹, ⁸⁸Sr: 20.3 ng.g⁻¹, ¹³⁸Ba: 2.6 ng.g⁻¹. Accepted recovery of reference materials ranged from 93% to 110%. Element compositions were expressed as mass elemental ratios (element:Ca) on the basis of the stoichiometry of Ca carbonate (380,000 µgCa.g⁻¹ otolith) (Campana, 1999). Data were processed using a VBA Macro and exported to ImageJ software (NIH, <http://rsb.info.nih.gov>) to generate images of element:Ca ratios.

3.1.8 Analysis of anglerfish otoliths and illicia using Laser ICPMS

The laser-ICPMS analysis of anglerfish otoliths and illicia was carried out at the Universidade de A Coruña using a CETAC Laser Ablation System LSX-213 G2+ coupled to a THERMO-FINNIGAN ICPMS Element XR. Prior to analysis samples were decontaminated by sonication in MilliQ water for 1min followed by soaking in 5% HNO₃ Suprapur for 15sec, and final sonication in MilliQ bath for 1 minute.

Analytical standards used in the analysis were NIST614, NIST616 (for otoliths and illicia) FEBS-1, NIES-22 (for otoliths only) and NIST1486 (for illicia only). In LA ICPMS analysis variability in the elemental signals can arise due to elemental fractionation, matrix effects and variation in ablation yield (Günther et al., 1999). To correct for this an element that is present at a known concentration within the sample can be used as an internal standard; concentrations of other elements are expressed relative to this standard. Calcium is present in otoliths at a reasonably consistent concentration of 38.8 wt% (Yoshinaga et al., 2000) and is therefore routinely used as an internal standard in LA ICPMS analysis of otoliths. In this analysis the minor isotope of calcium (⁴⁴Ca) provided the internal standard.

Two methods of data collection were employed in the pilot phase: spot transects and long lines. For the spot transects on the otoliths, a series of ablations of 40 µm diameter spaced 70 µm apart (centre to centre) were made along a transect with a scan speed of 10µm per second. On the illicia isolated spots of 25 µm diameter were ablated to align with putative growth marks. For the long lines a continuous scan was made across the section with a scan speed of 10 µm. The scan diameter was 40 µm on the otoliths and 25 µm on the illicia. In the main phase otoliths were analysed using long lines with a scan diameter of 50 µm.

In the pilot phase data were collected for: ²³Na, ²⁴Mg and ²⁶Mg, ²⁷Al; ³¹P, ³⁹K, ⁴⁴Ca, ⁵⁵Mn, ⁵⁶Fe, ⁶⁶Zn, ⁸⁸Sr, ¹³⁷Ba and ¹³⁸ Ba. Based on the results of the pilot phase (see section 4.1) the main phase analysis was restricted to ²³Na and ⁸⁸Sr.

Prior to statistical analysis the data were processed using Iolite software and quality controlled using established ICPMS data handling protocols at IMEDEA.

3.1.9 Stable isotope analysis

IRMS analysis of anglerfish otoliths

During the pilot phase 20 anglerfish otoliths were analysed for stable isotopes at the Laboratory of Geological Mass Spectrometry, University of Bergen (<https://www.uib.no/en/geo/56320/gms-lab>). Otolith material was drilled at multiple points along a transect from the dorsal edge towards the otolith centre using a NewWave Research Micromill. Between 7 and 12 points were drilled on each otolith, depending on the size of the otolith. Otolith material from each drilling was transferred to a glass tube and then analysed for isotopic composition (δ18O and δ13C) using a Kiel IV Carbonate Device coupled to a Thermo Scientific MAT253Plus isotope ratio mass spectrometer. Isotope measurements were calibrated against certified standards (CM12 and NBS-18).

SIMS analysis of hake otoliths and anglerfish otoliths and illicia

As part of the main phase, otoliths (hake and anglerfish) and illicia (anglerfish) were analysed for δ18O at the NORDSIM laboratory in the Swedish Museum of Natural History in Stockholm, Sweden. This laboratory is equipped with a secondary ionisation mass spectrometer (SIMS) which can collect stable isotope data from calcified structures at a fine spatial resolution the instrument used for the analysis was CAMECA ims 1280 ion microprobe.

To prepare the otoliths and illicia for SIMS analysis, the samples were recast into a 60mm diameter epoxy mount with grains of a calcite standard for the otoliths and Durango calcite for the illicia. The mounts were repolished using 3µm and 1µm diamond solutions. To facilitate navigation during analysis, a tiled image of each mount was generated using the Olympus cellSens software. The mounts were coated with a layer of gold before analysis in the ion microprobe machine.

Oxygen isotope measurements were taken from 10µm spots with a distance of 35-40µm between spots. Sample analyses were performed in blocks of 6, bracketed by two analyses of the standards. The results were reported in per mil (‰) relative to the Vienna Standard Mean Ocean Water (V-SMOW) standard with a mean reproducibility of ± 0.22‰. A total of 1517 measurements (1285 samples and 232 standard) were completed.

After the analysis images of the analysed sections were inspected for the presence of cracks in the otolith surface that could interfere with the accuracy of the analysis. Data points that coincided with surface cracks were removed prior to analysis. Missing data points accounted for 1.8% of the data; this did not impact on the ability to detect seasonal signals. Images were also used to identify the exact location of the analytical transect on each section and to relate this to the position of OTC marks.

Three chemically tagged hake were at liberty for over 2.5 years. For these otoliths a core to edge transect of the entire life history was taken to maximise the amount of information obtained (Table 3). For the other fish, transects from c.a. 150µm before the OTC mark to the edge were analysed.

Core to edge transects were analysed for all of the anglerfish illicia and for 8 of the anglerfish otoliths. For the remaining anglerfish otoliths a transects from the edge to ~200-3000µm was analysed to capture the previous 2 years of growth.

TASK 3 DEVELOPMENT OF AN OBJECTIVE METHOD TO INTERPRET THE OBSERVED PATTERNS

3.1.10 Underlying assumptions

In order for chemical constituents of otoliths or illicia to provide a reliable indicator of age, their deposition must follow a regular seasonal cycle. Given the logistic nature of fish growth it is also expected that the space between annual oscillations will get progressively narrower from the core to the edge of the structure. Annual patterns in microchemistry should align with annual growth marks, and this characteristic has been used in previous studies to verify their periodicity in otoliths from cod (*Gadus morhua*) and Atlantic bluefin tuna (*Thunnus thynnus*) (Hüssy et al., 2015; Siskey et al., 2016). However, the growth marks in calcified structures from hake and anglerfish are highly variable and difficult to interpret and so might not necessarily show good alignment with annual microchemistry patterns. To be used in age determination, seasonal variation in microchemistry must be consistent across age groups, sexes and geographic areas. The variability that exists between individuals and life-history stages must not override or confound the annual pattern.

The objectives of this task were to test these basic assumptions of annual periodicity for each of the elements and isotopes analysed, and to develop the optimal analytical method for processing the data and extracting and analysing any annual signals that occur.

3.1.11 Reanalysis of hake data

Previously collected trace element and isotope data for hake were plotted to visualise relationships between elemental concentrations along otolith transects and opacity measurements, which reflect changes in the visual appearance of the otolith and may be related to growth. After detrending the data, peak detection algorithms and spectral analysis approaches (described in section 3.4.5) were used to identify features which may reflect annual periodicity.

3.1.12 Seasonal microchemistry patterns in tagged hake otoliths

The time between tagging and recapture (time at liberty) of the OTC marked hake ranged from 347-1555 days (Tables 2 and 3). Microchemistry profiles were plotted against distance along the core to edge transect and the position of the OTC mark was marked. Profiles were examined for the presence of peaks both visually and statistically and the timing of such features was determined by relating to the position of the OTC marks.

3.1.13 Seasonal variation in edge chemistry of anglerfish otoliths and illicia

Concentrations of elements and isotopes at the edge of the otoliths and illicia were compared between samples collected at different time points within an annual cycle (pilot phase: quarter 3, 2017-quarter 1, 2018; main phase: quarter 4, 2017 – quarter 3 2018)) using general linear models (GLMs) and generalised linear mixed models (GLMMs). Length category was included as a factor in the analyses. Variation was also examined between ICES divisions and between males and females. The best fitting models were selected using Akaike information criterion (AIC) and log likelihood tests.

The data were visualised and analysed to establish the seasonal timing of any microchemical peaks. For analysis of elements in otoliths, the rate of change in elemental concentration along a 500µm transect, from the edge towards the core was estimated from the slope of the element~distance relationship for each individual. The rate of change in elemental concentration between quarters was statistically tested using GLMs. Length category was included as a factor in the analyses and variation within ICES areas and between sexes was also investigated.

3.1.14 Comparison of methods for detecting cycles in microchemistry data

Microchemistry data from calcified structures is typically “noisy” with high levels and multiple sources of variation. Data taken from a growth transect across an otolith or illicium is effectively a time series. An important property of this time series is that the temporal resolution at which the response is recorded decreases with increasing distance from the origin (due to logistic growth of the fish). In addition, the temporal resolution at which the data is collected (the age of the fish at any point along the transect) is not known. This presents a challenge when using time series methods to analyse otolith profiles.

Several approaches were compared here. Performance was first evaluated within a simulation framework. The methods were then applied to real otolith microchemistry data from five Kattegat cod (*Gadhus morhua*) otoliths with clearly defined annual bands and to data from the anglerfish and hake otoliths. Microchemical data were detrended prior to analysis to remove ontogenetic trends and to homogenise the level of variability across the time series. Raw chemical signals were first transformed by taking the natural logarithm, and detrended using a low degree of freedom (<5) additive model. The residuals from this model provided the response variable for subsequent analyse.

The signal detection approaches included in the comparison were:

*Argmax peak detection algorithm*⁵

This algorithm searches for local maxima (or minima) in a smoothed time series. The degree to which the data is smoothed and the number of data points across which the algorithm searches for a maximum (searching window) is defined by the user and can vary the outcome. The searching window is chosen based on the resolution of the data and the expected length of a cycle. So for example, if it is known that 100 data points represent 1 year then a searching window of 100 data points would be appropriate for detecting an annual maximum.

⁵ https://rpubs.com/mengxu/peak_detection

Argmax peak detection algorithm with varying window

The above algorithm was modified to allow the width of the searching window to decrease with increasing distance along the transect to reflect the logistic nature of otolith growth (the number of data points within one year decreases as distance from the core increases).

Automatic multiscale-based peak detection (APMD)

The APMD algorithm is suitable for the detection of peaks in noisy periodic and quasi-periodic signals (Scholkmann et al., 2012). The resolution at which the algorithm searches for peaks is not defined by the user but is selected algorithmically based on the data and can vary across the time series based on properties of the data.

Spectral analysis

Spectral analysis methods can be used to detect periodic patterns in time series, to establish their frequency and to test their significance. In most applications of spectral analysis methods, the time interval over which data is collected is known (e.g. daily, monthly or annual data). An otolith microchemistry profile describes how the response (elemental concentration) varies with the size of the otolith. Otolith size is linearly proportional to fish length and both are related to the age of the fish (the time variable) via a logistic function. This is typically described by the Von Bertalanffy growth model. As part of the AHA project a novel approach to spectral analysis has been developed which incorporates the properties of the Von Bertalanffy growth function. Two modes of implementing the approach were explored:

Lomb Scargle periodogram with grid search for the time variable

The Lomb-Scargle periodogram approach (Lomb, 1976; Scargle, 1983) is a form of spectral analysis that has previously been applied to the analysis of age-related trends in otolith microchemistry (Siskey et al., 2016). The advantage of this method is that it can deal with data that is irregularly spaced and can accurately detect trends in the presence of noise (VanderPlas, 2017).

The Lomb Scargle periodogram uses a Fourier transform to decompose a noisy time series (e.g. a microchemistry profile) into its constituent frequencies and to estimate the power of each frequency.

In this implementation the time variable (t) is expressed according to a logistic function:

$$t = \frac{-\log\left(1 - \frac{l}{Linf}\right)}{K}$$

Where l is the back calculated length of the fish at each point on the otolith (estimated from the linear relationship between fish length and otolith radius). K and $Linf$ are the parameters of the logistic relationship between l and t . A matrix of potential values for K and $Linf$ is created. The Lomb Scargle function from the lomb package (Ruf, 1999) in R-3.6.1 is used to generate a periodogram for each combination of K and $Linf$ in the matrix and to identify for each the frequency with the highest power across a defined range of frequencies. From this, the combination of K and $Linf$ for which the frequency with maximum power is statistically significant and is closest to one year is identified.

The output includes:

- An estimate of age (t) at each point along the transect for the model selected values of K and $Linf$
- A periodogram showing the power of each scanned frequency or period and the threshold above which a frequency has significant power
- The signal, which has an annual periodicity (frequency = 1) and which can be overlaid on the original data

Exploratory von Bertalanffy chirp functions

A function or signal with increasing (or decreasing) frequency in time is referred to as a chirp function. Standard chirp functions include linear and exponential forms, where the frequency changes linearly or exponentially over time, respectively (Smith, 1997). Instead of assuming linearly or strictly exponentially changing frequencies, we developed a von Bertalanffy chirp function whereby the frequency is assumed to follow a von Bertalanffy form over back-calculated length (or the distance along the otolith).

Chirp function derivation:

Solving the von Bertalanffy growth equation for age gives:

$$a = t_0 - \ln\left(1 - \frac{l}{L_\infty}\right) / K \quad (1)$$

We use this to define the length-domain phase as a function of length

$$\phi(l) = \phi_0 + 2\pi\left(t_0 - \ln\left(1 - \frac{l}{L_\infty}\right) / K\right) \quad (2)$$

where we can use ϕ_0 (radians) to define the position of the peaks with respect to age, e.g., for a Jan 1st birthdate we set $\phi_0 = -\pi/2$ for a mid-year peak. The corresponding length-domain function (e.g., strontium) is given by

$$x(l) = \sin(\phi(l)) \quad (3)$$

where amplitudes and base-levels can be set accordingly. An example is shown in Figure 3.

Raw chemical signals were transformed by taking the natural logarithm, and detrended using a low degree of freedom (<5) additive model. We scaled the residuals from this model to range between [-1,1]. To these detrended scaled data we fit the von Bertalanffy chirp functions. As the model (Equation 3) is highly nonlinear in the parameters, we implemented a maximum likelihood fitting approach used a global optimisation routine based on differential evolution (Ardia et al., 2016), assuming normally distributed likelihood. The models were run until convergence, estimating all the parameters of the model and a residual error variance. The chirp function was applied to the known age cod data and the outputs compared to the Lomb Scargle implementation.

TASK 4 COMPARISON OF RESULTS FROM DIFFERENT STRUCTURES IN ANGLERFISH

In the pilot phase of the analysis otoliths and illicia from the same fish were analysed and the occurrence of potentially annual signals in both structures was evaluated. Age readings from illicia and otoliths obtained via the ageing exchange allowed for comparison of chemically and visually derived age estimates.

The linear relationships between fish size and otolith radius and between fish size and illicia diameter were established based on measurements of images taken from each structure. This proportionality made it possible to identify the point on a growth transect in one structure that is equivalent to a point on the growth transect in the other. For example, if an annual feature is identified in a microchemistry profile from an otolith and occurs at a point 500 μ m from the core along a transect of 1000 μ m then this feature can be related to a growth feature that occurs half way along a core to edge transect on an illicium.

TASK 5 Development of growth models

3.1.15 Estimating age of chemically tagged hake using the modified Lomb Scargle periodogram

Length back-calculation

Fish length at each point on the hake otolith core to edge transects was estimated using the biological intercept method which is a linear regression with a biologically determined intercept (Campana, 1990). According to the biological intercept equation:

$$L_a = L_c + (O_a - O_c)(L_c - L_i)(O_c - O_i)^{-1}$$

Where L_a and O_a are respectively the fish and otolith size at point a on the transect, L_c and O_c are respectively the fish size and otolith size at capture and L_i and O_i are respectively the fish and otolith size at the biological intercept.

For the portion of the transect from the edge to the OTC mark the fish length and otolith size at the time of release provided the biological intercept parameters. For the portion from the OTC mark to the core the theoretical sizes of the fish and otolith at hatching (Palomera et al 2005) were used to estimate the intercept.

Processing of elemental signals

The modified Lomb Scargle approach described in section 3 was used to detect cycles in otolith profiles of phosphorous (^{31}P) which showed the strongest visual evidence of fluctuations. The range of Von Bertalanffy parameters for the grid search were set to $Linf=100-200$ and $K = 0.1-0.3$. The model output included an estimated age at each point on the otolith transects. From this the number of days between the OTC mark (time of tagging) and the otolith edge (time of recapture) was estimated for each fish and compared to the actual number of days at liberty to evaluate accuracy. The precision of the method was assessed by comparing age estimates obtained from two transects (proximal and distal) on the same otolith. Size at age in each year prior to tagging was also estimated from the back-calculated growth curves. These estimates were compared to mean size at age estimated the current growth model that is currently used in the stock assessment ($Linf=130$ cm, $K = 0.177$, length at age 0.75=15.84; ICES, 2013).

3.1.16 Estimation of anglerfish age using the modified Lomb Scargle periodogram

The modified Lomb Scargle approach was applied to strontium profiles from anglerfish otoliths. The range of Von Bertalanffy parameters for the grid search were set to $Linf=150-250$ and $K = 0.06-0.15$. The algorithm was applied to each individual and the outputs were examined (see example in Figure 4). The age estimates were accepted if they met these criteria:

- The frequency of the annual signal coincided with a clear peak in the periodogram
- The power of the annual signal was statistically significant
- The annual signal followed the broad visual trends in the data

When one or more of these criteria were not met the procedure was run again for that individual with a narrower range of Von Bertalanffy parameters.

3.1.17 Back-calculation of individual growth curves for anglerfish

Radii and fish length measurements were log transformed and linear models were fit using GLMs (Figure 5). The coefficients and intercept from these models were used to back-calculate fish length at each point along the microchemistry profiles (S_i) using the body proportional hypothesis (BPH) model (Francis 1990)

$$\frac{a + bS_i}{a + bS_c} \times L_c$$

Where S_c is the radius of the structure at capture L_c is the fish length and capture and a and b are the intercept and slope of the regression of fish length on structure radius.

Age estimates at each point along each microchemistry profile were obtained using the modified Lomb Scargle approach. This provided a growth curve for each individual for comparison with length distributions from the surveys and the predictions of current growth models

3.1.18 Comparison of microchemistry based anglerfish age estimates with mixture model estimates

A detailed analysis of length frequency distributions of white anglerfish from 15 years of survey data from three vessels has been conducted as part of a separate study involving members of the AHA consortium (Batts et al 2019). This includes a modal progression analysis and calculation of cohort specific growth curves using hierarchical mixture models. This approach is used to split the length frequency distributions into pseudo age cohorts as part of the age-based stock assessment for anglerfish (ICES, 2018).

In this study individual age cohort assignments were compared to age estimates derived from otolith microchemistry. First, length frequency distributions were constructed using data from the Irish groundfish survey sourced via the ICES DATRAS database⁶. The mixture model (described in Batts et al 2019) was used to estimate the mean length and the standard deviation of each mode in the distribution. Next, the size of each anglerfish in mid-November in each year of its life was estimated from the individual back-calculated growth curves. Finally, the mixture model was used to estimate for each fish, the probability of it belonging to each component in the survey length frequency distribution for each year of its life. The fish was assigned to the component with the highest probability. These "pseudo age estimates" were compared to the microchemistry derived age estimates.

4 RESULTS

Pilot phase: elements and isotopes in hake otoliths and in anglerfish otoliths and illicia

The results from the pilot phase were used to determine the optimal design for the main phase. Decisions were made regarding the most suitable techniques for sample preparation and analysis.

4.1.1 Reanalysis of previously collected hake data

Profiles of ²³Na and ⁸⁸Sr taken from 23 hake otoliths using wavelength dispersive spectroscopy as part of previous projects⁷ are shown in Figures 6 and 7. Fluctuations in the elemental profiles did not appear to align with otolith opacity measurements. The Lomb Scargle peak detection algorithm was applied to each of the 23 time series. While some features were identified that were consistent with Von Bertalanffy assumptions, none were above the threshold for statistical significance. An example is presented in Figure 8

4.1.2 Optimising methodologies for analysing trace elemental profiles in hake otoliths

Magnesium (Mg/Ca and the isotopic ratio ²⁶/²⁴Mg) has been reported in several taxa as having a "clock-like" behaviour probably in relation with seasonal variation of metabolic activity (Limburg et al. 2018). This makes these element/isotopes, good candidates as potential chemical chronometers in hake otoliths. Before using them on a "routine"

⁶ <https://www.ices.dk/marine-data/data-portals/Pages/DATRAS.aspx>

⁷ OTOMIC FAIR CT**98**-4365; IBACS QLRT-**2001**-01610, IDEADOS CTM**2008**-0489-CO3; EU DGXIV-**96**-075; year of project initiation highlighted in bold

basis, we aimed at specifying the conditions of use, as Mg isotopes are known to be interfered by other chemical compounds.

As expected, tests showed that measurements of ^{24}Mg and ^{26}Mg isotopes were subject to interference under certain analytical conditions (at low resolution or with a quadrupole ICPMS). This may lead to misinterpretation of results. In contrast, ^{25}Mg is not affected by interference from other compounds and should be used preferentially as its natural abundance (10 %) is not significantly lower than that of ^{26}Mg . Trials also showed that, in medium resolution, both isotopes show a clear temporal pattern while the isotopic ratio $^{24}/^{26}\text{Mg}$ did not (Figure 9). This suggests that the isotopic ratio, when measured without interference, does not provide any information in terms of temporal pattern which is not in accordance with results previously reported based on measurement with quadrupole ICPMS (cf supra). On the basis of this trial, although we worked in medium resolution, we systematically used ^{25}Mg for subsequent analyses.

Asymmetry in trace element composition

The two-dimensional maps of chemical elements on otolith transverse sections highlighted a clear proximo-distal asymmetry for some elements such as Mg, Mn, P and K, with concentration gradient directions that varied depending on the analysed element (Figures 10 and 11). Chemical imaging also revealed that elements of group II such as strontium Sr and barium Ba were symmetrically distributed between proximal (sulcus) and distal (antisulcus) sides of the otolith (Figure 12).

Such characteristics were systematically observed regardless of the analysed sample and do not seem to be species specific as shown by some analyses made in the framework of a concomitant project on European sea bass (BARFRAY⁸).

The results of the asymmetry analysis highlight

- 1) the need for rigorous sampling strategies in order to avoid analytical biases when using otolith chemical signatures as proxies of fish life traits or environmental parameters,
- 2) the need for thorough analyses of analytical settings before comparing otolith signatures issued from different studies, and
- 3) the need for further research on otolith biomineralization mechanisms.

4.1.3 Trace element analysis of anglerfish otoliths and illicia using Laser ICPMS

Analytical conditions

In addition to ^{44}Ca , five trace elements were reliably and consistently detected in the otoliths: ^{23}Na , ^{24}Mg and ^{26}Mg , ^{39}K , ^{88}Sr , ^{138}Ba . In the illicia ^{23}Na , ^{24}Mg , ^{66}Zn , ^{88}Sr and ^{138}Ba were accurately measured.

Three spot sizes were tested for their suitability analysing illicia (10 μm , 25 μm , 40 μm). A spot size of 25 μm was considered optimal in terms of accuracy and spatial resolution.

Although line scans have lower analytical sensitivity than spot measurements they still provided reliable, accurate and precise data in this analysis. The advantage of this method is that it provides a continuous profile across the growth transect and regions of interest do not need to be identified *a priori*. This feature is useful when the structure does not contain clear annual growth bands that could be used to identify putative growth seasons along the transect. Data is collected at a higher spatial resolution than with spots, providing more detailed time series and increasing statistical power. This is of particular advantage in the analysis of illicia; while the spot measurements provided 6 and 19 data points for a 30cm and 110cm fish respectively the line transects provided 30 and 184 data points for the same fish.

⁸ <https://wwz.ifremer.fr/bar/Projet-barfray/Description>

Variation in edge chemistry

Variation in otolith edge chemistry was detected across three elements: ^{23}Na , ^{39}K and ^{88}Sr . The best fitting (based on AIC values) GLMMs of elemental concentration included quarter, length category and their interaction. Fish collected in quarter 1 had higher concentrations of ^{88}Sr and lower concentrations of ^{23}Na in their otoliths than fish collected in quarter 3; the effect was more pronounced in fish from the smallest size category (<30cm). This indicates that these elements show seasonal trends that may have an environmental (e.g. related to temperature differences between quarters) or physiological basis (e.g. related to growth rate). For illicia, the models also indicated variation between quarters and an interaction between quarter and length category for ^{23}Na and ^{88}Sr . Although the AIC values indicated that the terms improved the fit of the models relative to the null model, Loglikelihood tests were not statistically significant. This likely reflects the small sample size of the pilot analysis. In addition, analysis of data from core to edge transects on illicia using GLMMs indicated that concentrations of ^{24}Mg , ^{66}Zn and ^{88}Sr varied between light and dark regions of the illicia. For ^{66}Zn and ^{88}Sr this effect was consistent across all length categories.

Patterns across transects

Elemental profiles across otolith and illicia core to edge transects were plotted and examined for the presence of peaks. A loess smoother was applied to emphasise broad trends. The argmax algorithm was used to identify peaks in the data. Scanning windows of 8 and 40 were used for the illicia and otoliths respectively. The purpose of this analysis was not to statistically test for the presence of peaks but to identify features in the data that would inform the design of the main phase of the analysis.

Peaks appeared reasonably consistently in otolith profiles of ^{88}Sr and in illicia profiles of ^{66}Zn . In the illicia the number of features was low, even in the largest fish (5 peaks in a 110cm fish). ^{88}Sr profiles were very variable but the number of peaks appeared to increase with size in a manner that was more consistent with expected growth patterns.

Peaks in the ^{66}Zn profiles did not consistently align with fluctuations in opacity across the transect (Figure 13).

Outcome of the pilot Laser ICPMS analysis

The analysis of illicia showed for the first time that trace elemental concentrations could be reliably determined and variation between groups could be detected. However, based on the appearance of the core to edge profiles it was concluded that the detection of annual signals, if they occur, would be difficult in larger slower growing fish due to the small size of the structure. Given their larger size, otoliths offered greater potential for consistently detecting annual patterns. Nonetheless, the otolith analysis also revealed variation between size classes that could potentially confound the detection of regular cycles. This could be tackled by detrending the data to remove ontogenetic variation. Longline scans were chosen as the most suitable analytical approach for the main phase due to their high spatial resolution. The elements that showed evidence of seasonal variation (^{23}Na , ^{39}K and ^{88}Sr) were prioritised for the main phase.

4.1.4 Anglerfish: stable isotope analysis using IRMS

Variation due to size, sex and season

No significant correlations between fish length and isotope concentrations were detected ($p > 0.05$). Analysis of the quarter 1 data revealed differences in $\delta^{13}\text{C}$ concentrations between males and females; the best fitting linear effects model of $\delta^{13}\text{C}$ concentrations included the fixed effect sex and the random effect *fish ID*. $\delta^{13}\text{C}$ concentrations were lower in males compared to females (Figure 14a). This analysis was based on data from 9 females and 5 males; the number of data points per individual ranged from 1 to 12.

There was no significant difference in $\delta^{18}\text{O}$ concentrations between males and females (collected in quarter 1); the addition of the sex term did not lower the AIC value relative to the null model (Figure 14b).

Levels of carbon and oxygen isotopes ($\delta^{13}\text{C}$ and $\delta^{18}\text{O}$) in the region corresponding to recent growth (the first 200 μm from the otolith edge) were compared between individuals from quarter 3 and quarter 1 using linear mixed effects models. *quarter* and *distance* (from otolith edge) were included as fixed effects and *fish ID* was included as a random effect to account for the non-independence of multiple measurements from the same otolith. The analysis showed that levels of the carbon isotope $\delta^{13}\text{C}$ were significantly lower in fish collected in quarter 3 compared to fish collected in quarter 1 ($p < 0.05$) (Figure 14c). The interaction between *quarter* and *distance* was also significant; the decrease in $\delta^{13}\text{C}$ from the otolith edge towards the centre of the otolith was more pronounced in fish collected in quarter 3 than quarter 1.

For the $\delta^{18}\text{O}$ concentrations, the model with the lowest AIC value included the terms *quarter*, *distance* and *fish ID*. However, the likelihood ratio test indicated that this model was not significantly different from the null model ($p = 0.051$). Plotted mean values did not indicate any marked differences in $\delta^{18}\text{O}$ values between fish from quarter 1 and quarter 3 (Figure 14d).

Trends in isotopic composition along otolith transects

Isotopic composition varied along the otolith transects, but not in a consistent fashion. Minima and maxima in $\delta^{13}\text{C}$ concentrations were apparent in some individuals but absent in others (Figure 15). $\delta^{18}\text{O}$ concentrations were highly variable, with little evidence of periodic fluctuation.

Outcome of the pilot stable isotope IRMS analysis

The need to microdrill the sample prior to analysis of stable isotopes made it difficult to isolate the region of interest at the otolith edge. This may explain why seasonal fluctuations in $\delta^{18}\text{O}$ (which reflects temperature variation) were not detected. While $\delta^{13}\text{C}$ did appear to vary seasonally, the level of variation was lower than that observed between males and females. Due to the complexities of sample preparation stable isotope analysis using IRMS is unlikely to provide a suitable method for microchemistry based age determination and so was not pursued further in the main phase of the analysis. Instead, oxygen stable isotope data were collected at a fine spatial resolution using SIMS.

Main phase: seasonal trends in elements and isotopes

4.1.5 Investigation of periodic signals in trace element profiles from chemically tagged hake

Elemental profiles were extracted from the 2D elemental maps using a protocol established as part of this project. Data were collected for: ^7Li ; ^{25}Mg ; ^{55}Mn ; ^{23}Na ; ^{31}P ; ^{85}Rb ; ^{88}Sr ; ^{138}Ba ; ^{63}Cu and ^{39}K . Clear signals are evident in these data, which can be related to annual cycles via the position of the OTC marks. An example is shown in Figure 16; the occurrence peaks in the elemental signal varies depending on the position of the transect, again highlighting the importance of consistency in this regard.

4.1.6 Analysis of oxygen stable isotope profiles from hake otoliths

The results of the SIMS oxygen isotope analysis are summarised in Table 7. The oxygen stable isotope profiles from otoliths of chemically tagged hake were analysed using the Lomb Scargle approach. There was some variation in relative $\delta^{18}\text{O}$ values across the transect from the OTC mark to the edge which indicates variation in the temperature of the surrounding water. However, the periodicity of the fluctuations did not correspond to the time at liberty and no clear annual or seasonal cycles were detected (see example in Figure 17).

4.1.7 Seasonal variation in trace elements at the edge of anglerfish otoliths

In the main phase core to edge profiles of ^{23}Na , and ^{88}Sr were obtained for 127 individuals, after data that did not pass quality control checks for accuracy and precision were discarded. For all individuals measurements of ^{39}K did not pass the quality control checks for accuracy and precision and were not included in the subsequent analysis.

The final dataset contained at least 30 individuals from each quarter and at least 21 individuals in each length category (Table 5). Although the number of individuals in some categories were low, particularly for the largest and smallest fish, the sample size was still sufficient to detect significant variation in elemental concentration between quarters and length categories.

Variation in mean standardised concentration of ^{88}Sr at the otolith edge (0-100 μm from the edge) was explained by quarter and length class (GLM, $p < 0.002$; $R^2 = 0.30$). Concentrations of ^{88}Sr were lower in samples collected in quarter 2 compared to quarters 1, 3 and 4. There was an increase in ^{88}Sr with fish length but no interaction between quarter and fish length (Figure 18).

Mean standardised concentration of ^{23}Na at the otolith edge varied significantly between quarters (GLM, $p < 0.04$; $R^2 = 0.04$) with no differences between length categories (Figure 18). Otolith edge ^{23}Na concentrations were higher in samples collected in quarter 3 compared to quarter 4.

Samples were collected from three broad regions: 7b-c; 7e-f and 7g,j,k. Only one region (7g,j,k) was sampled in all four quarters. In this area seasonal difference in ^{88}Sr at the otolith edge were less pronounced and not significant. Variation between length categories remained significant. A small but significant difference in otolith edge ^{23}Na concentrations was detected in area 7g,j,k.

In quarter 2 samples were collected from all four broad areas. In these samples regional variation occurred in otolith edge concentrations of ^{88}Sr ($p = 0.03$) and ^{23}Na ($p = 0.002$).

The rate of change in elemental concentration along the otolith transect from the edge towards the core (0-500 μm) was measured using the slope of a linear model describing the element~distance from edge relationship for each individual. The mean slope was negative and significantly lower in individuals collected in quarter 1 compared to quarters 2, 3 and 4 ($p = 0.01$). This suggest that in samples from quarter 1 ^{88}Sr concentrations decrease along the transect running from the otolith edge towards the core and that this decrease is more pronounced than in other seasons (Figure 18). No significant differences in slope were detected for ^{23}Na .

To visually examine temporal changes in ^{88}Sr at a finer scale, detrended ^{88}Sr values on the outer edge (50 μm) of the otolith were plotted against collection month and a loess smooth was fitted to the general trend. Contrary to the trends detected in the first 500 μm , edge concentrations of ^{88}Sr appeared to reach a peak in June. The nature of the relationship was reasonably consistent across length categories but was most pronounced in the smallest fish and least pronounced in the 42-52 cm size category (Figure 19).

Overall, the main phase LA ICPMS analysis confirmed that concentrations of ^{88}Sr and ^{23}Na in anglerfish otoliths show small but significant levels of seasonal variation which may be indicative of an annual cycle that could support age determination. Patterns varied between size categories and areas and the timing of seasonal peaks was not certain but the evidence suggested that ^{88}Sr reach a maximum in spring or summer.

4.1.8 Stable isotope profiles in otoliths and illicia of anglerfish

Oxygen isotope ($\delta^{18}\text{O}$) profiles in otoliths showed a high degree of variability between individuals and some featured large fluctuations. When profiles were examined across all individuals some general trends emerged; relative $\delta^{18}\text{O}$ appeared to rise from the edge towards the core in samples collected in quarter 3 and to fall in those collected in quarter 2 (Figure 20). No significant differences in $\delta^{18}\text{O}$ at the otolith edge were detected between quarters ($p > 0.05$).

Mean values of $\delta^{18}\text{O}$ at the edge of the illicia appeared to increase from quarter 1 to quarter 4 (Figure 21), however, there was no statistically significant difference in edge chemistry between quarters ($p = 0.37$). Individual core to edge transects showed no evidence of regular fluctuations in $\delta^{18}\text{O}$ that might be indicative of seasonal fluctuations in water temperature (Figure 22).

Comparison of peak detection approaches

4.1.9 Simulation outputs

Data were simulated to represent time series with peaks that occurred with random frequency and with varying numbers of peaks in each series. Four peak detection procedures were compared with this simulation framework:

- A loess smoother and argmax peak detection algorithm with a fixed window: 8 observations wide
- A loess smoother and argmax algorithm with a fixed window: 20 observations wide
- A loess smoother and argmax algorithm with a window that decreased exponentially as a function of distance along the transect
- Adaptive smoother and automatic peak detection algorithm (AMPD)

The results showed variation in accuracy between methods. The argmax algorithm tended to overestimate the number of peaks particularly when the true number of peaks was low, when time series were long and when the width of the window was fixed at 8 observations. The AMPD algorithm error showed less bias although it did tend to overestimate the number of peaks when the time series was long and the number of peaks was low (Figures 23 and 24).

4.1.10 Application to data from independently aged cod (*Gadus morhua*)

Phosphorous (^{31}P) profiles from five cod otoliths showed clear visual peaks which generally corresponded to age (all were determined to be 6 years old from counts of translucent bands). The minima generally aligned with the position of the translucent bands. These profiles were ideal for testing the performance of cycle detection methods as they were characteristic of otolith microchemistry data (unlike the simulated data) and the expected number of peaks could be independently determined. The basic argmax algorithm detected 7 peaks in 3 of these otolith profiles and 6 on the other two (Figure 25). Additional peaks which did not correspond to growth structures were generally detected towards the beginning of the transect.

4.1.11 Lomb Scargle age estimation

The modified Lomb Scargle approach was used to estimate age from each ^{31}P profile. In this case the length-otolith radius relationship was not known so the search range for *Linf* was set to reflect the maximum otolith size (6500-8000 μm). *K* was allowed to vary from 0.15 to 0.4.

Age was correctly estimated by the LS algorithm for 4 otoliths (age 6.25-6.75), the best fitting solution for the 5th produced an age of 7.25 years. For some otoliths the first solution was not the optimal (the extracted signal did not follow the clear visual peaks in the data). In these cases the annual signal was not the one with the maximum power. When the routine was rerun with a narrower range of searching values the annual signal was correctly identified. Where age not already known the first outputs would have been rejected due to poor fit to the data.

4.1.12 Estimation using the chirp function

Example fits to the cod data show variable performance reflecting both the model and the underlying data (Figure 27). For three of the five series the model captures the increasing frequency of the peaks well (IDs: k_04_1_01; k_14_2_3; k_17_1_2). For fish ID k_06_1_03 the model picks out only two peaks and attributes much of the observations to residual variability. While for fish ID k_06_1_02 to fit the peaks for lengths greater than 25cm the model fits two peaks between 10 and 25cm whereas only one appears in the data.

4.1.13 Age estimation of chemically tagged hake otoliths from phosphorous profiles

In the LA ICPMS data extracted from the 2D elemental maps, phosphorous concentrations showed consistent fluctuations that appeared to have an annual periodicity (as indicated by the OTC mark on the otolith). The data contained some very pronounced peaks as well as smaller scale fluctuations. When the Lomb Scargle method

was applied to these data, significant cycles were detected in all otoliths which were consistent with Von Bertalanffy growth. For some otoliths the detected cycles fit to broad visual trends in the data (e.g. Figure 28a) while in others sub-annual fluctuations that were not consistent with Von Bertalanffy growth were also apparent (e.g. Figure 28b). Although distal and proximal transects from the same otolith showed similar trends, some features were more apparent in transects from the proximal side compared to the distal side (Figure 28c).

4.1.14 Age estimation of anglerfish otoliths from strontium profiles

Otolith strontium (^{88}Sr) profiles showed the most promise as an indicator of age in anglerfish otoliths. The element varied seasonally at the edge of the otolith and cycles could be visually identified in core to edge transects. Nonetheless, the signals were much more variable than those observed in the otoliths of cod and peaks were less distinct. A lot of this variability was removed by detrending using a GAM smoother, however some high frequency fluctuations which were unlikely to reflect age remained. Using the Lomb Scargle approach putative annual signals which were consistent with Von Bertalanffy growth and which appeared to fit visible cycles in the data were extracted for 109 (86%) of the profiles examined. The remainder were rejected. The Lomb Scargle method could not extract annual signals for any of the fish less than 22cm in length (10 fish). This may be because these fish were less than one year old and did not contain a complete annual growth cycle in their otoliths. All of the detected annual signals were above the threshold for statistical significance. In some cases they were the dominant signal with the highest power on the periodogram. In other cases they were a secondary signal. For some individuals more than one solution met the criteria for selection. In these cases the periodogram showed two statistically significant adjacent peaks and two plausible estimates of age could be extracted from the data (see example in Figure 29).

4.1.15 Hake: accuracy and precision of microchemistry based age determination

Variation between transects

The age and growth estimates derived from otolith phosphorous profiles from chemically tagged hake otoliths varied between distal and proximal transects on the same otolith (Table 7) (average percent error = 10.1%, Coefficient of variation = 14.3%). There was no systematic bias between estimates from the proximal and distal transects (paired t-test, $p=0.3$).

Estimated versus observed growth rates

During the period at liberty, chemically tagged hake grew at a rate of 0.42 mm day⁻¹. Individual growth curves derived from the phosphorus signals produced a mean estimated growth rate of 0.38 mm day⁻¹ (Table 8). A paired t-test showed that the difference between observed and actual growth rates was not significant ($p=0.4$). The absolute error rate of the growth rate estimates ranged from 0 to 80%; the mean error rate was 23%.

Relationship between estimated age and length

Estimated total ages of the 14 chemically tagged hake that were aged using otolith microchemistry ranged from 2 to 4 years (average of two estimates per fish), 13 of the 14 were estimated to be under 4 years old. Mean back-calculated lengths at age 1, 2 and 3 were 19.4cm \pm 3.0cm, 35.4cm \pm 4.9cm and 39.5cm \pm 3.8cm, respectively. These estimates are based on a very small number of fish and can not be generalised to the population. However, they are reasonably consistent with the predicted mean length at age from the revised growth model for European hake (De Pontual et al 2013) that is used in the stock assessment ($L_{\infty} = 130$, $K=0.177$; $L_1=21.1$, $L_2=38.8$, $L_3=53.6$), with the exception of the largest size class. The results of this study show that the microchemistry method can be used to estimate recent growth rates with moderate accuracy (mean error 23%). Future work should focus on applying the approach to a larger sample size that is more representative of the population size structure; this would help to establish the extent of the divergence between the growth model used in

the stock assessment and microchemistry based age estimates. Anglerfish: comparative evaluation of microchemistry age estimates

Comparison with age estimates based on visual growth marks

Outputs from the Lomb Scargle routine included for each anglerfish, an estimate of total age at capture, an estimate of age at each point on the microchemistry transect and the corresponding back calculated length at each point on the transect. This data can be used to identify the position on the otolith growth trajectory corresponding to the end of each year. Although the microchemistry profiles from the illicia were not suitable for age estimation, the otolith microchemistry profiles can be related to features on the illicia by finding the equivalent proportional distances on the illicia transect (see example in Figure 30). This provides a useful framework for comparing the three age estimation techniques and potentially corroborating identified growth marks.

The results from the ageing exchange showed that the age estimates were highly variable between readers and between structures (Figure 31), as has been previously reported. The quality of the sections may have contributed to this as they were prepared for the purpose of microchemistry analysis rather than age determination. One expert reader deemed 25% of the illicia sections to be unreadable.

There was a notable bias between the age estimates obtained from illicia and microchemistry; the age estimates obtained from strontium profiles were consistently higher than those estimated from the interpretation of growth marks in the illicia provided by two of the readers. In the future, the sharing of images like the one presented in Figure 30 with expert readers will be useful for evaluating the relationship between putative annual features in strontium profiles and growth marks in illicia.

Comparison with length cohort assignments

Length distributions from the individual back-calculated growth curves were overlaid on the length frequency distributions from the Irish groundfish survey for the corresponding years (Figure 32). The anglerfish samples used in the study were stratified by length category and the size distribution is therefore not representative of the population. However, some correspondence between the progression of cohorts in the study samples and the survey samples is evident. For example, in 2017 the lengths of the smallest fish in the study sample overlap with the right tail of the first mode and the left tail in the second mode in the survey length distribution; in the previous year these fish overlap with the left tail of the first mode.

Fish assigned to each age class by the mixture model were generally larger than those assigned to the corresponding age class by the microchemistry method (Figure 33). This indicates that growth rates from the individual back calculated growth curves were lower than the growth rates indicated by the modal analysis of the survey data.

Each mixture assignment to an age class had an associated probability. For the smallest lengths (estimated age 0 according to microchemistry) the mean probability of assignment model to the first component of the mixture distribution was 1 as the values were from the extreme left or outside of the survey distribution. The group that were assigned to age-1 using microchemistry were assigned to age-0 by the mixture model with a mean probability of 0.8. The mixture model tended to assign fish to a lower age class than the microchemistry method but the certainty the assignments was low for age groups 3-7 (Figure 34).

The mean difference between the age estimates obtained from the two methods was 0.85 ± 0.08 . When the group assigned to age-0 by the microchemistry method were excluded the mean difference was $1.14 (\pm 0.09 \text{ 95\% confidence interval})$.

Comparison with published growth curves

The back-calculated length data together with the otolith chemistry derived age estimates provided a complete growth history for each fish that followed a typical Von Bertalanffy curve (Figure 35a). Sex was only recorded for a subset of the samples making statistical comparison between the sexes difficult. However, the plotted growth

histories indicated that the females in the sample grew faster than the males, as is consistent with current knowledge of the species (Figure 35b). The mean back-calculated lengths at age were consistently lower than the mean lengths at age predicted by published growth curves for the species (Table 9).

5 DISCUSSION AND CONCLUSIONS

The optimal approach to measuring annual cycles

This study has applied a wide range of approaches to the analysis and detection of age related microchemistry signals in hake and anglerfish. Laser ICPMS, operating at a fine spatial resolution (line scans or elemental mapping) appears to offer the optimal analytical method for measuring annual microchemistry cycles. By collecting data continuously (within the limits of machine speed), this approach ensures that peaks are recorded at a sufficiently high resolution to be detected and providing high statistical power compared to spot-based techniques. The data from previous projects that were reanalysed as part of this study were collected using spot based LA ICPMS analysis methods and showed no evidence of statistically significant annual cycles. Bulk analyses methods that require the desired portion of the otolith to be isolated prior to analysis using a micro drill do not have sufficiently high or precise spatial resolution to detect age related trends. SIMS provides a means of analysing stable isotopes at a relatively fine spatial resolution, without the need to drill the sample, and may provide sufficient data for detecting annual cycles in species that are exposed to strongly seasonal environments. However, LA ICPMS machines are more accessible for scientists in Europe, the sample preparation is more straightforward and the technique is less costly. It is recommended that in future investigations that aim to develop microchemistry based age estimation methods for other species, the collection of elemental data using LA ICPMS and the collection of data from line scans or elemental maps be prioritized.

Evidence for age related microchemistry trends

In anglerfish, strontium profiles in otoliths showed the strongest evidence of seasonal fluctuations. In hake, phosphorous signals were the most closely aligned with annual cycles, as indicated by overlaying the position of the OTC mark on the otolith chemistry profile. Cycles in both of these elements have been shown to be related to age cod (Hüssy et al., 2015) and Atlantic bluefin tuna (Siskey et al., 2016). The levels variation in edge chemistry between fish collected at different times of year were low and were also influenced by size and geographic location which could make the consistent detection of age related trends more difficult. Some of the peaks that occurred in the elemental data that were not consistent with Von Bertalanffy growth and sub-annual peaks were noted between the OTC mark and the edge of tagged hake otoliths. Estimates of accuracy and precision indicate that phosphorous cycles may provide a reasonable but not entirely accurate indicator of age for hake. As with any other ageing method estimates based on microchemistry are prone to error. The most useful application of the methods presented here is likely to be for corroborating other sources of data describing age and growth.

Strontium is present in high concentrations in the otolith relative to other trace elements and so is not analytically difficult to reliably detect. Strontium substitutes for calcium in the aragonite matrix of the otolith (Doubleday et al 2013) and its uptake is known to be temperature dependant in marine conditions (Arai et al 1996; Bath et al 2003). Seasonal peaks in otolith strontium have been reported in other species and have been associated with maturation and reproduction (Granzotto et al 2003; Clarke and Friedland 2004). It is therefore plausible that the features identified in the anglerfish otolith strontium profiles are related to seasonal change. However, in this study, the exact timing of the cycle was unclear; the statistical comparisons indicated that otolith strontium concentrations were lower in quarter two while plots of detrended strontium values indicated a peak occurred in June. While further work is needed to establish its timing and periodicity, strontium signals in otoliths are likely to provide a chemical marker of seasonal change that may be useful in age estimation.

As shown by the LA ICPMS analysis of the hake otoliths, several elements are unevenly distributed in the otolith. It is therefore important to consistently measure along the same transect (distal or proximal) when analysing microchemistry profiles in transverse sections. Despite the occurrence of asymmetry, similar elemental trends were detected along distal and proximal transects. The hake otolith analysis indicated that strontium is homogeneously distributed in the otolith and should therefore be less subject to variability between transects than heterogeneously distributed elements such as phosphorus. In the anglerfish analysis the otoliths were polished on the longitudinal plane; all of the transects were on the proximal side of the otolith so elemental measurements were not affected by proximal/distal asymmetry. However, some of the elements that were analysed here and that did not show evidence of annual cycles in anglerfish (e.g. phosphorus) might display different profiles if analysed on the distal plane. Further development of microchemistry based age determination methods for anglerfish could evaluate the effect of the sample preparation method (sectioning and polishing) on elemental profiles. The longitudinally polished sections used here were quite thick making it difficult to locate the otolith core and identify the primary growth axis in larger individuals. Due to time constraints it was not possible to test the suitability of different sectioning methods. Thin transverse section or a longitudinal section polished on both sides may be more suitable. It is recommended that this is considered in the future development of this method.

The optimal approach to detecting annual cycles

A novel approach was developed for detecting cycles in microchemistry data, which incorporates properties of Von Bertalanffy growth. This approach has distinct advantages over standard peak detection methods as it accounts for the fact that peaks will occur at a higher frequency (relative to transect length) towards the end of the transect due to logistic growth.

The Lomb Scargle periodogram performed well relative to other methods when applied to simulated data and could accurately recover annual signals from microchemistry profiles in otoliths from 6 year old cod. However, additional input from the user was required to find the optimal fits. The protocol presented here also requires a range of potential *Linf* and *K* parameters across which the model will search. This potentially introduces bias into the model and if growth is very different to the assumed possible range this will not be detected. The assessment of how well a putative annual signal from the periodogram fits the observations is subjective. When there are multiple adjacent peaks in the periodogram this makes it difficult to recover the true annual signal and could lead to ageing error. For 14% of the samples an annual signal that was consistent with Von Bertalanffy growth could not be recovered from the periodogram. This may reflect problems with sample preparation or may indicate individual variability in the occurrence of annual otolith strontium cycles. It also partly reflects the fact that annual cycles can not be detected in small fish that have not completed one year of growth; in that case individuals could be assigned to age-0 although that does introduce a degree of subjectivity.

As with any new technique, further development and refinement of the statistical approaches to age estimation presented here are needed. This could involve further refinement of the chirp function and testing of the von Bertalanffy assumption against other forms (constant, random, other growth model). For the errors, here they are assumed independent and identically distributed but an autocorrelated assumption is more likely to fit the data better.

While otolith chemistry profiles are effectively time series and can be analysed as such, ignoring the logistic properties of fish growth when detecting peaks can lead to errors, as was demonstrated by the comparison of statistical approaches in this study. Signal processing methods are increasingly being applied to the analysis of age and growth data; it is recommended that the biological properties underlying these data are considered in their analysis.

Insights into age and growth of hake and anglerfish

The microchemistry based growth estimates for hake varied between transects from the same otolith and were in some cases inaccurate. However, the mean growth estimates were reasonably consistent with the current growth model that informs the stock assessment, with the possible exception of the largest size class. This corroborates the existing evidence that the previous international ageing criteria for hake underestimated growth (de Pontual et al., 2006; Piñeiro et al., 2007; Mellon-Duval et al., 2010; de Pontual et al., 2013). If applied to a larger reference sample, the microchemistry method presented here could be used to comprehensively evaluate the accuracy of the current growth model and to assess variability in growth rates between the sexes and across years, information this is currently lacking from the stock assessment.

For anglerfish, growth rates estimated using microchemistry were consistently lower than estimates from the mixture model that is used to split the length frequency data into age cohorts prior to stock assessment. The latest anglerfish benchmark found that this approach is robust as the identified cohorts can be tracked in the frequency distribution across survey years (ICES, 2018). The discrepancy between the two methods may indicate that the microchemistry method overestimates age due to sub-annual patterns in the microchemistry data. Alternatively, the length splitting approach may underestimate age, possibly due to underrepresentation of small fish in the data and misidentification of the first component. It is recommended that the consequences of the second alternative for the stock estimates and biological reference points be investigated within a management strategy evaluation framework.

For white anglerfish in ICES Divisions 7b-k and 8a,b,d the length splitting approach currently supports a robust assessment and provides a more reliable alternative to direct ageing. Microchemistry based age estimation could complement this approach if used to quantify differences in growth between the sexes. The time at which the first annual signals appear in the otolith could be validated using otolith microstructure, which would help to confirm if the first component in the survey length frequency distribution is fully representative of the age-0 cohort. For black anglerfish and for other stocks of white anglerfish, which do not have an age structured assessment, microchemistry based age estimation, in combination with other direct ageing methods could be used to estimate growth parameters and to evaluate the accuracy of stock estimates and reference points. Given their biological similarity, it is likely that the microchemistry patterns observed in white anglerfish will be detectable in otoliths from black anglerfish and other stocks of white anglerfish. International tagging studies are recommended as a measure to improve knowledge of anglerfish growth (ICES, 2018). Where possible, these studies should incorporate chemical tagging using OTC or alizarine red (Do, et al 2006; Vigola, 1997). This would allow the accuracy of otolith microchemistry based age determination for anglerfish to be assessed.

Comparison with age readings from illicia and with the predictions from published growth models showed that age estimates from analysis of strontium profiles are high relative to other approaches. The deviation from current growth models may be partly explained by the fact that the length at age estimates use back-calculated data. It is well established that size selective fishing mortality can remove faster growing fish from the population and as a consequence back-calculated lengths-at-age, which are taken from the slower growing survivors, are lower than those observed in the stock (the Rosa Lee phenomenon, Lee 1912). The purpose of this study was to test and develop a range of microchemistry based age determination methods using fish from a broad size range and geographic area. An assessment of growth at the population level was beyond the study scope. Future application of microchemistry based age determination to anglerfish should expand the size of the study group so that growth can be estimated from age at capture as well as from back-calculated lengths and the effect of size selectivity assessed.

The statistical approach to identifying peaks in microchemistry data while accounting for Von Bertalanffy growth provides an alternative and an objective age-estimation method that could be used to corroborate age estimates based on the interpretation of growth marks in hake otoliths and in anglerfish otoliths and illicia. As demonstrated here, features on the otolith chemistry profiles can be aligned with corresponding visual

features on the otolith and on the illicia from the same fish. This provides a framework for comparing age estimates across readers and different methods, being useful for determining where discrepancies arise. The results of this project will be disseminated to ICES WGBIOP.

Conclusions and extent to which project objectives have been addressed

The project aimed to:

1. Analyse microchemistry patterns in otoliths and illicia of hake and anglerfish
2. Develop statistical approach for detecting seasonal patterns in microchemistry
3. Relate detected seasonal trends to visual growth marks and length distributions
4. Use available information to refine growth models for associated stocks

In relation to the first objective, the AHA project has demonstrated for the first time that otolith composition of anglerfish and hake varies seasonally and has identified the optimal methods for measuring age related microchemistry patterns in these stocks.

In line with objective 2, a novel statistical technique has been developed to process these time series while incorporating their biological properties. Strontium (anglerfish) and phosphorous (hake) profiles in otoliths show promise as indicators of age and provide some insight that can inform the assessment of the stocks.

To address objective three, an approach was developed to visually relate microchemistry patterns to the visual growth marks identified by expert readers on images of anglerfish otoliths and illicia; this provides a framework for corroborating direct age estimates using microchemistry based approaches. In addition, the comparison of anglerfish back-calculated lengths with the survey length distributions highlighted that the microchemistry based method of age estimation method underestimates growth relative to length cohort analysis. Future development microchemistry based age determination should be carried out in parallel with analysis of length frequencies and visual growth marks and could be achieved following the framework outlined here.

To address objective 4, the microchemistry based growth estimates for hake and anglerfish were compared to the current growth models used in stock assessment. For hake estimated back calculated lengths at age across the growth transect were reasonably consistent with the current growth model used in the stock assessment (with the possible exception of the larger size classes). The results corroborate existing evidence that the previous international ageing criteria underestimated growth rates. For anglerfish growth rates estimated using microchemistry were slower than those used in the stock assessment; it is recommended that the implications for stock assessment of possible growth over estimation be considered within a management strategy evaluation framework. However, further work is needed before evidence from microchemistry can be used to refine the growth models used in stock assessment as microchemistry methods may underestimate growth.

The application of microchemistry techniques to age determination is a relatively new technique; as these methods develop, rigorous testing and refinement are required and sources of error should be quantified. The microchemistry based age determination methods presented here are resource intensive and are unlikely to provide a routine method of age estimation. Nonetheless, they have practical application for corroborating other sources of data describing age and growth and for investigating variability in growth rates. It is recommended that the methods presented here be applied to a wider range of stocks (including black anglerfish) within a large sampling program that ensures full representation of size structure, maturity stages and sexes in the stocks of interest and that incorporates tag recapture. This would facilitate a comprehensive evaluation of growth rate variability, information that is currently lacking from the stock assessment and could support the refinement of existing growth models.

Table 1: Summary of the numbers of individuals, for hake and anglerfish, analysed in both pilot and main phase.

• Pilot phase					

			<ul style="list-style-type: none">• Main phase		

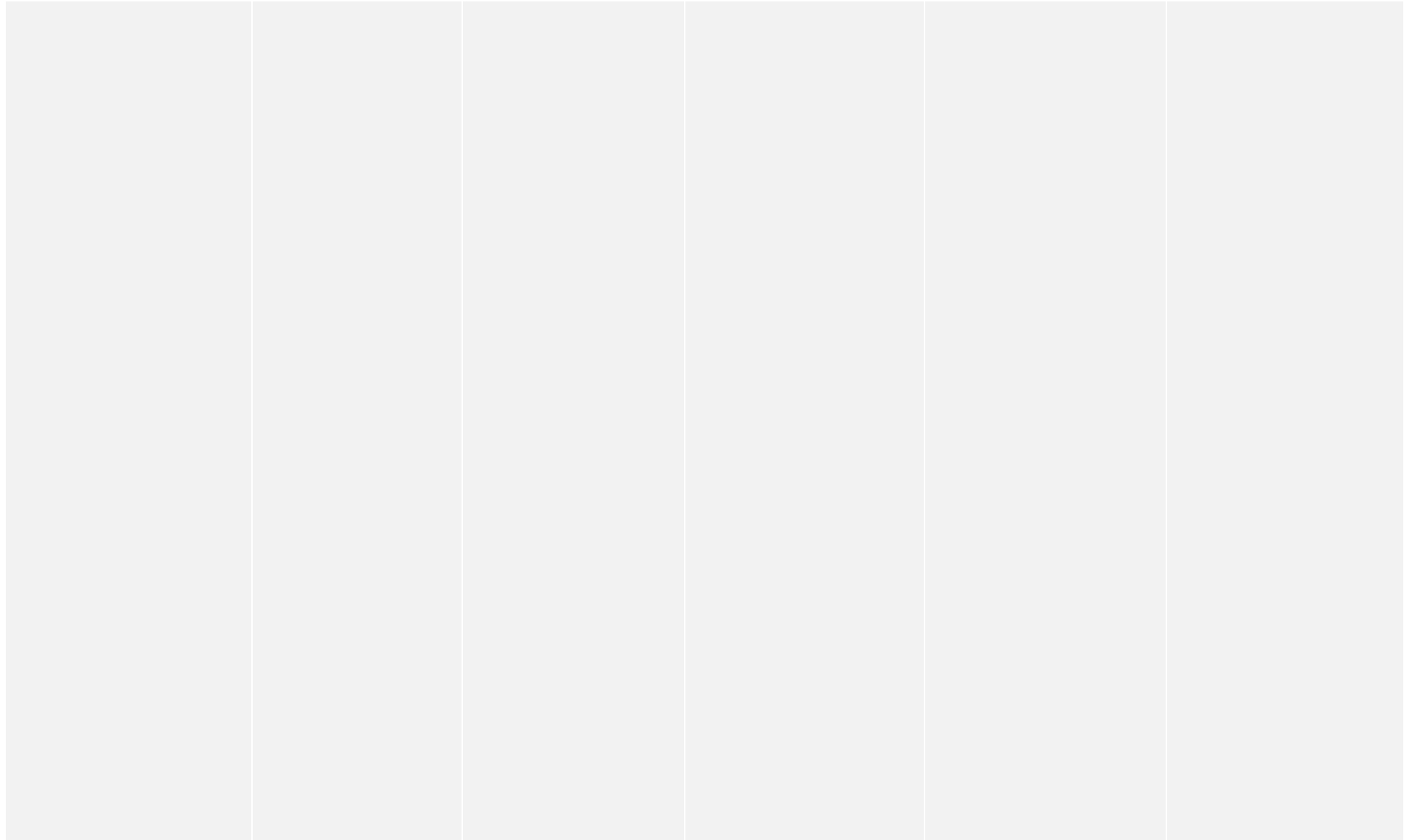


Table 2. Origin of hake otoliths used for the trace element analysis. Slide reference indicates that otolith had been prepared prior to the current project (see section 3.3.1). New preparations were made to complete the samples. Two otoliths (ID 8493 and ID 7521) did not show an OTC mark and date or length at recapture appeared to be misreported at the time of collection. For otolith 5154 the difference in size between the release and recapture dates indicated that the date of recapture had been misreported. These samples were excluded from further analysis.

Table 3. Tagged hake otoliths samples analysed with ion probe-SIMS. Four previously prepared samples were discarded because of the lack of the OTC mark. Instead, the most valuable samples were analysed from the core to edge (Core) rather than from the OTC tag to the edge (OTC). TL total length.

--	--	--	--	--	--	--

Table 4: Sample size used in the pilot phase (PP) and main phase (MP) of the anglerfish analysis. Sample number refers to number of individuals sampled by size category and quarter. In the pilot phase, otoliths and illicia from each individual were analysed using LA ICPMS and IRMS. In the main phase, the otoliths were analysed using LA-ICPMS and a subsample were analysed using SIMS. In the main phase illicia were imaged and ages were estimated by expert readers.

		• Size category (cm)							

Table 5: Numbers of anglerfish otoliths in each category included in the final analysis of the LA ICPMS data from the main phase after exclusion of unreliable data.

	• Size category (cm)				

Table 6. Summary of the results of $\delta^{18}\text{O}$ measured in otoliths of tagged hakes. Mean values represent the mean of all measurements obtained in each otolith. SD standard deviation. $\pm \%$: averaged precision i.e averaged the overall one sigma uncertainty on an analysis, which includes the within run uncertainty (std. error of the mean) and the standard deviation on the standards, propagated together. Note that this statistics come from data that still need to be validated.

[Redacted Table Header]						

Table 7: Age and growth estimates for chemically tagged hake, derived from otolith phosphorous profiles.

Table 8: Growth rates for chemically tagged hake calculated from measured body size at the time of tagging and recapture and estimated from the individual growth curves derived from otolith phosphorous signals.

--	--	--	--	--	--	--	--

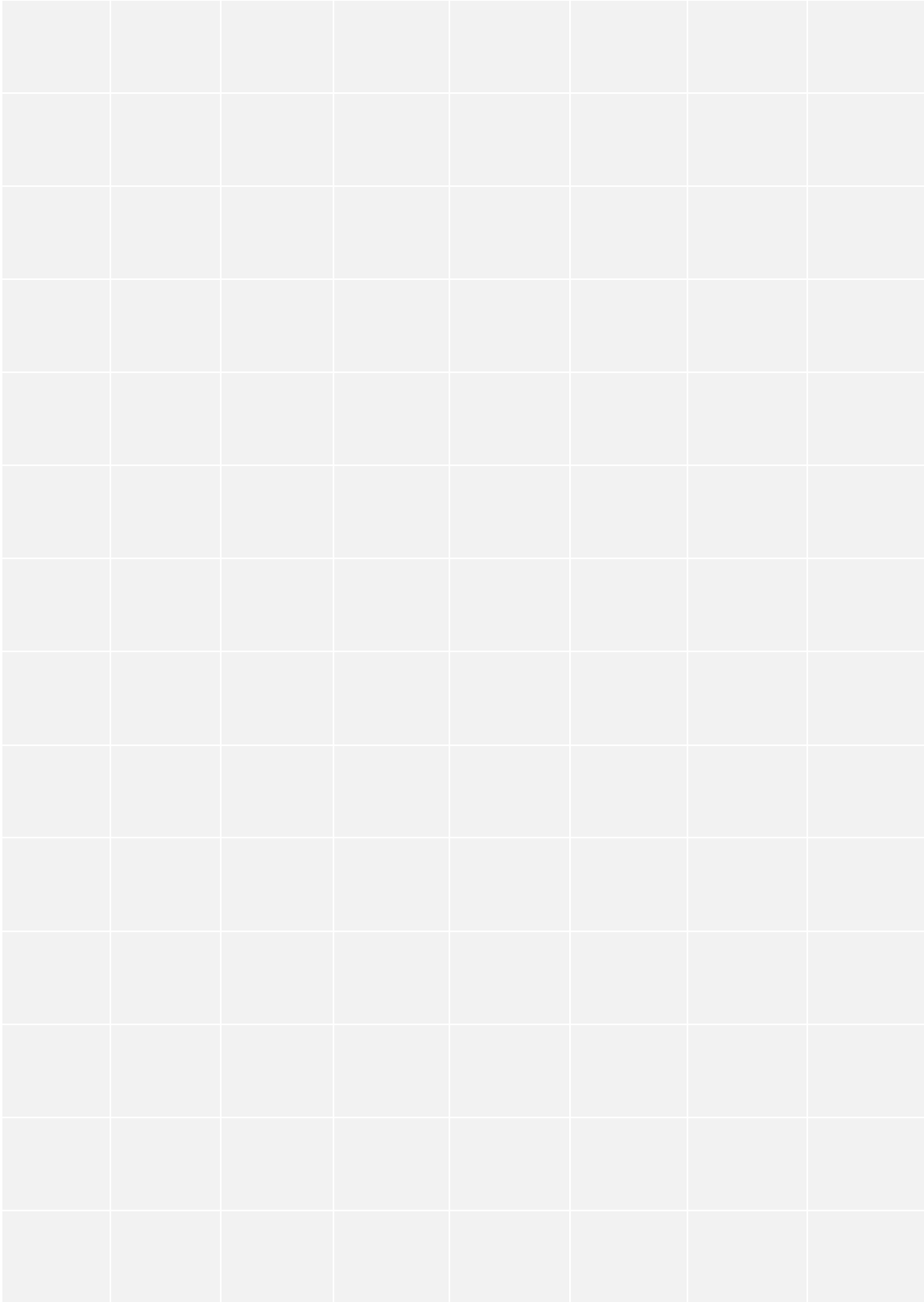


Table 9: Mean length at each age as estimated by back-calculation using peaks identified from strontium profiles in anglerfish otoliths compared to mean lengths at age estimated using two published growth models.

Age	Mean back-calculated length	sd	n	95% CI	Mean model estimated length at age	
					Batts et al. (2019)	Landa et al (2013)
1	13.3	3.7	109	0.4	20.8	24.9
2	25.2	6.7	106	0.7	37.3	36.5
3	33.5	8.1	71	1	52.5	47.1
4	42.2	10.9	39	1.7	66.3	56.8
5	52.8	14.3	22	3.1	79	65.7
6	60.3	14	9	4.7	90.6	73.8
7	80.3	15.3	3	8.9	101.2	81.3
8	88.3		1		110.9	88.1
9	95.5		1		119.8	94.4
10	102		1		127.9	100.1

Figure 1: Images of sectioned otoliths from collections of chemically tagged hake held by IFREMER. a) Fluorescence microscope image with the position of the chemical (OTC) mark indicated by a red arrow. b) Image showing the four growth transects along which otolith growth was measured (OTC mark to otolith edge).

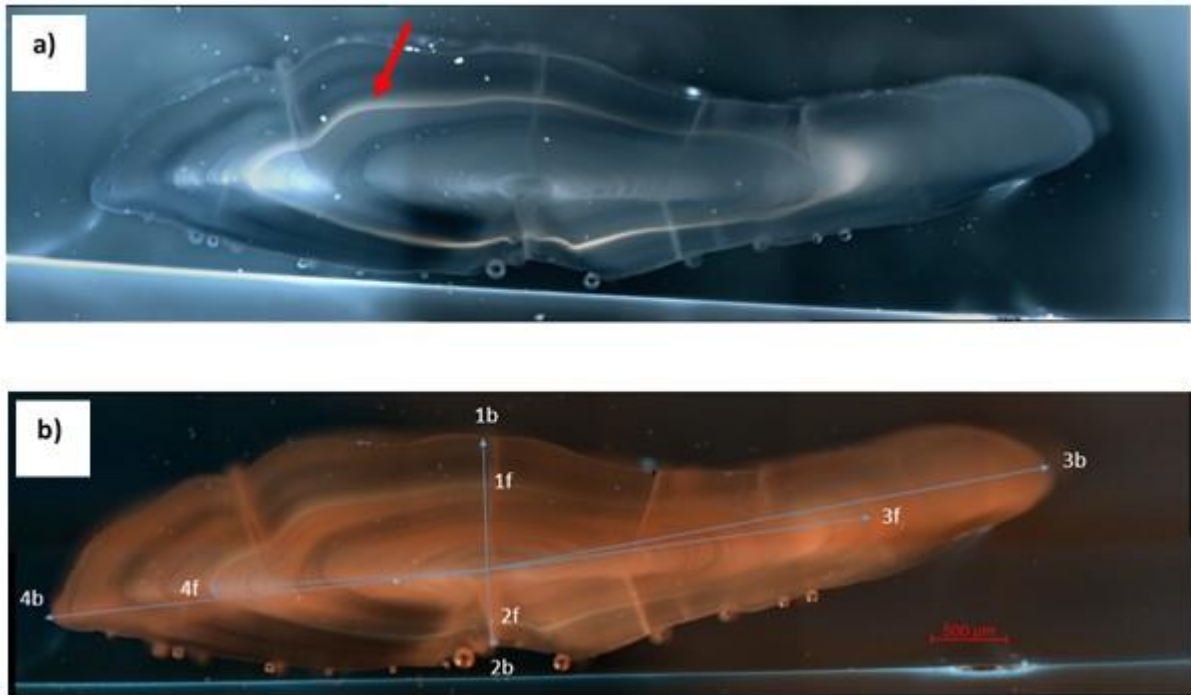


Figure 2: Image of an illicium (left) and an otolith (right) showing the axis that were measured for the construction of back calculation equations.

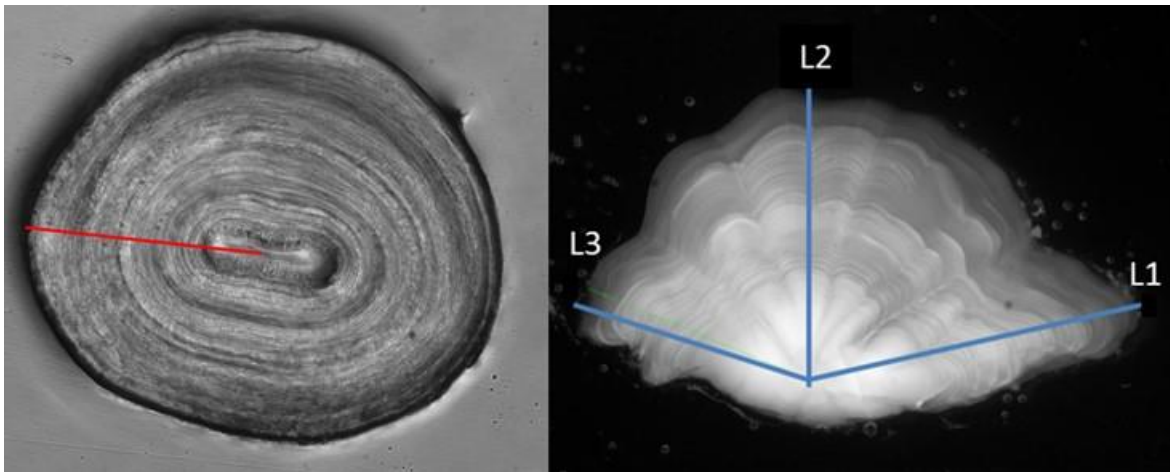


Figure 3: A vonBertalanffy chirp function with the phase given by the reverse von Bertalanffy function with ($L_{\infty} = 100, K = 0.2, t_0 = 0, \varphi_0 = -\pi/2$). X-axis is back-calculated fish length

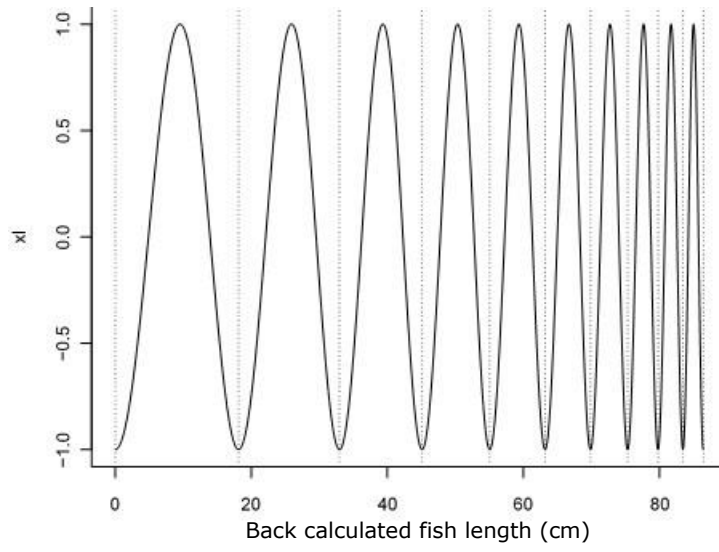


Figure 4: Example outputs from the modified Lomb Scargle method. The top panels show the detrended elemental data (blue points) with the putative annual signal extracted by the model overlaid (black line). The bottom panels show the periodogram with the period of the putative annual cycle indicated by the vertical line. The dashed horizontal line shows the threshold for statistical significance. In the example on the left one clear signal dominates the series and is easily isolated. In the middle plot the period of the selected signal does not coincide with a peak in the periodogram. The routine is repeated with a different range of parameters for the grid search. The results of this iteration are shown on the right; now the extracted signal aligns with the peak and the result is accepted. In this example (MP-Q2-9) there is a visible peak at the beginning of the time series and another just before estimated age 2; these features are not consistent with the constrains of the Von Betalanffy growth function that are incorporated into the signal detection process and are therefore not detected as part of the annual signal.

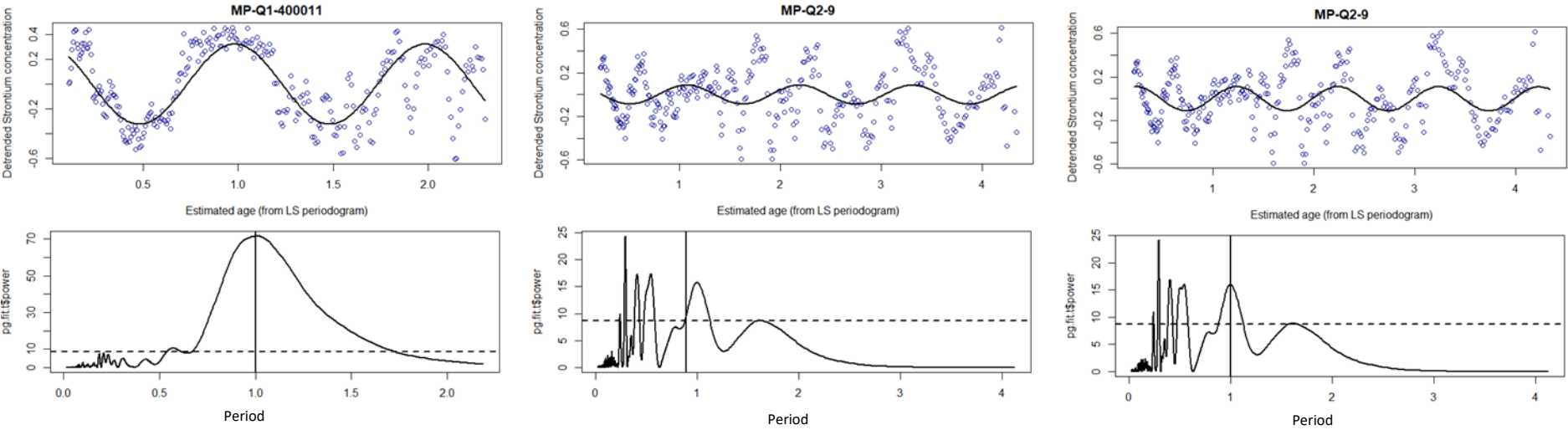


Figure 5: Plots of the linear relationships between otolith and illicia radii and fish length for anglerfish. L1, L2 and L3 refer the three axes that were measured in each otolith (depicted in Figure 2).

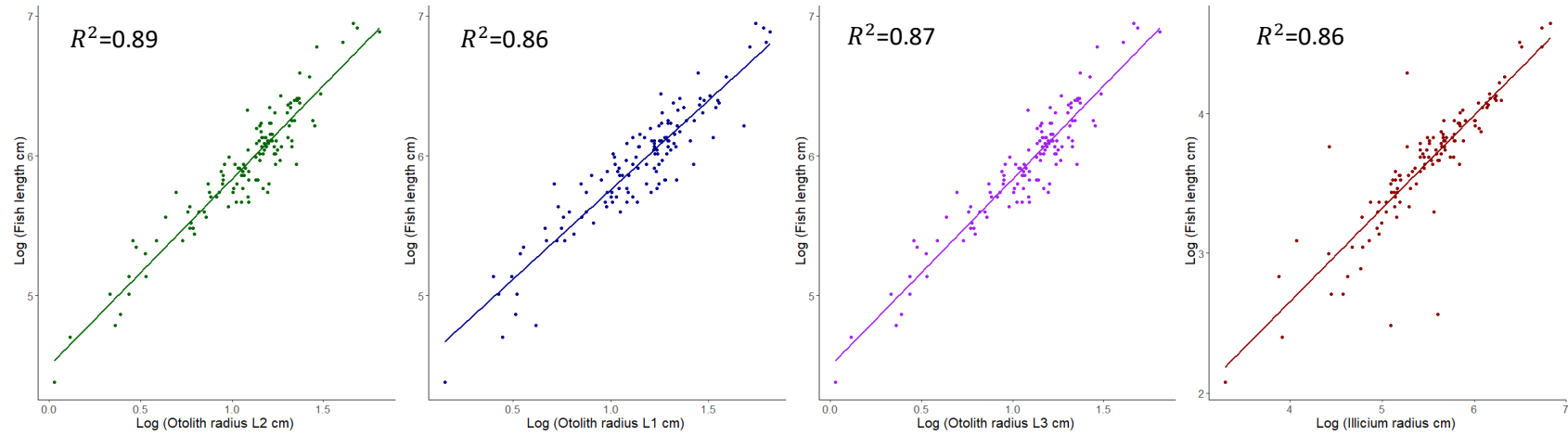


Figure 6: Strontium profiles from hake otoliths collected as part of previous projects (OTOMIC FAIR CT**98**-4365; IBACS QLRT-**2001**-01610, IDEADOS CTM**2008**-0489-CO3; EU DGXIV-**96**-075). Blue shaded areas indicate the locations of translucent areas on the otolith transects.

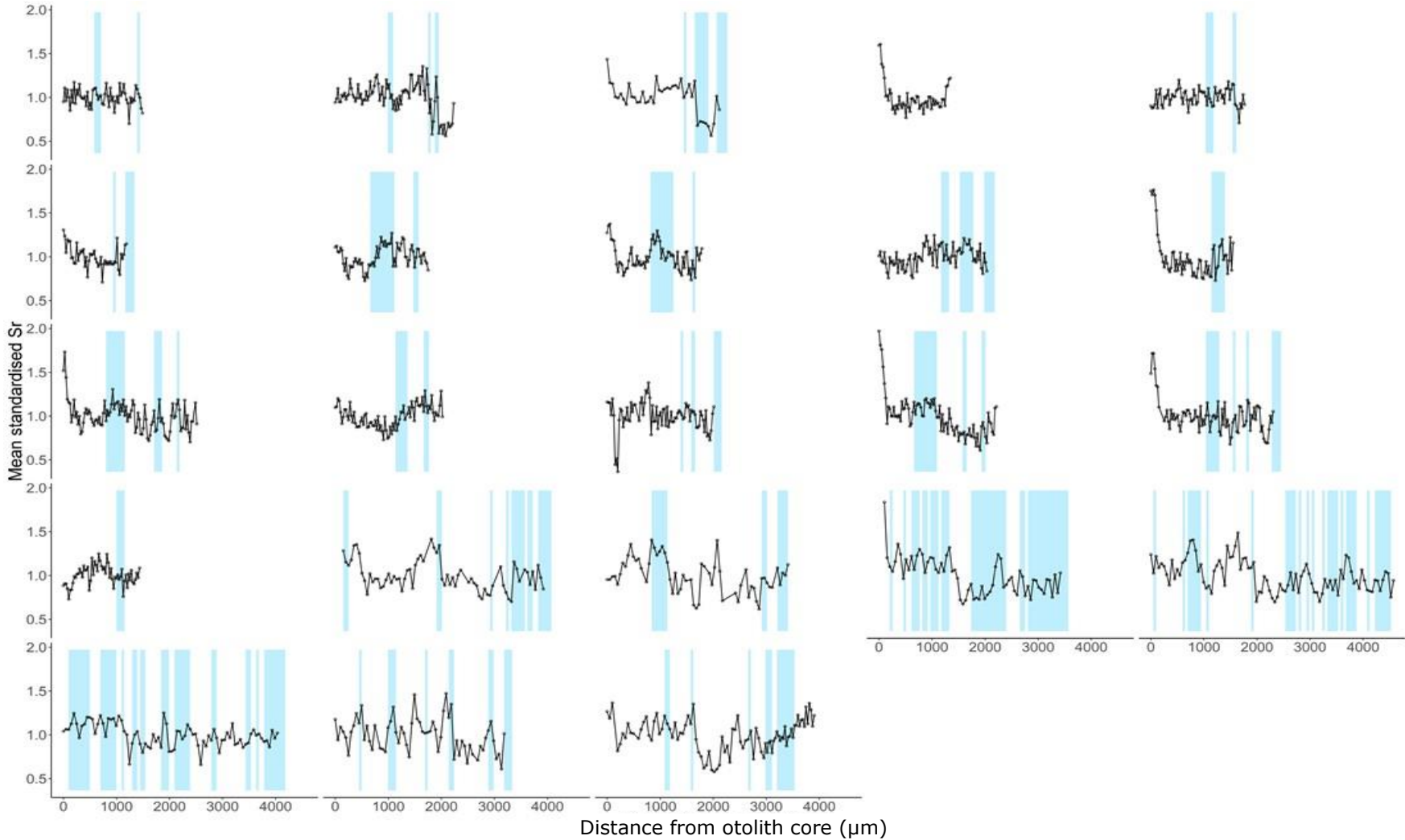


Figure 7: Sodium profiles from hake otoliths collected as part of previous projects OTOMIC FAIR CT**98**-4365; IBACS QLRT-**2001**-01610, IDEADOS CTM**2008**-0489-CO3; EU DGXIV-**96**-075. Blue shaded areas indicate the locations of translucent areas on the otolith transects

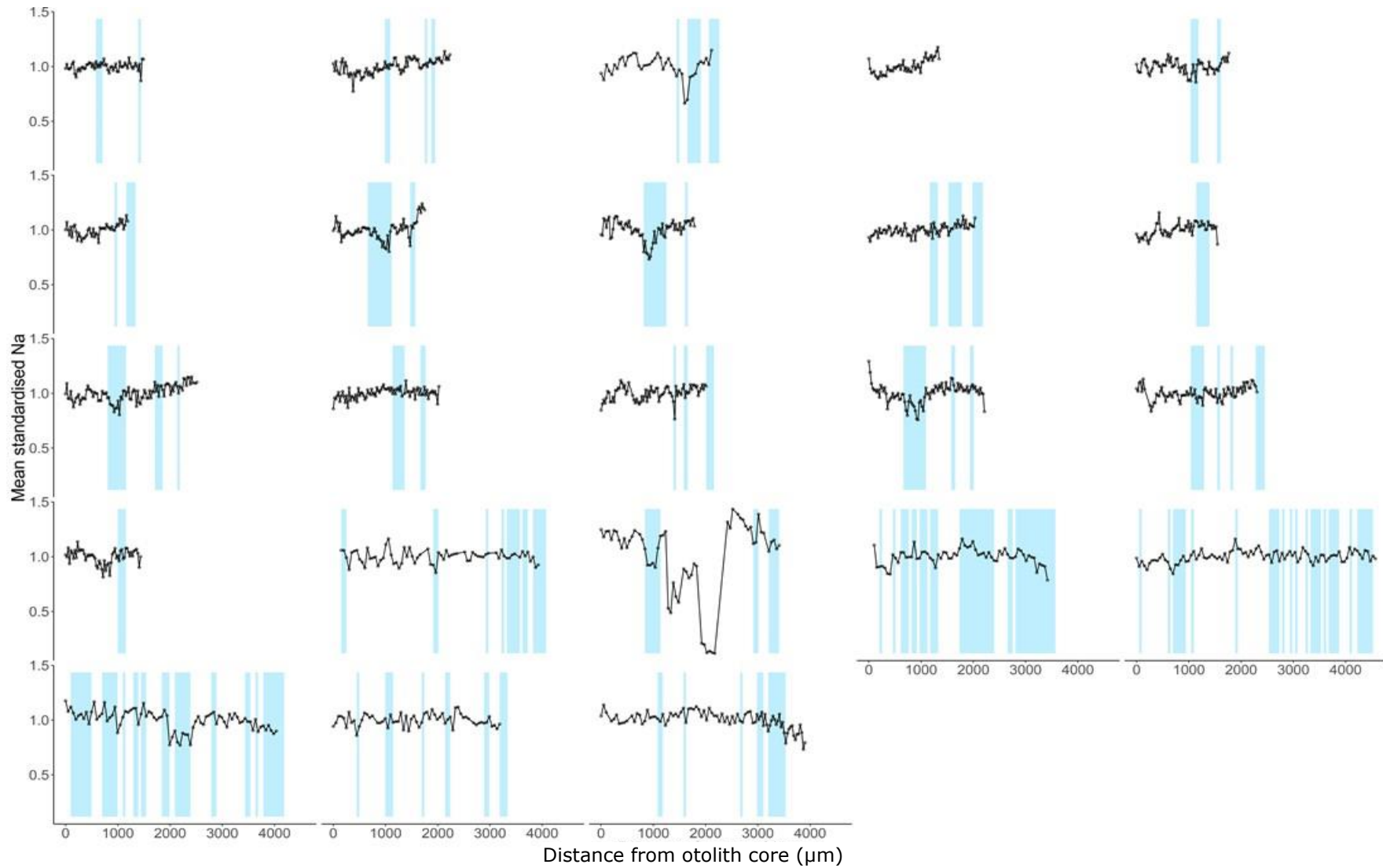


Figure 8: Results from a Lomb Scargle analysis of otolith chemistry profiles from a 70cm hake. The peak with annual periodicity is indicated with the vertical black line in the bottom panel; the normalised power falls below the significance threshold (horizontal dashed line). The detected signals are therefore not significant and not considered to be indicative of age.

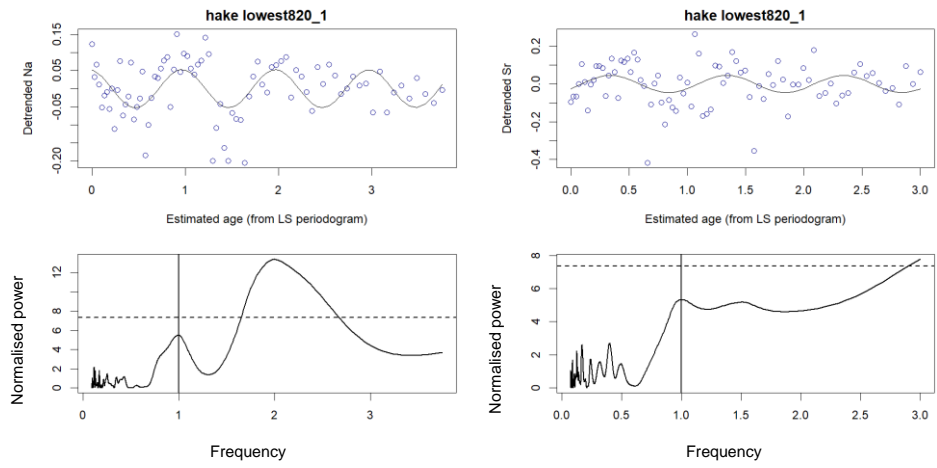


Figure 9: 2D mapping of ^{24}Mg and ^{26}Mg and the resulting isotopic ratio $^{24}/^{26}\text{Mg}$ from hake otoliths.

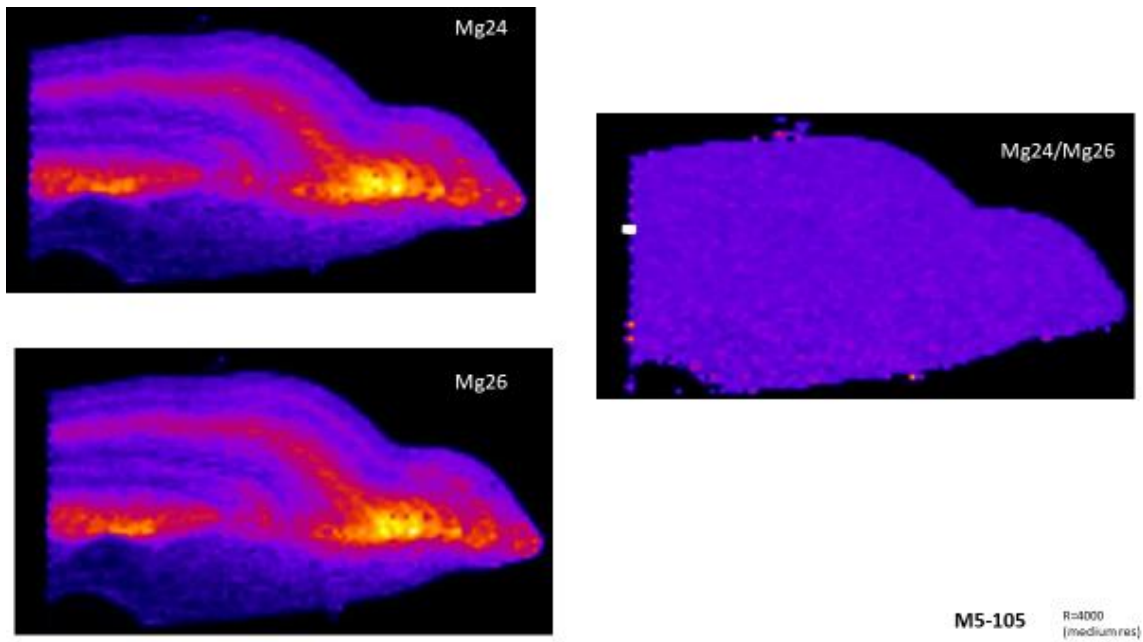


Figure 10: 2D mapping of $^{25}\text{Mg}/\text{Ca}$ (left) and $^{55}\text{Mn}/\text{Ca}$ (right) on M5-M123 hake otolith showing that concentrations of these two elements are much lower on the proximal side (sulcus) than on the distal side (anti sulcus).

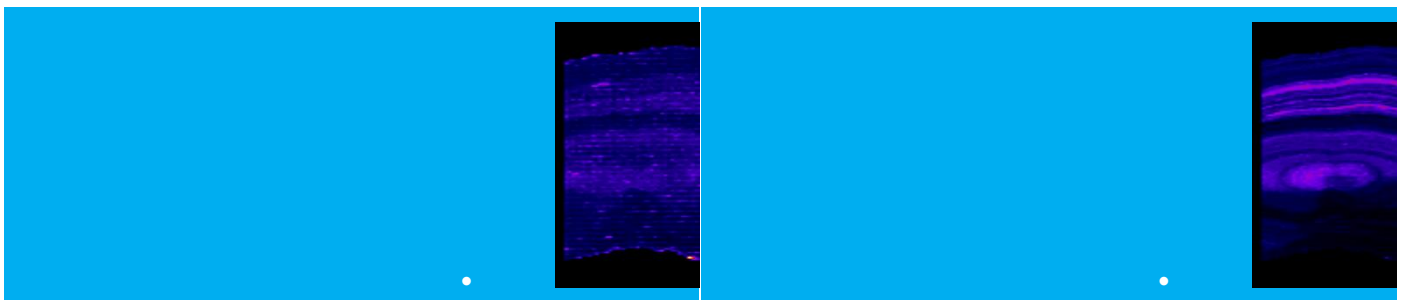


Figure 11. 2D mapping of $^{31}\text{P}/\text{Ca}$ (left) and $^{39}\text{K}/\text{Ca}$ (right) on M5-M123 hake otolith showing that concentrations of these two elements are much higher on the proximal side (sulcus) than on the distal side (anti sulcus).

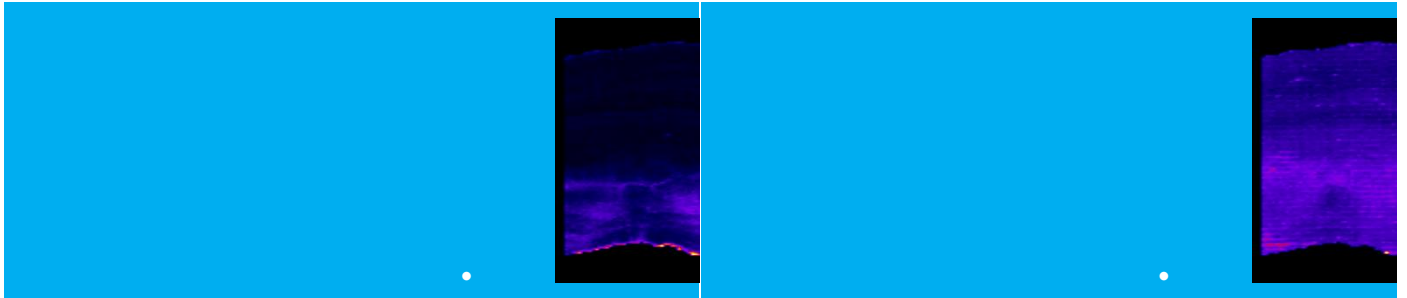


Figure 12. 2D mapping of $^{88}\text{Sr}/\text{Ca}$ (left) and $^{138}\text{Ba}/\text{Ca}$ (right) on M5-M123 hake otolith showing that concentrations of these two elements do not show any asymmetry.

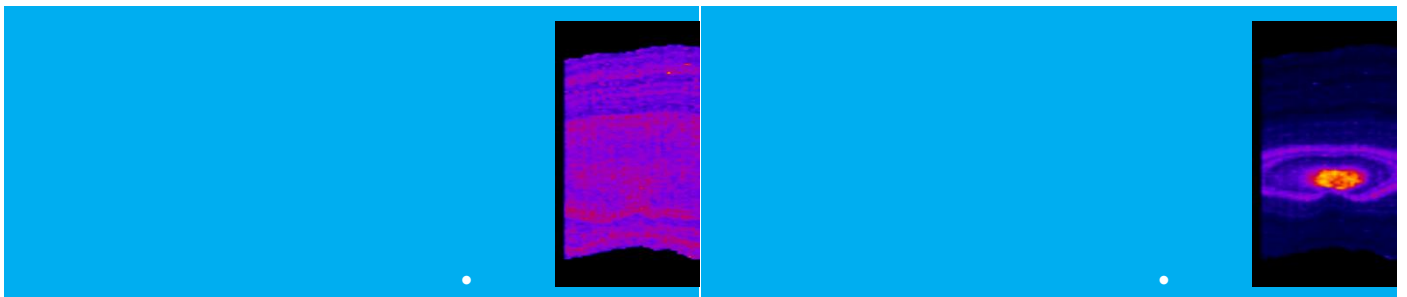


Figure 13: Plot showing relationships between zinc and opacity profiles in anglerfish illicia.

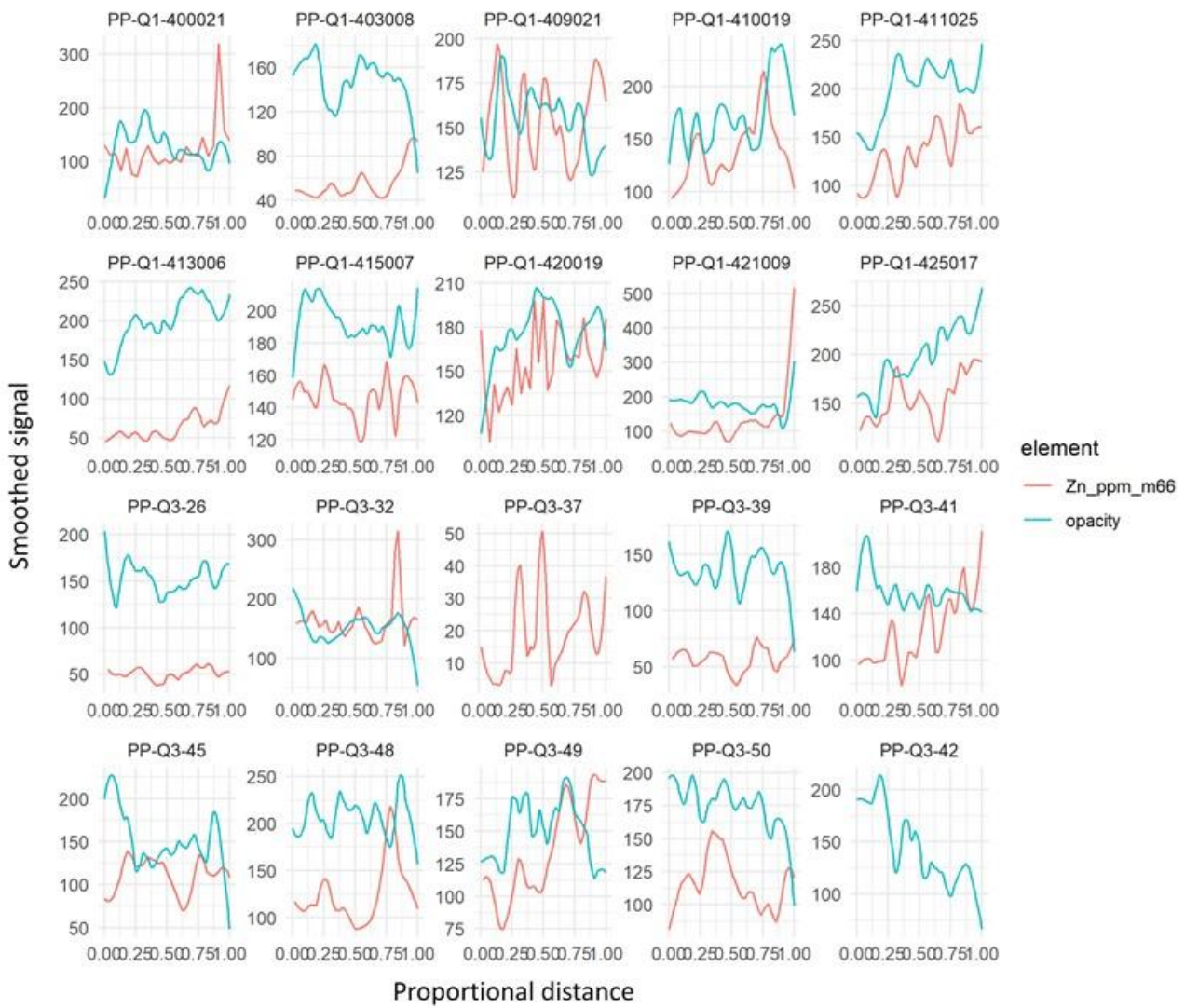


Figure 14: Boxplots showing the distribution of $\delta^{13}\text{C}$ (a and c) and $\delta^{18}\text{O}$ (b and d) concentrations at edge of anglerfish otoliths. Data for males and females are compared in plots a) and b) (quarter 1 data only). Data from fish collected in quarter 1 and quarter 2 are compared in plots b) and c). Medians are indicated by the dark line, the upper and lower edges of the boxes represent the 75th and 25th percentiles respectively, whiskers represent the data extremes.

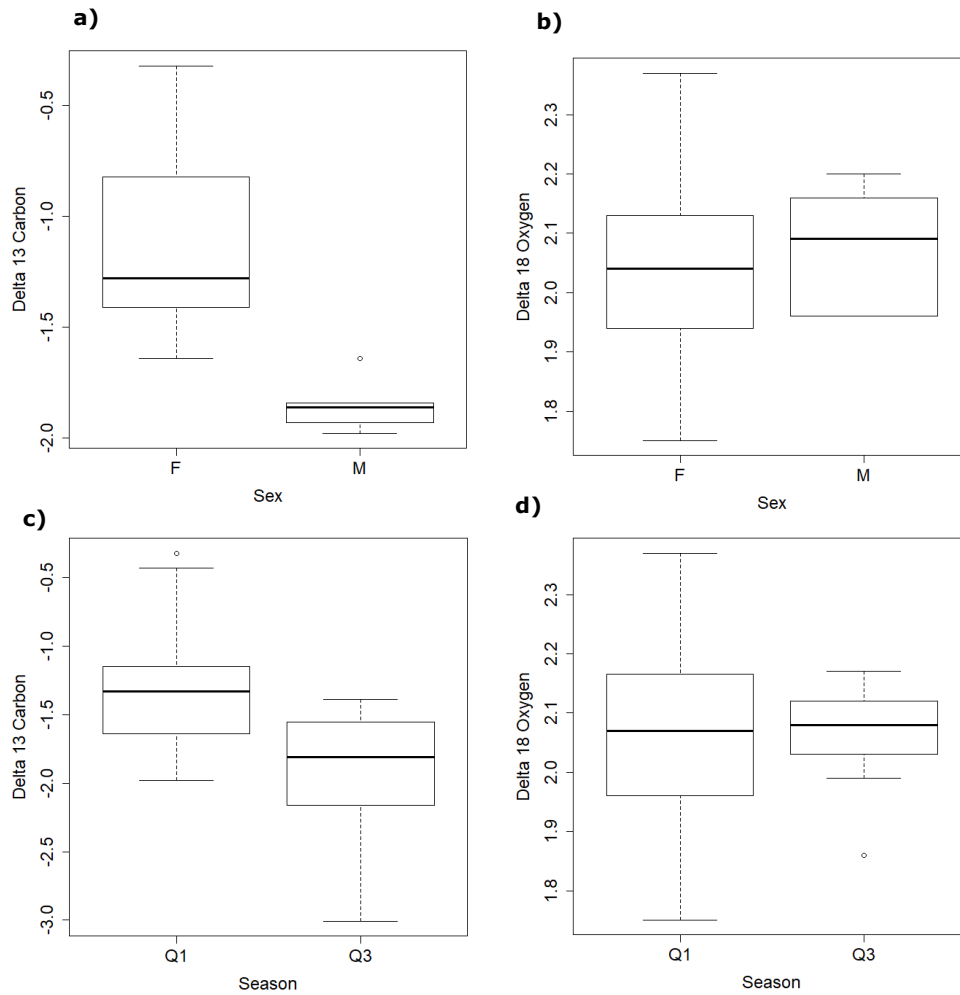


Figure 15: Example plots showing concentrations of $\delta^{13}\text{C}$ (left) and $\delta^{18}\text{O}$ (right) along anglerfish otolith transects. Data shown in the upper plot is from a fish collected in quarter 3 2017, data shown in the lower plot is from a fish collected in quarter 1 2018.

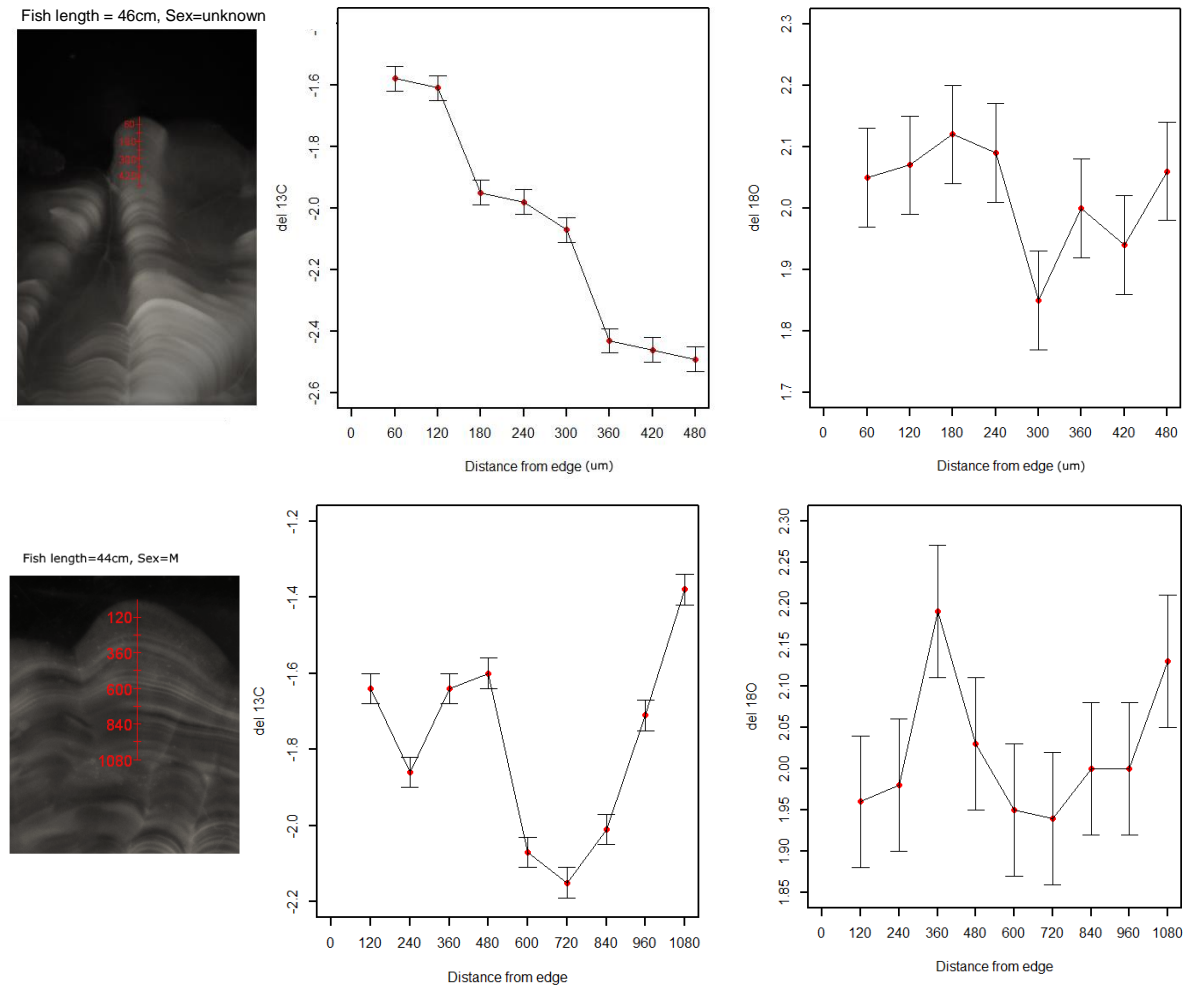


Figure 16: Concentration of Mn/Ca on M5M123 otolith. Transect extracted on the proximal side, OTC at 1576 μm (top left), transect extracted on the distal side, OTC at 1892 μm (top right), corresponding chemical image (bottom left).

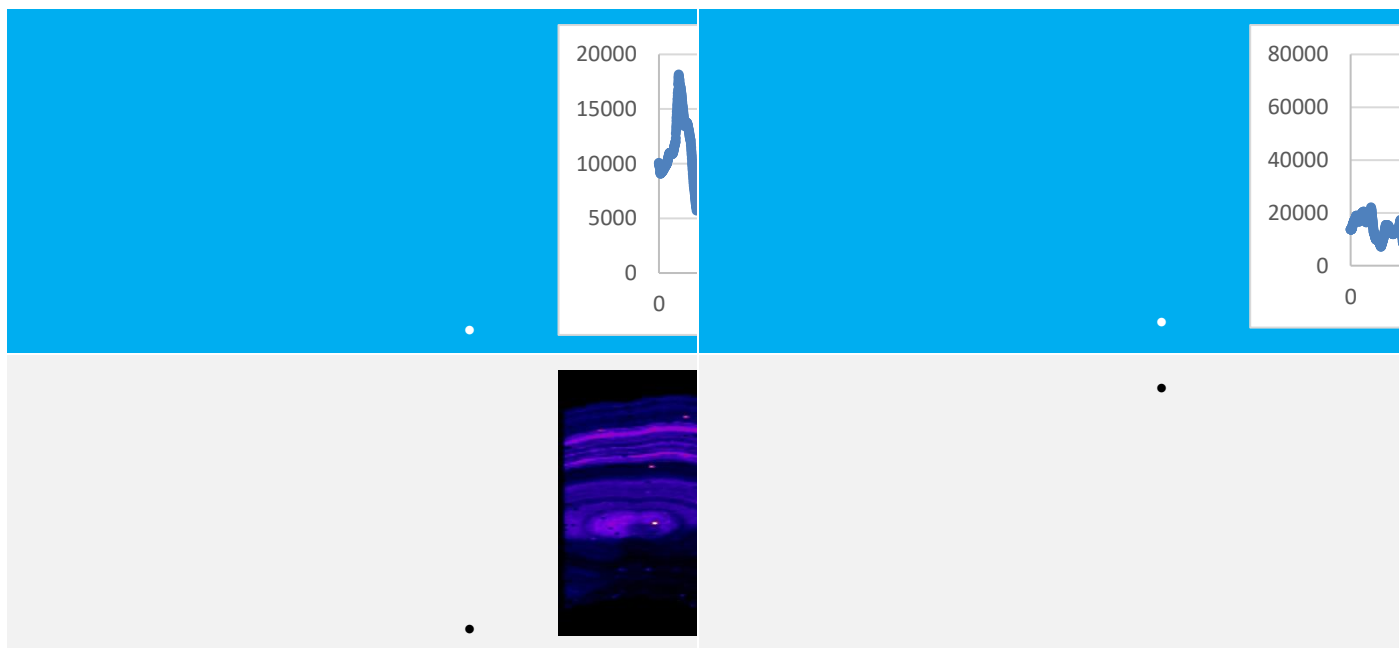


Figure 17: Example outputs from the Lomb Scargle analysis of oxygen stable isotope profiles from chemically tagged hake otoliths. The top panels show the detrended oxygen isotope data (blue points) with the dominant signal extracted by the model overlaid (black line). The point on the otolith corresponding to the time of tagging (OTC mark) is indicated with a vertical blue line. The time of recapture (otolith edge) is indicated with a vertical red line. The dates beside each line refer to the time of release and capture. The bottom panels show the periodogram with the period of the putative annual cycle indicated by the vertical line. The dashed horizontal line shows the threshold for statistical significance. In plot (a) almost three full cycles are completed within a period of just over 1 year while in plot (b) 1.5 cycles are completed within the 474 days of liberty. This shows that the fluctuations in oxygen stable isotopes do not show a regular seasonal or annual pattern. The detected signals are not statistically significant.

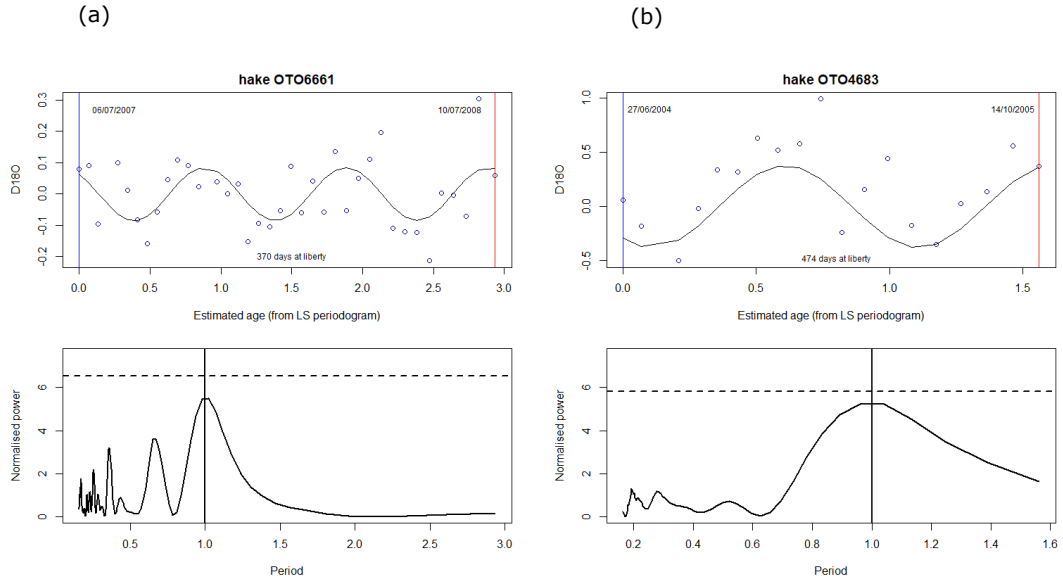


Figure 18: Plots displaying how concentrations of ^{23}Na and ^{88}Sr in anglerfish otoliths vary between quarters, length classes and ICES divisions. The regional comparison is based on samples collected in quarter 2 only.

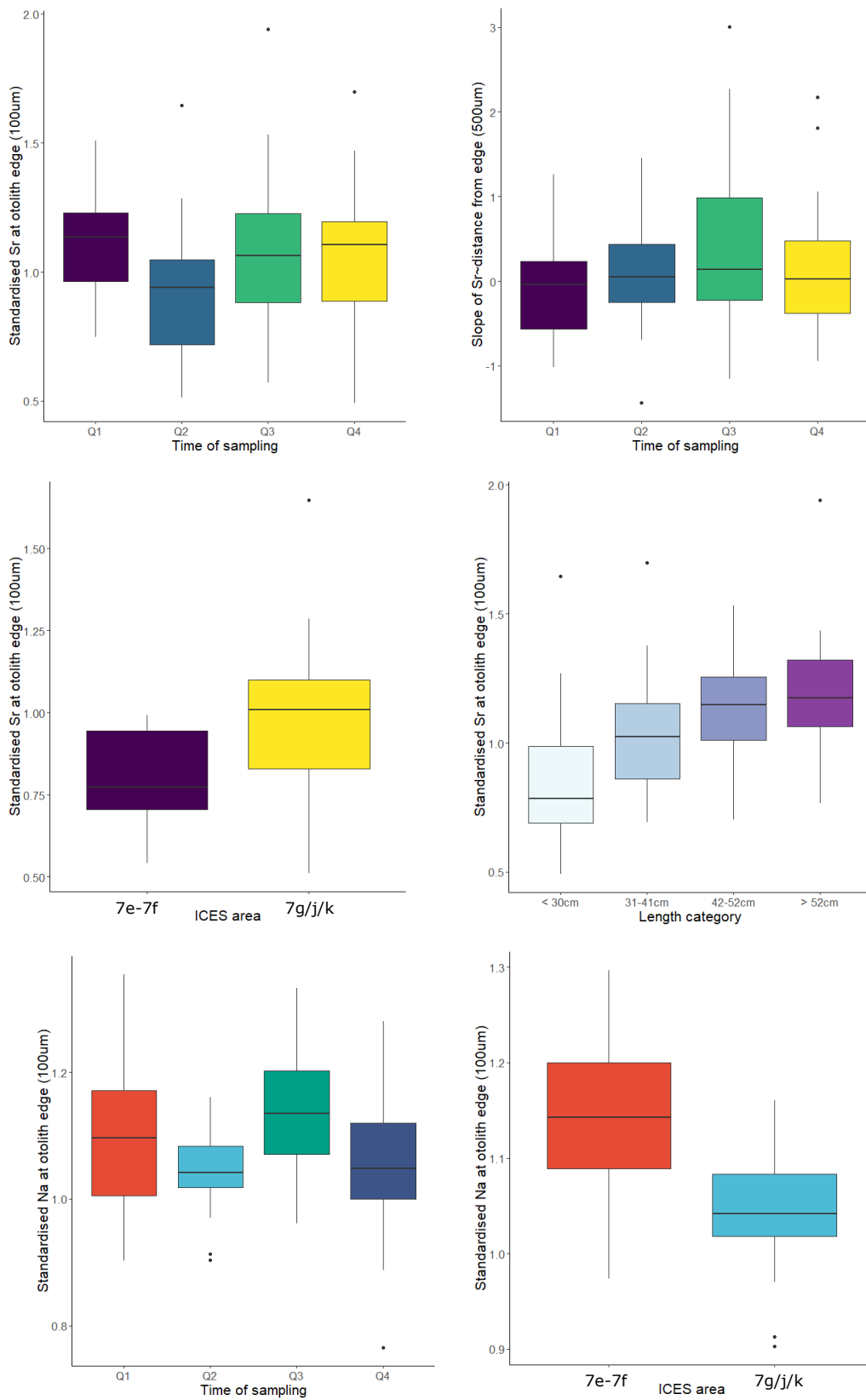


Figure 19: Plot showing how detrended ^{88}Sr concentrations at the otolith edge ($40\mu\text{m}$) vary across samples collected in different months. Measurements are shown as black dots. The blue line is a loess smooth used to highlight broad trends in the data.

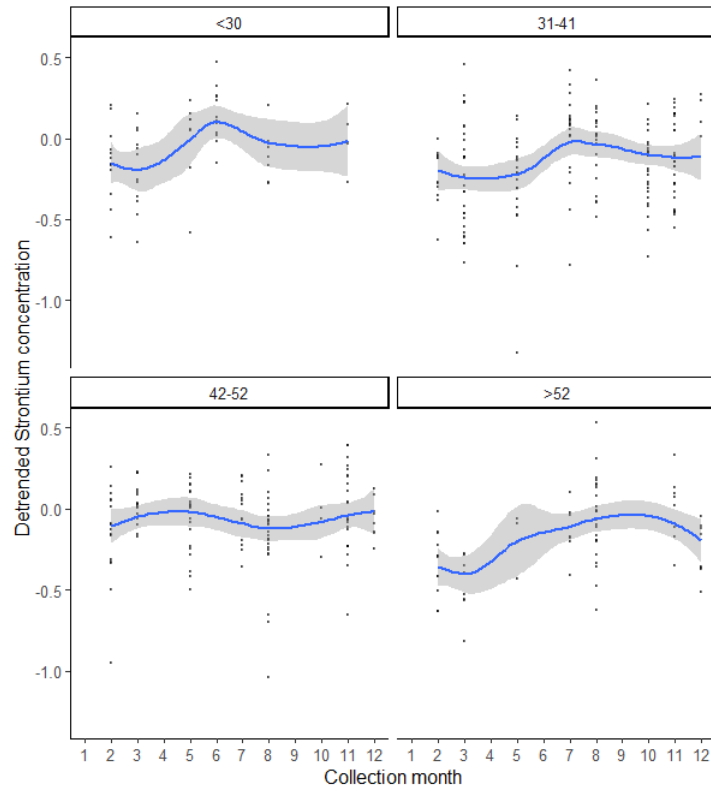


Figure 20: Relative $\delta^{18}\text{O}$ values across edge to core transects on individual anglerfish otoliths. Colours indicate the time of year (quarter) when the fish was collected.

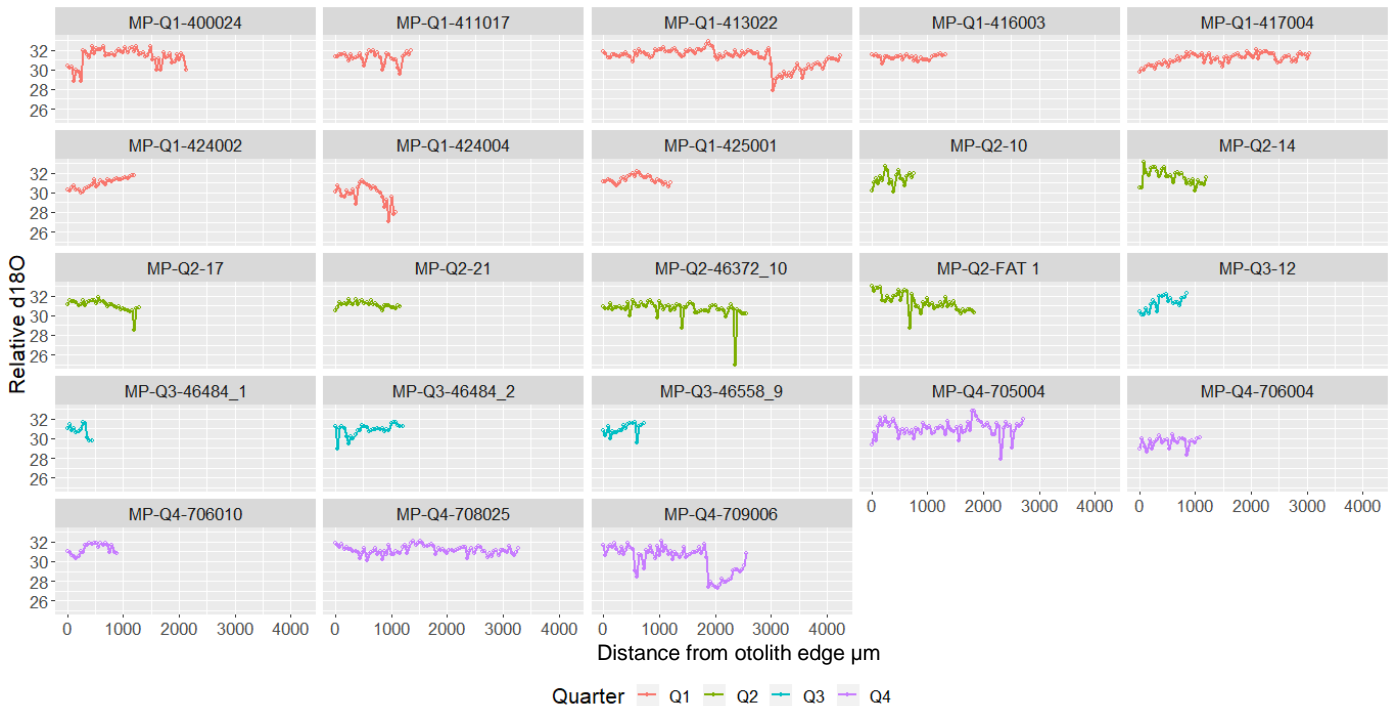


Figure 21: Boxplots showing the distribution of $\delta^{18}O$ concentrations at the edge of anglerfish illicia collected in each quarter. Medians are indicated by the dashed line, the upper and lower edges of the boxes represent the 75th and 25th percentiles respectively, whiskers represent the data extremes. There was no significant difference between quarters ($p=0.37$)

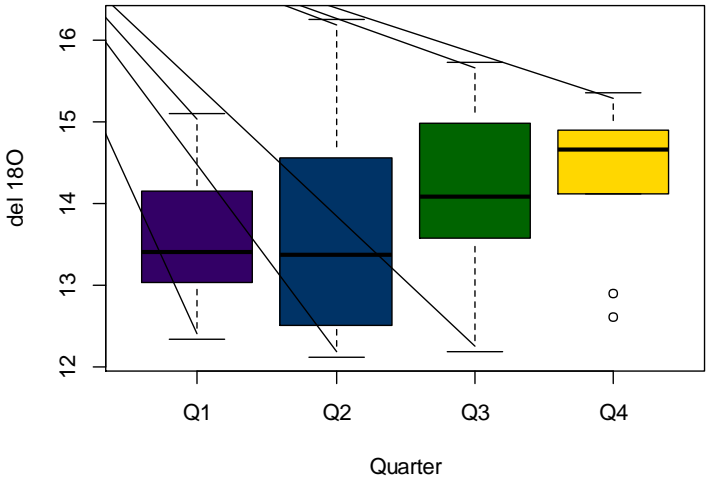


Figure 22: Relative $\delta^{18}O$ values across edge to core transects on individual anglerfish illicia. Colours indicate the time of year (quarter) when the fish was collected.

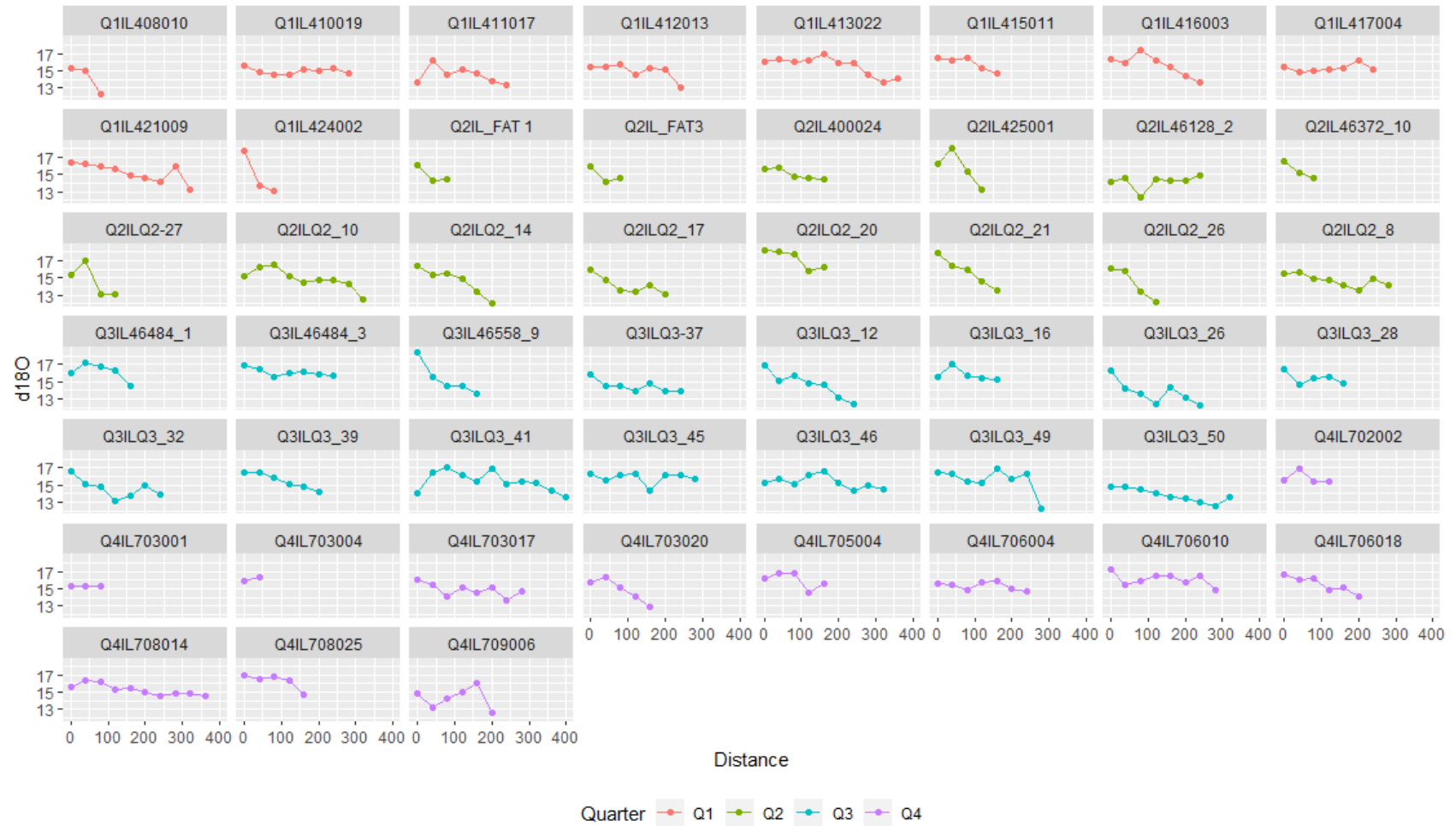




Figure 23: Example simulations of random peak detection. Simulated true series are shown as black lines, observations with error from the simulated series are shown in grey, true peaks are denoted with a vertical dashed line. Points denote peaks detected using: fixed window of eight observations (red triangles); fixed window of 20 observations (red crosses, mostly covered by decreasing window peaks); decreasing window (blue crosses); adaptive smoother and automatic peak detection algorithm (green x).

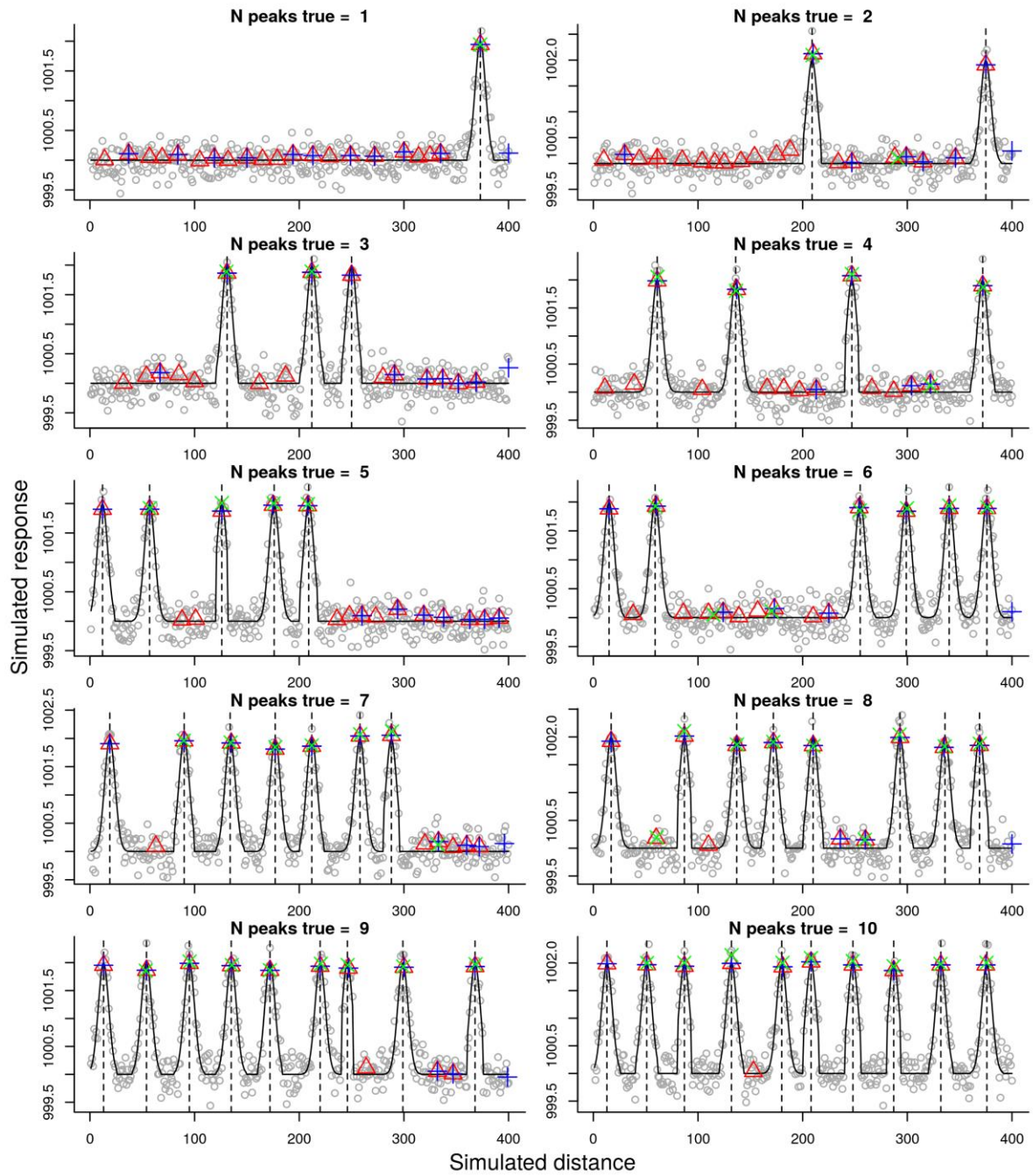




Figure 24: Scatterplots summarising the results of the method comparison based on simulated data. The true number of peaks are shown on the x axis and the number detected by each method are shown on the y axes. n_op1_w8: fixed window of eight observations; n_op1_w20: fixed window of twenty observations; n_op2: decreasing window; n_gam_ampd: adaptive smoother and automatic peak detection algorithm). Rows denote the length of the time series (T) and scale the height of the peaks. 1:1 line shown for reference.

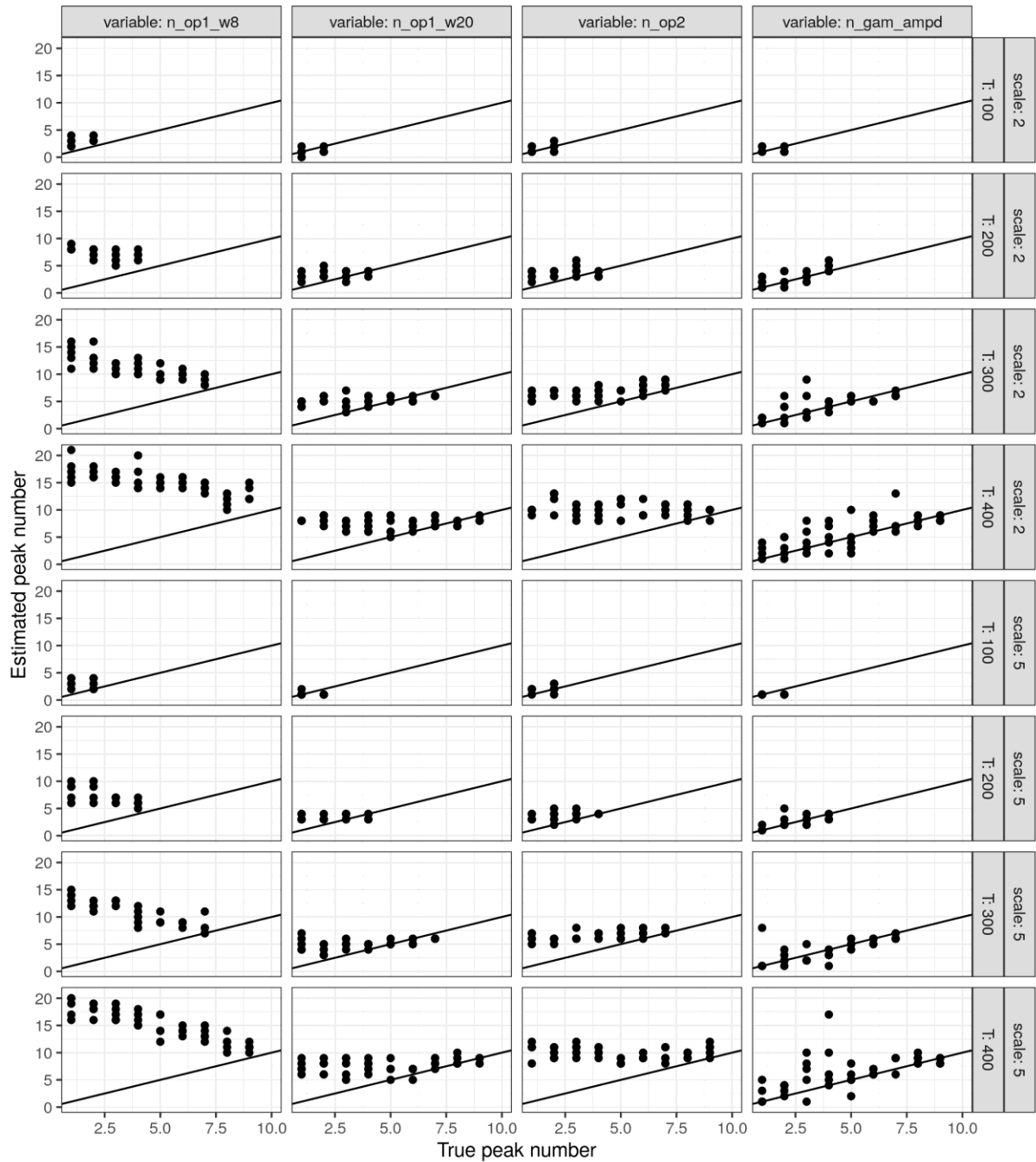
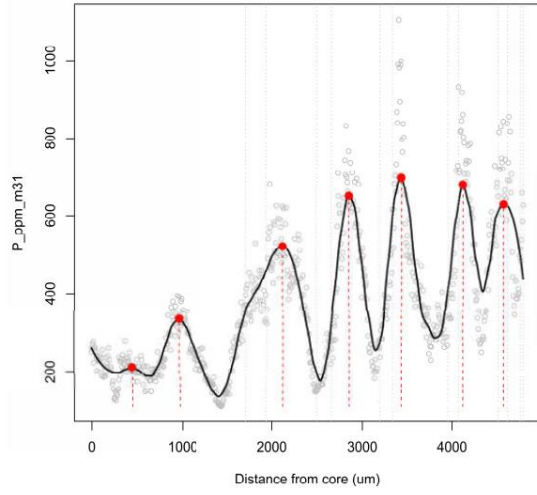
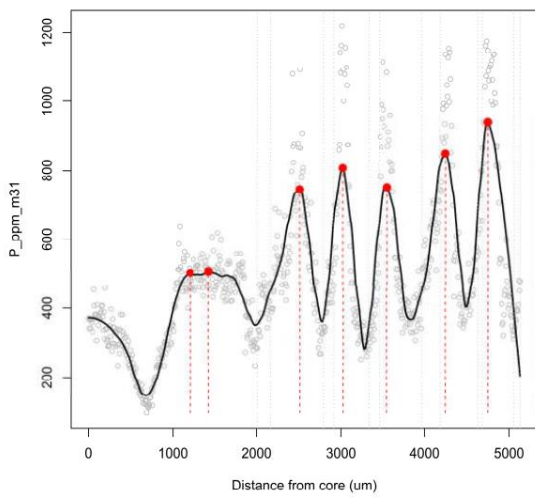


Figure 25: Plots showing the occurrence of peaks in Phosphorous (^{31}P) profiles from otoliths of 6 year old cod (*Gadus morhua*). Grey points indicate the observations. The black line is a loess smoother with a span equal to 100 divided by the time series length. The beginning and end of each translucent band on the otolith is indicated by the dashed vertical lines. The red dots indicate local maxima identified by the argmax peak detection algorithm.

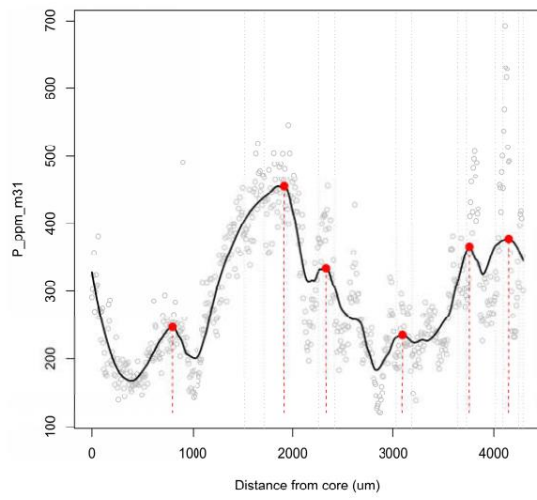
k_04_1_01.csv w = 20, span = 0.212766, age = 6



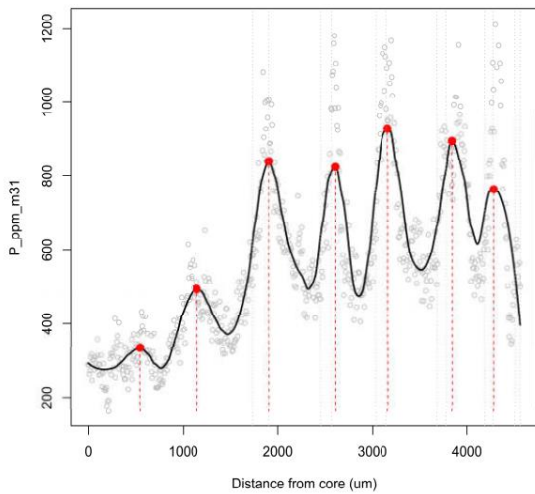
k_06_1_02.csv w = 20, span = 0.2010724, age = 6



k_06_1_03.csv w = 20, span = 0.2388535, age = 6



k_14_2_3.csv w = 20, span = 0.2262443, age = 6



k_17_1_2.csv w = 20, span = 0.206044, age = 6

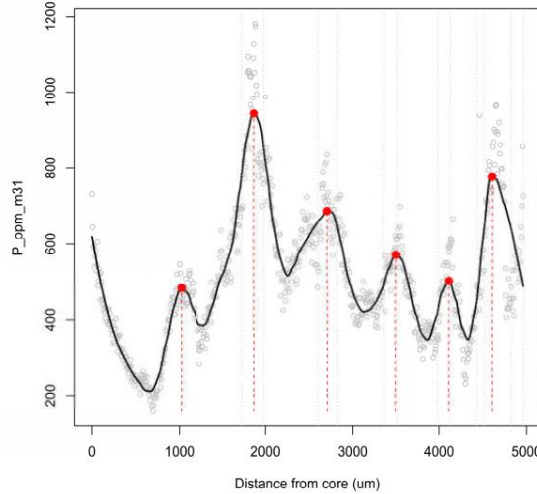


Figure 26: The annual signal extracted from ^{31}P profiles in 6 year old cod otoliths using the modified Lomb Scargle approach (black line) overlaid on the detrended ^{31}P measurements.

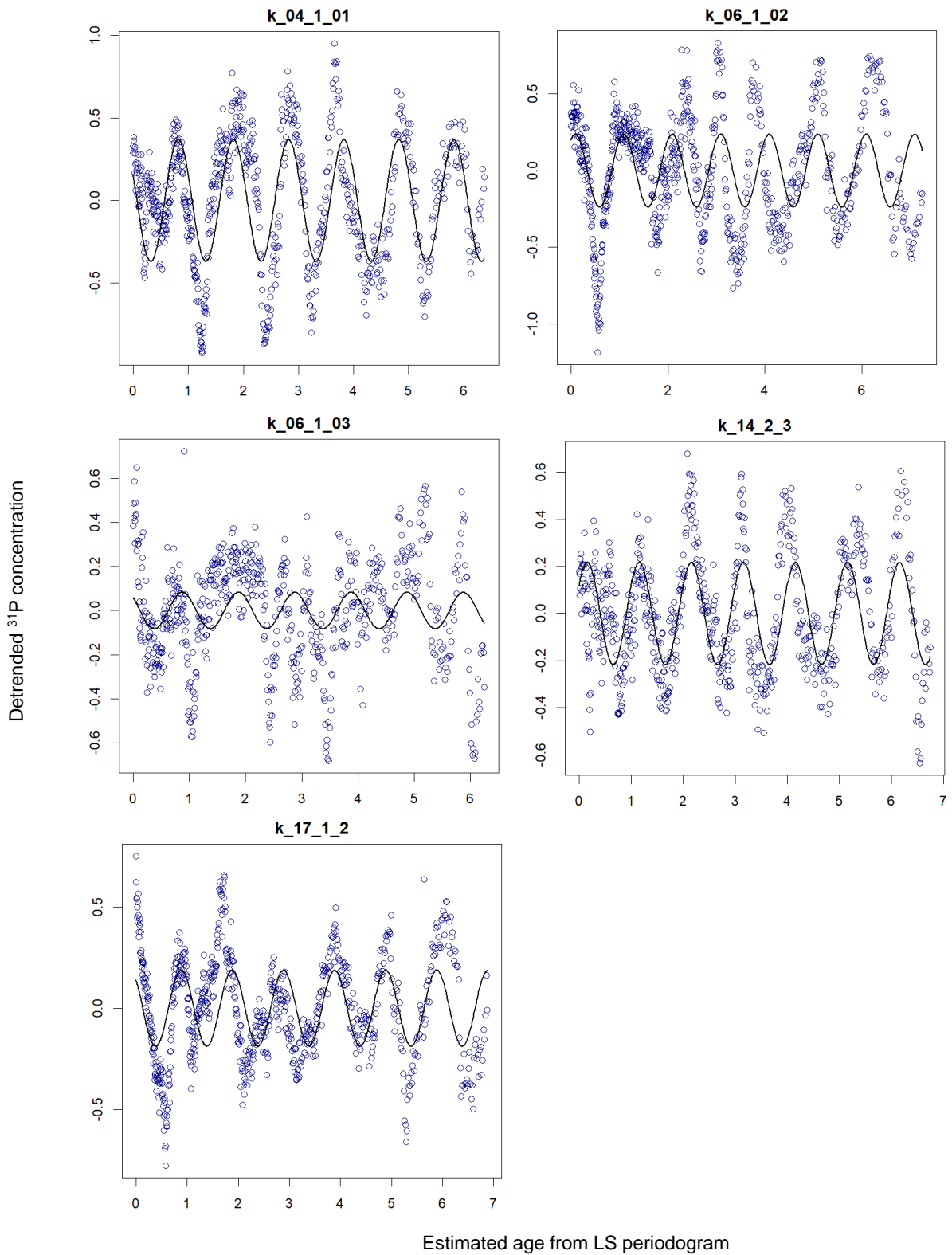


Figure 27: Chirp function fits to 31P profiles in otoliths from 6 year old cod.

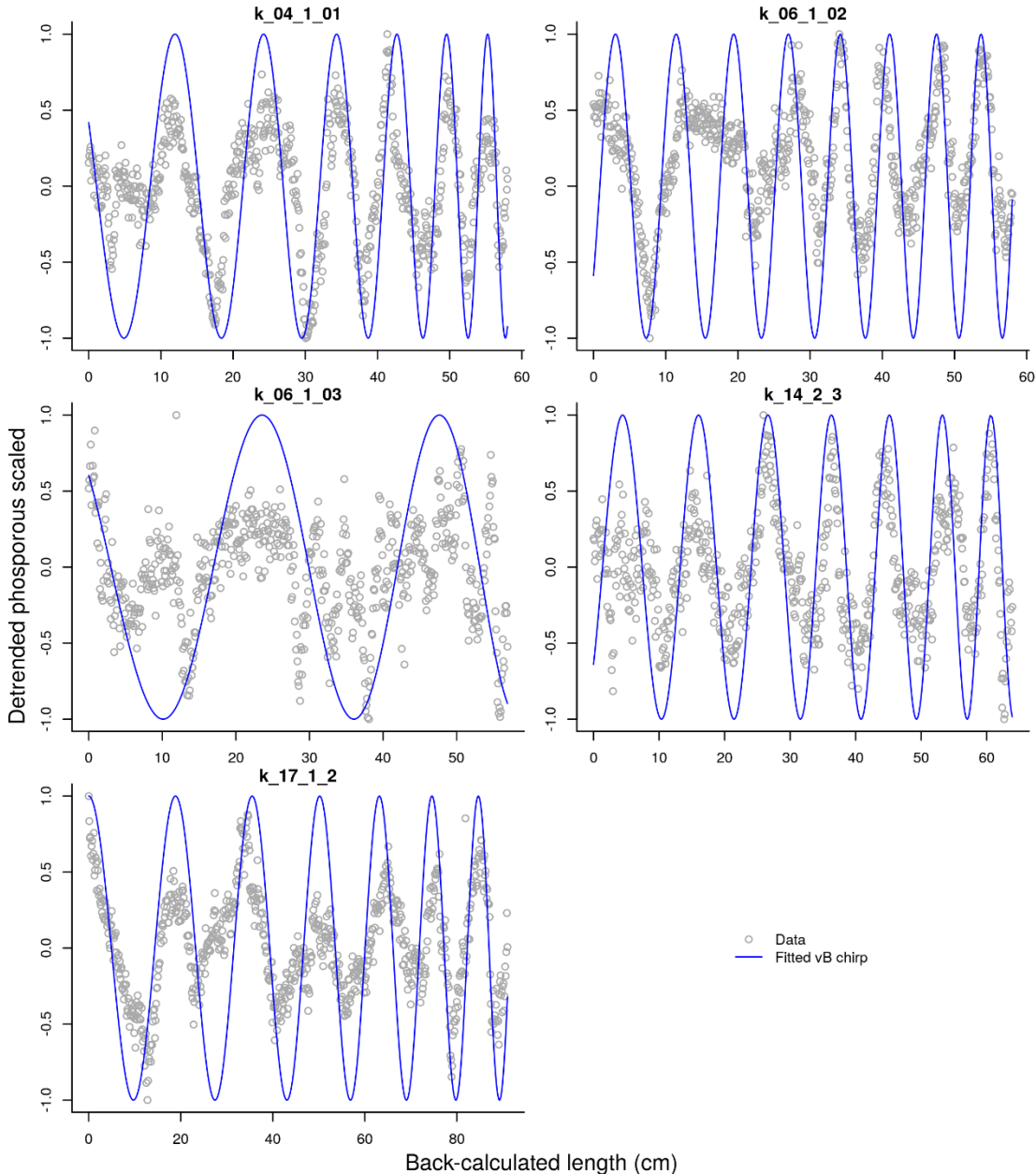


Figure 28: Example outputs from the modified Lomb Scargle method applied to 2D image LA ICPMS data from chemically tagged hake otoliths. The top panels show the detrended elemental data (blue points) with the putative annual signal extracted by the model overlaid (black line). The point on the otolith corresponding to the time of tagging (OTC mark) is indicated with a vertical blue line. The time of recapture (otolith edge) is indicated with a vertical red line. The dates beside each line refer to the time of release and capture. The bottom panels show the periodogram with the period of the putative annual cycle indicated by the vertical line. The dashed horizontal line shows the threshold for statistical significance. In example (a) the annual signal extracted by the Lomb Scargle method fits to the general visual trend in the data, other fluctuations occur at high frequencies. In example (b) in the middle there are two prominent sub-annual peaks in the middle of the time series; these features are not consistent with the constraints of the Von Betalanffy growth function that are incorporated into the signal detection process and are therefore not detected as part of the annual signal. (b) and (c) show data from two transects taken from the same otolith. The peaks in phosphorus concentration are more pronounced on the proximal transect (b) compared to the distal transect (c), although both show similar trends.

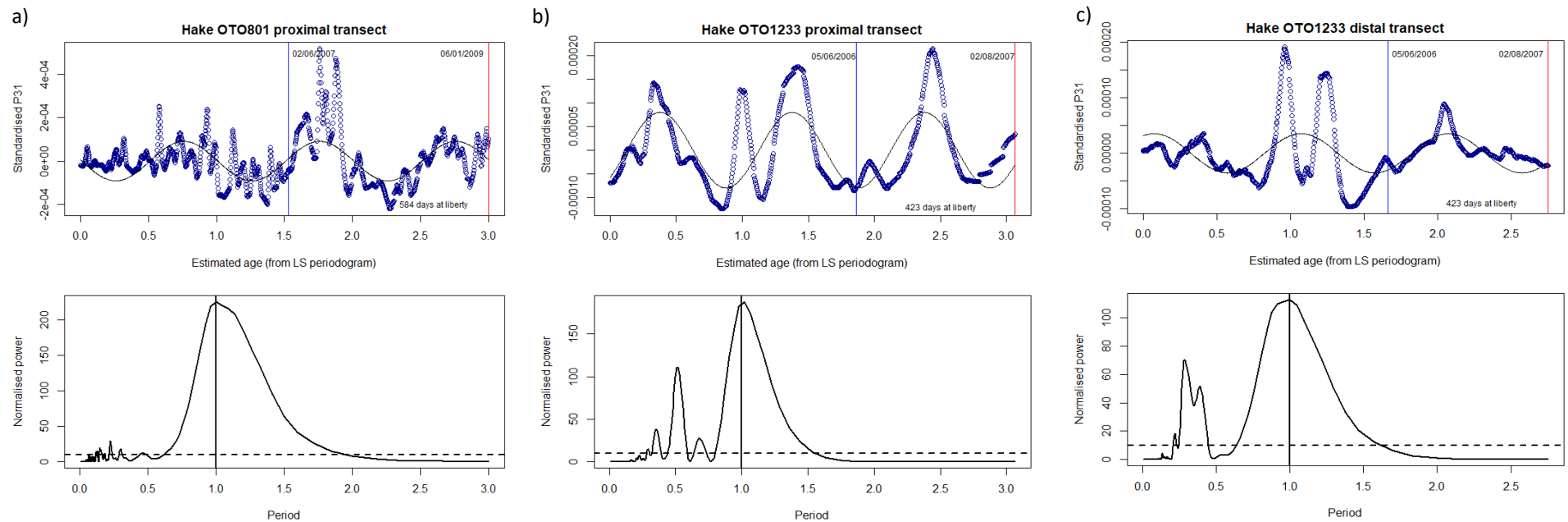


Figure 29: Example plots from an individual anglerfish for which annual cycles in strontium profiles are difficult to isolate using the Lomb Scargle approach.

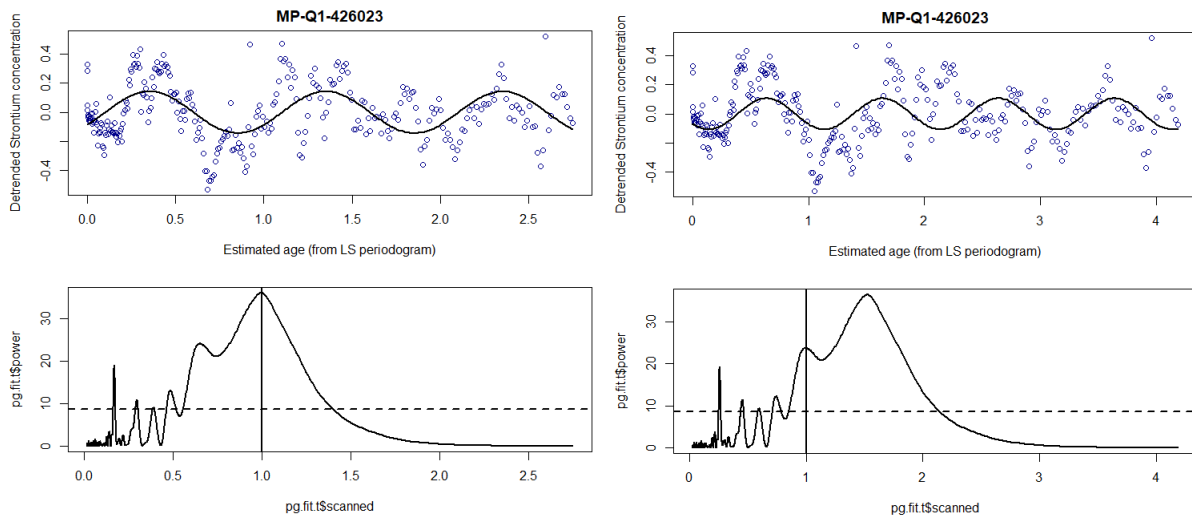


Figure 30: Strontium profile for one individual (blue points in left panel) overlaid with the annual signal extracted by the modified Lomb Scargle algorithm (black line in left panel) showed alongside an otolith (centre) and illicium (right) from the same individual. The red dots on the otolith and illicium images mark the position on the transects that correspond to the end of each year in the annual cycle (the minima). The ages estimated by expert readers for this individual were 4 and 5 (two otolith readings) and 3, 3 and 5 (three illicia readings).

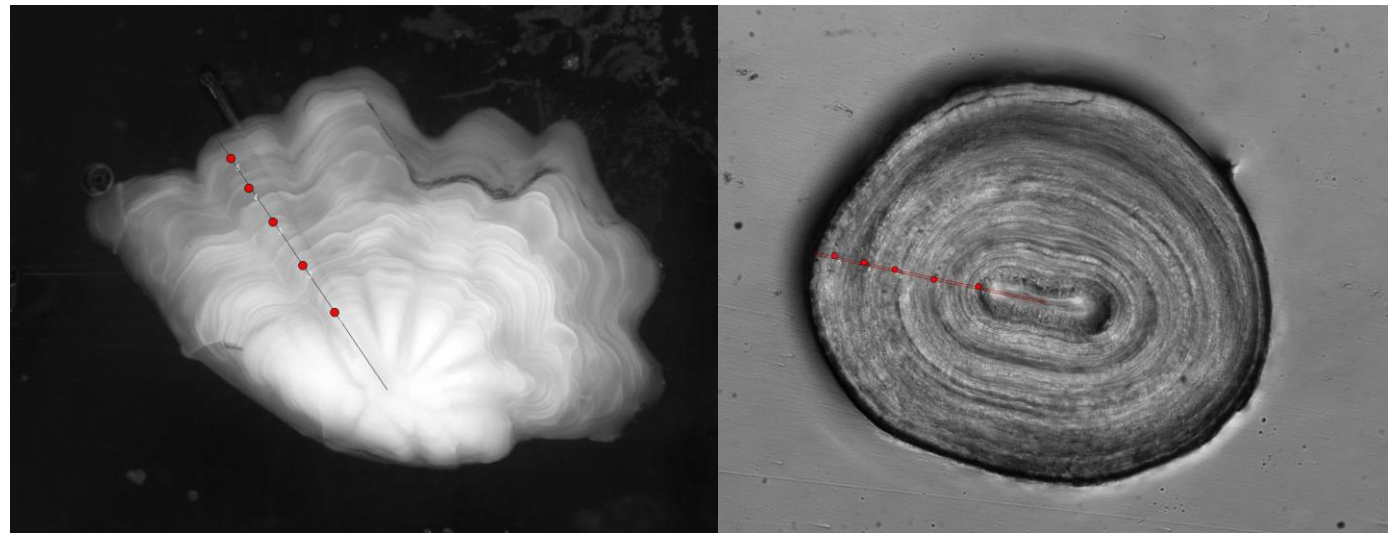
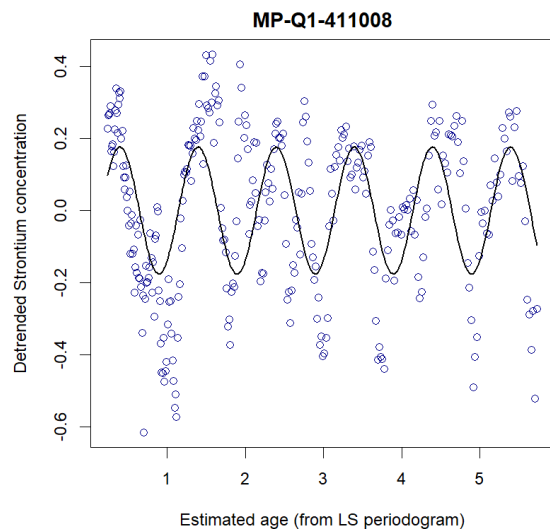


Figure 31: Plots showing the correspondence between age estimates derived from the strontium profiles and those provided by three expert readers based on visual examination of otolith and illicium images. The blue points are individual age estimates, the grey line shows a 1:1 relationship (perfect agreement).

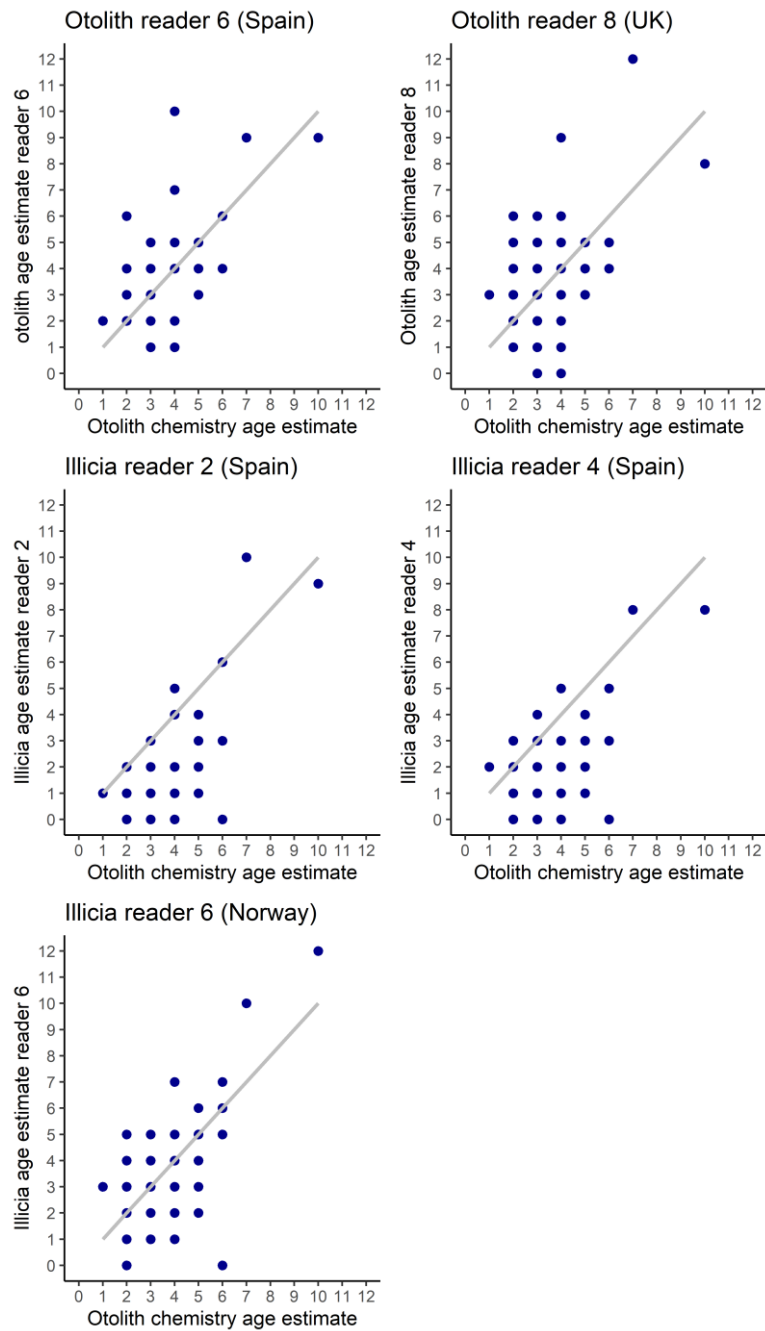


Figure 32: Frequency distribution of the back-calculated lengths from individual growth curves for the anglerfish samples in this study overlaid on the frequency distribution of lengths from the Irish groundfish survey.

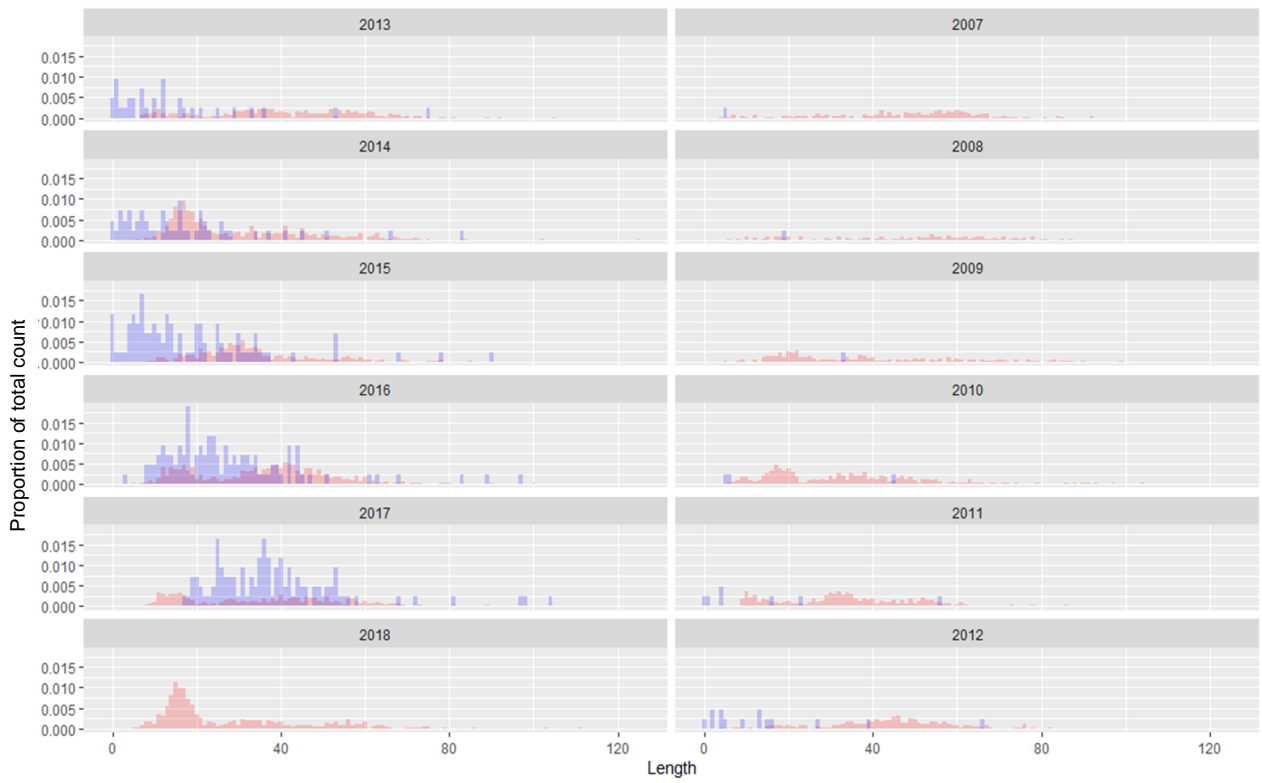


Figure 33: Boxplot showing the distribution of lengths of fish assigned to each age class using the mixture mode (orange) and the microchemistry method (green).

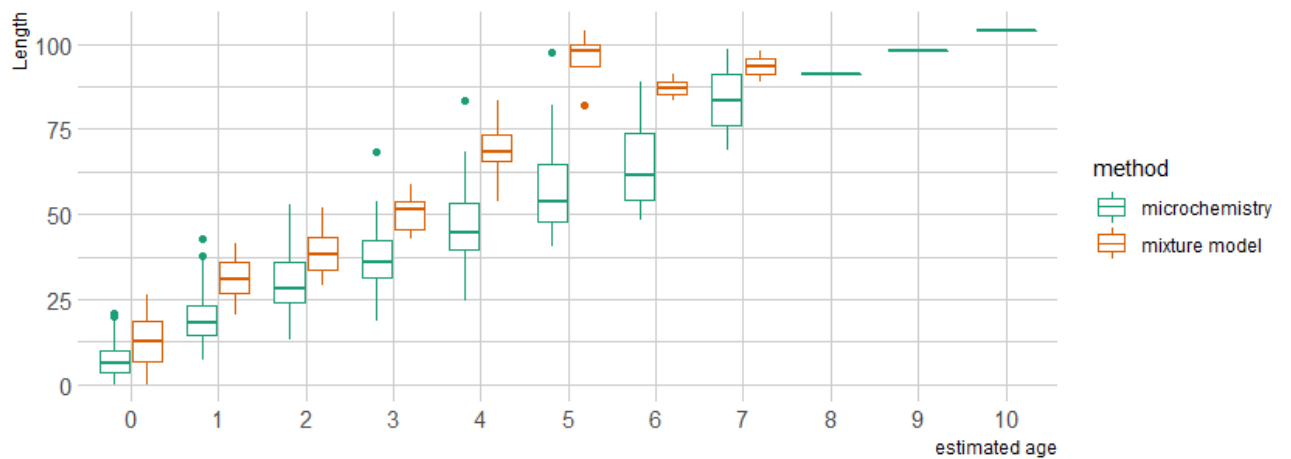


Figure 34: Mean probabilities of mixture model assignments to pseudo age cohorts for each age group as estimated using microchemistry

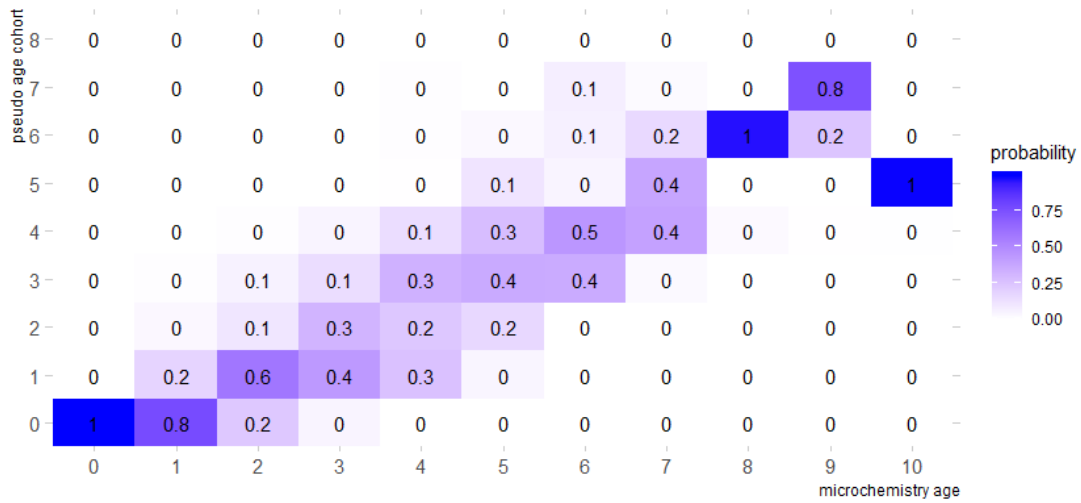
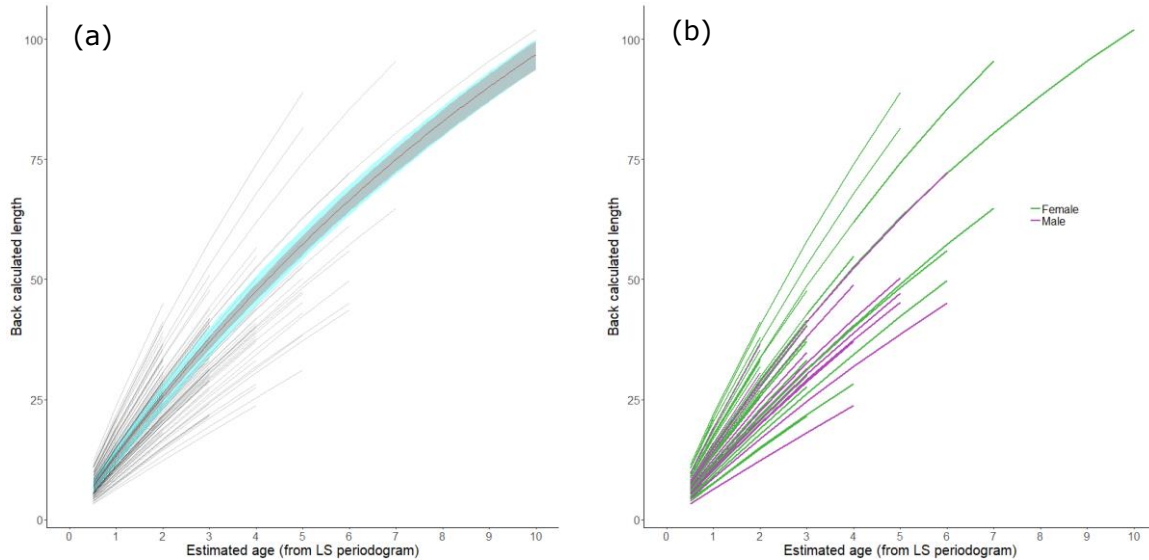
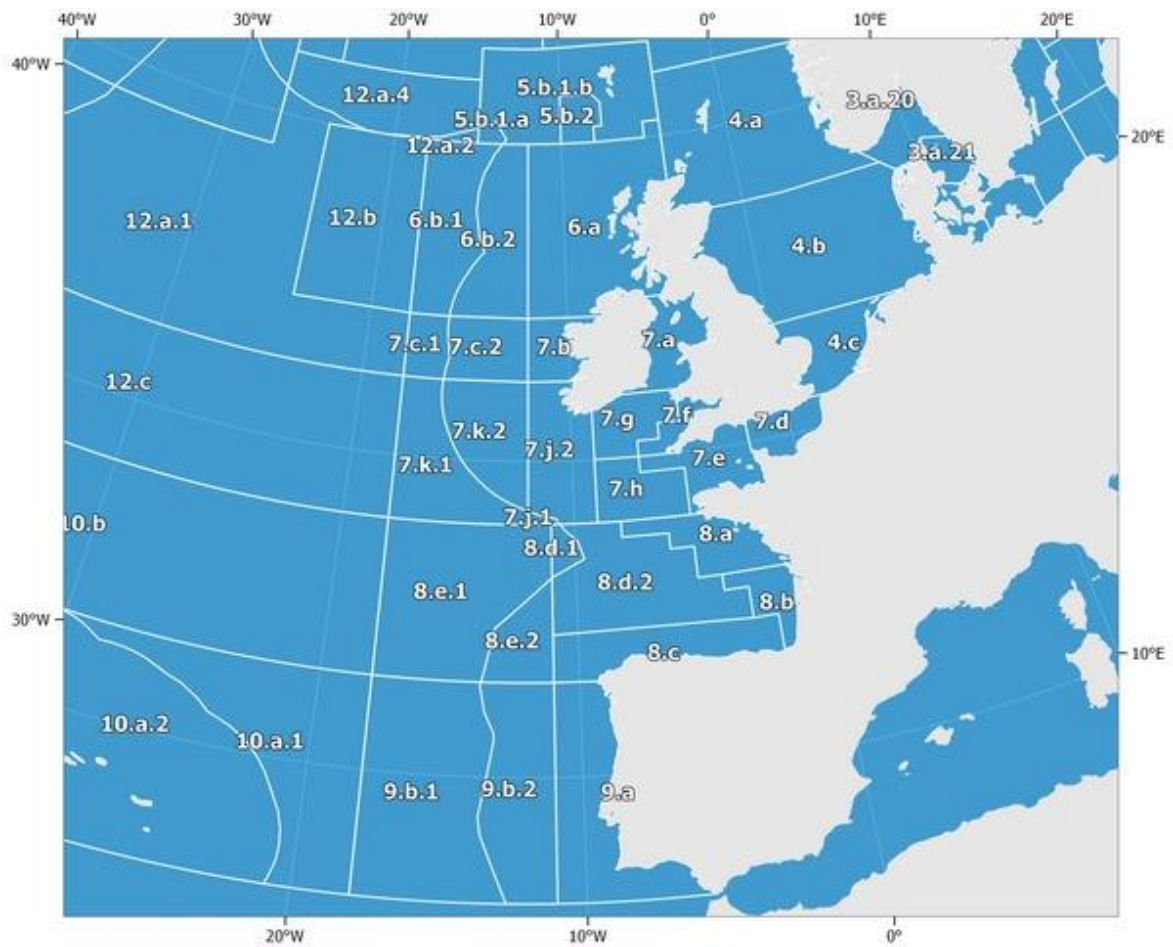


Figure 35: (a) Back-calculated growth histories, reconstructed using the age estimates from the strontium profiles (grey lines), with the best fitting Von Bertalanffy growth curve shown in red and 95% confidence limits shown in grey (bootstrap estimates) and cyan (delta estimates). (b) From the subset of the sample for which sex information was available: back-calculated growth histories for the females (green) and the males (purple)



Annex 1: Map of ICES area boundaries in the Northeast Atlantic

(from www.fao.org). The study focused on hake from ICES Divisions 7 and 8a (northern stock) and from ICES Division 8c/7a (southern stock) and on white anglerfish (*Lophius piscatorius*) from ICES Divisions 7b-k and 8a,b,d.





6 ANNEX 2: LIST OF PROJECT PARTICIPANTS

Name	Affiliation	Country
Deirdre Brophy	Galway Mayo Institute of Technology (GMIT)	Ireland
Cóilín Minto	GMIT	Ireland
Roxanne Duncan	GMIT	Ireland
Hans Gerritsen	Marine Institute	Ireland
Beatriz Morales-Nin	Mediterranean Institute for Advanced Studies (IMEDEA)	Spain
Silvia Pérez-Mayol	IMEDEA	Spain
Audrey Geffen	University of Bergen (UiB)	Norway
Hélène De Pontual	Institut Français de Recherche pour l'Exploitation de la Mer (IFREMER)	France
Kelig Mahé	IFREMER	France
Ching-Maria Villanueva	IFREMER	France
Karin Hüsey	National Institute of Aquatic Resources (DTU Aqua)	Denmark



7 ANNEX 3: GLOSSARY OF ABBREVIATIONS AND ACRONYMS USED IN TEXT

AIC	Akaike Information Criterion
APMD	Automatic Multiscale-Based Peak Detection
Ba	Barium
Ca	Calcium
CFP	Common Fisheries Policy
Cu	Copper
DATRAS	Database of Trawl Surveys
GLM	General Linear Model
GLMM	Generalised Linear Mixed Model
ICES	International Council for the Exploration of the Sea
IRMS	Isotope Ratio Mass Spectrometry
K	Potassium
La	Lanthanum
LA ICPMS	Laser Ablation Inductively Coupled Plasma Mass Spectrometry
Li	Lithium
Mg	Magnesium
Mn	Manganese
Na	Sodium
NIST	National Institute of Standards And Technology
OTC	Oxytetracycline
P	Phosphorous
Rb	Rubidium
SIMS	Secondary Ionisation Mass Spectrometry
Sr	Strontium
V-SMOW	Vienna Standard Mean Ocean Water
WGBIOP	Working Group on Biological Parameters
Y	Yttrium
Zn	Zinc



8 ANNEX 4: PROTOCOL FOR THE ANALYSIS OF ANGLERFISH ILLICIA AND OTOLITHS

Identifying elements in illicia likely to show age related trends

Laser-Ablation Inductively Coupled Plasma-Mass Spectrometry (LA-ICPMS) was the surface-based analytical technique selected to quantify the chemical composition of both otoliths and illicia. A review of the literature using Web of Science was conducted to collate information pertaining to the analysis of illicia (Table A1) using LA-ICPMS. Elements that tend to display potentially age-related trends in fin spines and vertebrae were identified: Sr, Zn, Ba, Mn and Cu. This list is similar to the suite of elements that have proved useful for age validation using otolith microchemistry.

A preliminary microchemical analysis was performed in four monkfish illicia using a Hitachi S3400N SEM with a Bruker ACS XFlash 4010 detector at Universitat de les Illes Balears. The purpose of the analysis was to qualitatively characterise the chemical composition of the illicia and the resin used for embedding the structure and to identify potential contamination issues due to sample preparation. SEM was used in backscattered mode on 150 x 100 µm surface samplings in both illicia and surrounding resin,

Moreover, due to the small size of illicia (mean diameter 0.2 mm) and the need for a good signal for LA-ICPMS analysis, three laser beam sizes (10µm, 25µm, 40µm) were tested to obtain the best relation between response analysis and spatial resolution.

Laser-ablation ICPMS analysis

The LA-ICPMS analysis of anglerfish otoliths and illicia was carried out at the Universidade de A Coruña using a CETAC Laser Ablation System LSX-213 G2+ coupled to a Thermo-Finnigan ICPMS Element XR. Core-to-edge continuous line scans were shot in both otolith (40 µm diameter) and illicia (25 µm diameter) with a scan speed of 10 µm.s⁻¹.

Due to the different composition of bone and otoliths the reference standards common to both tissues were: NIST612, NIST614 and NIST616. Additionally, a specific bone meal standard (NIST1486) pressed as a pellet was used in the illicia analysis; whereas FEBS-1 (Sturgeon et al. 2005) and NIST-22 (Yoshinaga et al. 2000) pressed as pellets were used only for otoliths. All reference materials were shot following the bracketing procedure, being measured at the beginning and end of each working session and every 5 scans on the CS.;. A suite of elements could be quantified: ⁷Li, ²³Na, ²⁴Mg, ²⁶Mg, ²⁷Al, ³¹P, ³⁹K, ⁴³Ca, ⁴⁴Ca, ⁵⁵Mn, ⁵⁶Fe, ⁶⁶Zn, ⁸⁸Sr, ¹³⁷Ba, ¹³⁸Ba, ²⁰⁶Pb, ²⁰⁷Pb and ²⁰⁸Pb.

In LA-ICPMS analysis variability in the elemental signals can arise due to elemental fractionation, matrix effects and variation in ablation yield (Günther et al., 1999). To correct for this an element that is present at a known concentration within the sample can be used as an internal standard. Calcium is present in both otoliths and illicia at a reasonably consistent concentration, thus a value of 38.8 wt% of ⁴³Ca in otoliths and 26.0 wt% of ⁴³Ca in illicia was used as internal standard.

The raw data were processed using software Iolite (Melbourne University, Melbourne), a semiautomatic program for LA-ICPMS data reduction and calculation of isotope concentrations. Briefly, the procedure consisted of: i) cutting of the continuous line scans in 0.57 s sections (representing 5.7 µm length portions), ii) subtraction of the signal background for each portion, iii) temporal drift and internal standard corrections,

and iv) calculation of the isotope concentration and limits of detection using one single reference material. The last step (iv) was repeated for each reference material. Accuracies and precisions for each reference material were calculated.



Table A1: . Summary of studies dealing with the chemical composition of fish fin rays/spines and vertebrae.

Author&year	species	structure	analytical method	elements	Settings	units	Observations	Species
Feldite et al. 2008	Tilapia,chinese tilapia, common carp	vertebrae, flesh, liver	ICP-OES+Flame Atomic Absortion for Hg	As,Cd,Pb,Hg	Rearing in waste water for a long period	mg/kg dry weight	Vaues in vertebrae there are values in flesh and liver	Chinese Carp
Vas 1991	10 shark species	up to 8 tissues depending species	Atomic Absorption spectrophotometry	Cu,Mn,Fe,Cd,Ni,Pb,Zn	British&Atlantic waters	ug/g fresh w	values vertebrae	<i>S.canicula</i>
Veinott et al. 1999	white sturgeon	pectoral fin rays	LA-ICPMS	88Sr,44Ca	growth zones, estuary,2 rivers	ppm		<i>Arcipenser transmotanus</i>
Allen et al 2009	green sturgeron	pectoral fin rays	LA-ICPMS		migrations, water samples, reared and wild annuli	mmol	ratios to Ca x103 for Sr/Ca and x105 for Ba/Ca	<i>Acipenser medirostris</i>
Smith&Whitledge 2011	lake sturgeron	pectoral fin rays	LA-ICPMS		chemical marking juveniles water enriched 86SrCO3	88Sr/86Sr ratios		<i>Acipenser fulvescens</i>
Pollard et al.1998	snapper	dorsal spines	ICPMS	86Sr	experimental marking with SrCl2 incorporation at different concentrations	ug/g		<i>Pagrus auratus</i>
Kock et al. 1996	Artic charr	opercula	GFAAS	Pb	presence in different lakes	ug/g dry weight		<i>Salvelinus alpinus</i>
Tillet et al. 2011	bull and pig-eye sharks	vertebrae	LA-ICPMS	Li,Mg,Al,P,Ca,Mn,Fe,Cu,Zn,Sr,La,Ba,U	age, nursery habitats,migration	element/Ca		<i>Carcharhinus leucas,C.amboinensis</i>
Kennedy et al. 2000	salmon	vertebrae	Mass spectrometer	87Sr/86Sr	water composition,incorporation, natural marking otoliths,scales vertebrae	87Sr/86Sr		<i>Salmo salar</i>
Behrens Yamada et al.2016	salmon	vertebrae	X-ray fluorescence	P,S,K,Ca,Mn,Cu,Zn,Br,Sr	Sr enriched in water and food, natural differences due to genetics	ug/g	No data only MANOVA results	<i>Oncorhynchus nerka</i>
Lewis et al. 2017	black tip shark	vertebrae	LA-ICPMS	li,Mg,Mn,Sr,Ba,Pb	differences intra e intervertebrae and effects of handling and storage	umol/Ca mol	Data only in a graph tables statistical tests	<i>Carcharhinus limbatus</i>
Balazik et al. 2012	Atlantic sturgeon	pectoral fin spines	EDXRF	Sr/Ca	diadromy in adult and juveniles plus experimental work salinity		provide ratios at distances from the primordium	<i>Acipenser oxyrinchus</i>
Jarik et al. 2011	danube sturgeon	pectoral fin spines	NMP+PIXE	Sr/Ca for salinity and Zn/Ca for season	comparation of different age zones juvenile-adult		there are 4 different patterns in Sr/Ca maps	<i>3 species H.uso, A.stellatus,A.gueldenstadti</i>
Gillanders 2001	damselfish	otoliths,eye lenses,scales and spines	ICPMS	Mn,Sr,Ba,Pb	correlation between tissues	ug/g		<i>Parma microlepis</i>
Luque et al. 2016	bluefin tuna	first dorsal spine	LAICPMS	Sr,Ba,Mg,Mn,Li,Co,Pb,Ni,Cu,Zn,Ca	increment has effects onSr,Ba,Mn,Zn,Cu	ug/g	changes between opaque and translucent and age	<i>Tunnus thynus</i>
Davies et al.2011	albacore tuna	otoliths and first dorsal spine	LAICPMS	Mn,Ba,Mg,Sr	differences opaque translucent band in contamination and in concentration	ppm	decontamination treatment	<i>Thunnus alalunga</i>
Scharer et al. 2012	smalltooth sawfish	vertebrae	LAICPMS	Ca,P,Sr,Ca	Ca and P highly variable between bands, Sr/Ca varied with bands in relation to river salinity	mmol mol-1	age validation	<i>Pristis pectinata</i>
Smith &Whitledge 2010	smallmouth bass	pectoral fin rays	LAICPMS	Ca,Sr,Ba	reconstructing environment history ray core and edge analysed	mmol/mol		<i>Micropterus dolomieu</i>
Phelps et al. 2012	sturgeon	pectoral fin rays	LAICPMS	Sr,Ca	water, lab keep age 0 and river fish	umol/mol	profiles Sr/Ca at distance from core	<i>Scaphirhynchus spp</i>
Arai&Miyazaki 2002	Russian sturgeon	pectoral fin rays	X-ray microprobe	Sr,Ca	migrations		profiles Sr:Ca from the core	<i>Arcipenser guldenstadti</i>
Rude et al. 2014	muskellunge	pelvic fin ray	LAICPMS	Sr,Ca	differentiation of stcked and wild fish	umol/mol	profiles Sr:Ca from the core in different age groups	<i>Esox masquinongy</i>
Ugarte et al. 2012	tuna species	first dorsal spine	ICPMS	B,Mg,Al,V,Cr,Mn,Fe,Cu,Ni,Cu,Zn,As,Se,Rb,Sr,Y,Pd,Cd,Ba,La,Ce,lr,Hg,Pb	relation to muscle	ug/kg	5 elements results	<i>albacore, bluefin tuna</i>
Clarke et al.2007	artic grayling	pectoral fin spines	LAICPMS	Sr,Ba,Mn	comparisons with otoliths and scales	mmol/mol	otoliths and fin ray correpated to water composition	<i>Thymallus arcticus</i>
Wolff et al. 2013	june sucker	pelvic fin ray	LAICPMS	87Sr/86Sr	differentiation stocked and wild fish			<i>Chasmistes liorus</i>

9 REFERENCES

- Ardia, D., Mullen, K.M., Peterson, B.G., and Ulrich, J. (2016). 'DEoptim': Differential Evolution in 'R'. version 2.2-4
- Batts, L., Minto, C., Gerritsen, H., and Brophy, D. 2019. Estimating growth parameters and growth variability from length frequency data using hierarchical mixture models. *ICES Journal of Marine Science*.
- Gillanders, B. M. 2001. Trace metals in four structures of fish and their use for estimates of stock structure. *Fishery Bulletin*, 99: 410-419.
- Günther, D., Jackson, S. E., and Longerich, H. P. 1999. Laser ablation and arc/spark solid sample introduction into inductively coupled plasma mass spectrometers. *Spectrochimica Acta Part B: Atomic Spectroscopy*, 54: 381-409.
- Hüssy, K., Gröger, J., Heidemann, F., Hinrichsen, H. H., and Marohn, L. 2015. Slave to the rhythm: seasonal signals in otolith microchemistry reveal age of eastern Baltic cod (*Gadus morhua*). *ICES Journal of Marine Science*, 73: 1019-1032.
- ICES. 2014. Report of the Benchmark Workshop on Sprat Stocks (WKSPRAT), 11–15 February 2013, Copenhagen, Denmark. ICES CM 2013/ACOM:48. 220 pp.
- ICES. 2018. Report of the Benchmark Workshop on Anglerfish Stocks in the ICES Area (WKANGLER), 12–16 February 2018, Copenhagen, Denmark. ICES CM 2018/ACOM:31. 177 pp.
- ICES. 2019. Inter-benchmark of Hake (*Merluccius merluccius*) in subareas 4, 6, and 7 and divisions 3.a, 8.a–b, and 8.d, Northern stock (Greater North Sea, Celtic Seas, and the northern Bay of Biscay) (IB- Phake). ICES Document 4: 1. 28 pp.
- Jardim, E., Millar, C. P., Mosqueira, I., Scott, F., Osio, G. C., Ferretti, M., Alzoriz, N., et al. 2014. What if stock assessment is as simple as a linear model? The a4a initiative. *ICES Journal of Marine Science*, 72: 232-236.
- Jaric, I., Lenhardt, M., Pallon, J., Elfman, M., Kalauzi, A., Suci, R., Cvijanovic, G., et al. 2011. Insight into Danube sturgeon life history: trace element assessment in pectoral fin rays. *Environmental Biology of Fishes*, 90: 171-181.
- Laurenson, C. H., Johnson, A., and Priede, I. G. 2005. Movements and growth of monkfish *Lophius piscatorius* tagged at the Shetland Islands, northeastern Atlantic. *Fisheries Research*, 71: 185–195
- Limburg, K. E., and Elfman, M. 2017. Insights from two-dimensional mapping of otolith chemistry. *J Fish Biol*, 90: 480-491.
- Lomb, N. R. 1976. Least-squares frequency analysis of unequally spaced data. *Astrophysics and Space Science*, 39: 447-462.
- Luque, P. L., Zhang, S., Rooker, J. R., Bidegain, G., and Rodriguez-Marin, E. 2017. Dorsal fin spines as a non-invasive alternative calcified structure for microelemental studies in Atlantic bluefin tuna. *Journal of Experimental Marine Biology and Ecology*, 486: 127-133.
- Mellon-Duval, C., de Pontual, H., Métral, L., and Quemener, L. 2010. Growth of European hake (*Merluccius merluccius*) in the Gulf of Lions based on conventional tagging. – *ICES Journal of Marine Science*, 67: 62–70.
- Methot, R. D., and Wetzel, C. R. 2013. Stock synthesis: A biological and statistical framework for fish stock assessment and fishery management. *Fisheries Research*, 142: 86-99.
- Payan, P., Edeyer, A., De Pontual, H., Borelli, G., Boeuf, G., and Mayer-Gostan, N. 1999. Chemical composition of saccular endolymph and otolith in fish inner ear: lack of spatial uniformity. *American Journal of Physiology-Regulatory Integrative and Comparative Physiology*, 46: R123-R131.
- Phelps, Q. E., Whitley, G. W., Tripp, S. J., Smith, K. T., Garvey, J. E., Herzog, D. P., Ostendorf, D. E., et al. 2012. Identifying river of origin for age-0 Scaphirhynchus sturgeons in the Missouri and Mississippi rivers using fin ray microchemistry. *Canadian Journal of Fisheries and Aquatic Sciences*, 69: 930-941.
- Pracheil, B., George, R., and Chakoumakos, B. 2019. Significance of otolith calcium carbonate crystal structure diversity to microchemistry studies. *Reviews in Fish Biology and Fisheries*.

-
- Ruf, T. 1999. The Lomb-Scargle Periodogram in Biological Rhythm Research: Analysis of Incomplete and Unequally Spaced Time-Series. *Biological Rhythm Research*, 30: 178.
- Scargle, J. 1983. Studies in astronomical time series analysis. II - Statistical aspects of spectral analysis of unevenly spaced data. *The Astrophysical Journal*, 263.
- Scholkmann, F., Boss, J., and Wolf, M. 2012. An Efficient Algorithm for Automatic Peak Detection in Noisy Periodic and Quasi-Periodic Signals. *Algorithms*, 5: 588-603.
- Siskey, M. R., Lyubchich, V., Liang, D., Piccoli, P. M., and Secor, D. H. 2016. Periodicity of strontium: Calcium across annuli further validates otolith-ageing for Atlantic bluefin tuna (*Thunnus thynnus*). *Fisheries Research*, 177: 13-17.
- VanderPlas, J. 2017. Understanding the Lomb-Scargle Periodogram. *The Astrophysical Journal Supplement Series*, 236.
- Yoshinaga, J., Nakama, A., Morita, M., and Edmonds, J. S. 2000. Fish otolith reference material for quality assurance of chemical analyses. *Marine Chemistry*, 69: 91-97.
- Campana SE (1990) How reliable are growth back-calculations based on otoliths? *Canadian Journal of Fisheries and Aquatic Sciences [CAN J FISH AQUAT SCI]* 47: 2219-2227
- Campana SE (1999) Chemistry and composition of fish otoliths: pathways, mechanisms and applications. *Marine Ecology-Progress Series* 188: 263-297
- Chang M-Y, Geffen AJ, Kosler J, Dundas SH, Maes GE (2012) The effect of ablation pattern on LA-ICPMS analysis of otolith element composition in hake, *Merluccius merluccius*. *Environmental Biology of Fishes* 95: 509-520 doi 10.1007/s10641-012-0065-7
- Chen Y, Hunter M, Vadas R, Beal B (2003) Developing a growth-transition matrix for the stock assessment of the green sea urchin (*Strongylocentrotus droebachiensis*) off Maine. *Fishery Bulletin* 101: 737-744
- Clarke, L. M., & Friedland, K. D. (2004). Influence of growth and temperature on strontium deposition in the otoliths of Atlantic salmon. *Journal of Fish Biology*, 65(3), 744-759. doi:10.1111/j.0022-1112.2004.00480.x
- Clarke AD, Telmer KH, Shrimpton JM (2007) Elemental analysis of otoliths, fin rays and scales: a comparison of bony structures to provide population and life-history information for the Arctic grayling (*Thymallus arcticus*). *Ecology of Freshwater Fish* 16: 354-361 doi 10.1111/j.1600-0633.2007.00232.x
- Crozier WW (1989) Age and growth of angler-fish (*Lophius piscatorius* L.) in the north Irish Sea. *Fisheries Research* 7: 267-278 doi http://dx.doi.org/10.1016/0165-7836(89)90060-X
- Davies CA, Brophy D, Jeffries T, Gosling E (2011) Trace elements in the otoliths and dorsal spines of albacore tuna (*Thunnus alalunga*, Bonnaterre, 1788): An assessment of the effectiveness of cleaning procedures at removing postmortem contamination. *Journal of Experimental Marine Biology and Ecology* 396: 162-170 doi 10.1016/j.jembe.2010.10.016
- de Pontual H, Geffen AJ (2002) Otolith microchemistry. In: Panfili J, de Pontual H, Troadec H, Wright PJ (eds) *Manual of Fish Sclerochronology*, Ifremer-IRD coedition, Brest, France, pp 245-301
- de Pontual H, Groison AL, Pineiro C, Bertignac M (2006) Evidence of underestimation of European hake growth in the Bay of Biscay, and its relationship with bias in the agreed method of age estimation. *ICES Journal of Marine Science* 63: 1674-1681 doi 10.1016/j.icesjms.2006.07.007
- de Pontual H, Jolivet A, Garren F, Bertignac M (2013) New insights on European hake biology and population dynamics from a sustained tagging effort in the Bay of Biscay. *Ices Journal of Marine Science* 70: 1416-1428 doi 10.1093/icesjms/fst102
- DeLong AK, Collie JS, Meise CJ, Powell JC (2001) Estimating growth and mortality of juvenile winter flounder, *Pseudopleuronectes americanus*, with a length-based model. *Canadian Journal of Fisheries and Aquatic Sciences* 58: 2233-2246 doi 10.1139/f01-162

- Do, H.H.; GrønkJær, P.; Simonsen, V. (2006) Otolith morphology, microstructure and ageing in the hedgehog seahorse, *Hippocampus spinosissimus* (Weber, 1913). *Journal of Applied Ichthyology*, Vol. 22, p. 153-159.
- Doubleday, Zoë & Harris, Hugh & Izzo, Chris & Gillanders, Bronwyn. (2013). Strontium Randomly Substituting for Calcium in Fish Otolith Aragonite. *Analytical chemistry*. 86. 10.1021/ac4034278.
- Drouineau H, Mahevas S, Bertignac M, Duplisea D (2010a) A length-structured spatially explicit model for estimating hake growth and migration rates. *Ices Journal of Marine Science* 67: 1697-1709 doi 10.1093/icesjms/fsq042
- Drouineau H, Mahévas S, Bertignac M, Duplisea D (2010b) A length-structured spatially explicit model for estimating hake growth and migration rates. *ICES Journal of Marine Science* 67: 1697-1709 doi 10.1093/icesjms/fsq042
- Elsdon TS, Wells BK, Campana SE, Gillanders BM, Jones CM, Limburg KE, Secor DH, Thorrold SR, Walther BD (2008) Otolith chemistry to describe movements and life-history parameters of fishes: Hypotheses, assumptions, limitations and inferences. *Oceanography and Marine Biology: an Annual Review*, Vol 46 46: 297-+ doi 10.1201/9781420065756.ch7
- Francis RICC (1988) Maximum likelihood estimation of growth and growth variability from tagging data. *New Zealand Journal of Marine and Freshwater Research* 22: 43-51 doi 10.1080/00288330.1988.9516276
- Geffen AJ, Morales-Nin B, Pérez-Mayol S, Cantarero-Roldán AM, Skadal J, Tovar-Sánchez A (2013) Chemical analysis of otoliths: Cross validation between techniques and laboratories. *Fisheries Research* 143: 67-80 doi <http://dx.doi.org/10.1016/j.fishres.2013.01.005>
- Gillanders, B. M. 2001. Trace metals in four structures of fish and their use for estimates of stock structure. *Fishery Bulletin*, 99: 410-419.
- Granzotto, Angela & Franceschini, Gianluca & Malavasi, Stefano & Molin, Gianmario & Pranovi, Fabio & Torricelli, Patrizia. (2003). Marginal increment analysis and Sr/Ca ratio in otoliths of the grass goby, *Zosterisessor ophiocephalus*. *Italian Journal of Zoology*. 70. 5-11. 10.1080/11250000309356489.
- Hampton J, Fournier DA (2001) A spatially disaggregated, length-based, age-structured population model of yellowfin tuna (*Thunnus albacares*) in the western and central Pacific Ocean. *Marine and Freshwater Research* 52: 937-963 doi 10.1071/mf01049
- Harwood AJP, Dennis PF, Marca AD, Pilling GM, Millner RS (2008) The oxygen isotope composition of water masses within the North Sea. *Estuarine, Coastal and Shelf Science* 78: 353-359 doi <http://dx.doi.org/10.1016/j.ecss.2007.12.010>
- Hüssy K, Gröger J, Heidemann F, Hinrichsen HH, Marohn L (2015) Slave to the rhythm: seasonal signals in otolith microchemistry reveal age of eastern Baltic cod (*Gadus morhua*). *ICES Journal of Marine Science* 73: 1019-1032 doi 10.1093/icesjms/fsv247
- ICES (2010) Report of the Workshop on Age estimation of European hake (WKAEH), 9-13 November 2009, Vigo, Spain. ICES CM 2009/ACOM:42. 68 pp.
- ICES (2011) Report of the anglerfish (*Lophius piscatorius*) illicia and otoliths exchange 2011
- ICES (2016) EU request to provide a framework for the classification of stock status relative to MSY proxies for selected category 3 and category 4 stocks in ICES subareas 5 to 10 (Version 4). In Report of the ICES Advisory Committee, 2016. ICES Advice 2016, Book 5, Section 5.4.2. 11 pp.
- ICES (2017) Report of the Benchmark Workshop on Widely Distributed Stocks (WKWIDE), 4-11 May 2017, Copenhagen, Denmark. ICES CM 2017/ACOM:36. 534 pp.
- Jaric, I., Lenhardt, M., Pallon, J., Elfman, M., Kalauzi, A., Suci, R., Cvijanovic, G., et al. 2011. Insight into Danube sturgeon life history: trace element assessment in pectoral fin rays. *Environmental Biology of Fishes*, 90: 171-181.
- Kastelle CR, Helser TE, McKay JL, Johnston CG, Anderl DM, Matta ME, Nichol DG (2017) Age validation of Pacific cod (*Gadus macrocephalus*) using high-resolution stable

-
- oxygen isotope ($\delta O-18$) chronologies in otoliths. *Fisheries Research* 185: 43-53 doi 10.1016/j.fishres.2016.09.024
- Landa J, Barrado J, Velasco F (2013) Age and growth of anglerfish (*Lophius piscatorius*) on the Porcupine Bank (west of Ireland) based on illicia age estimation. *Fisheries Research* 137: 30-40 doi 10.1016/j.fishres.2012.07.026
- Landa J, Duarte R, Quincoces I (2008) Growth of white anglerfish (*Lophius piscatorius*) tagged in the Northeast Atlantic, and a review of age studies on anglerfish. *ICES Journal of Marine Science* 65: 72-80 doi 10.1093/icesjms/fsm170
- Lee, R. M. 1912. An investigation into the methods of growth determination in fishes. Conseil Permanent International pour l'Exploration de la Mer, Publications de Circonstance, 63. 35 pp.
- Li L, Høie H, Geffen AJ, Heegaard E, Skadal J, Folkvord A (2008) Back-calculation of previous fish size using individually tagged and marked Atlantic cod (*Gadus morhua*). *Canadian Journal of Fisheries and Aquatic Sciences* 65: 2496-2508 doi 10.1139/F08-157
- Limburg, K. E., and Elfman, M. 2017. Insights from two-dimensional mapping of otolith chemistry. *J Fish Biol*, 90: 480-491.
- Linley TJ, Krogstad EJ, Nims MK, Langshaw RB (2016) Geochemical signatures in fin rays provide a nonlethal method to distinguish the natal rearing streams of endangered juvenile Chinook Salmon *Oncorhynchus tshawytscha* in the Wenatchee River, Washington. *Fisheries Research* 181: 234-246 doi 10.1016/j.fishres.2016.04.004
- Loewen TN, Carriere B, Reist JD, Halden NM, Anderson WG (2016) Linking physiology and biomineralization processes to ecological inferences on the life history of fishes. *Comparative Biochemistry and Physiology a-Molecular & Integrative Physiology* 202: 123-140 doi 10.1016/j.cbpa.2016.06.017
- Luque PL, Zhang S, Rooker JR, Bidegain G, Rodriguez-Marin E (2017) Dorsal fin spines as a non-invasive alternative calcified structure for microelemental studies in Atlantic bluefin tuna. *Journal of Experimental Marine Biology and Ecology* 486: 127-133 doi 10.1016/j.jembe.2016.09.016
- Mace PM, Fenaughty JM, Coburn RP, Doonan IJ (1990) Growth and productivity of orange roughy (*Hoplostethus atlanticus*) on the north Chatham Rise. *New Zealand Journal of Marine and Freshwater Research* 24: 105-119 doi 10.1080/00288330.1990.9516406
- Maunder MN, Piner KR (2014) Contemporary fisheries stock assessment: many issues still remain. *ICES Journal of Marine Science* 72: 7-18 doi 10.1093/icesjms/fsu015
- Minto C, Flemming JM, Britten GL, Worm B (2014) Productivity dynamics of Atlantic cod. *Canadian Journal of Fisheries and Aquatic Sciences* 71: 203-216 doi 10.1139/cjfas-2013-0161
- Montgomery SS, Walsh CT, Haddon M, Kesby CL, Johnson DD (2010) Using length data in the Schnute Model to describe growth in a metapenaeid from waters off Australia. *Marine and Freshwater Research* 61: 1435-1445
- Morales-Nin B, Swan SC, Gordon JDM, Palmer M, Geffen AJ, Shimmield T, Sawyer T (2005) Age-related trends in otolith chemistry of Merluccius merluccius from the north-eastern Atlantic Ocean and the western Mediterranean Sea. *Marine and Freshwater Research* 56: 599-607 doi 10.1071/mf04151
- Nobuaki Arai, Wataru Sakamoto, Kuniko Maeda, (1996) Correlation between Ambient Seawater Temperature and Strontium-calcium Concentration Ratios in Otoliths of Red Sea Bream *Pagrus Major*, *Fisheries science*, 1996, Volume 62, Issue 4, Pages 652-653, Released June 30, 2008, Print ISSN 0919-9268, <https://doi.org/10.2331/fishsci.62.652>, https://www.jstage.jst.go.jp/article/fishsci1994/62/4/62_4_652/_article/-char/en
- Palomera, I. Olivar, M. & Morales-Nin, B. (2005). Larval development and growth of the European hake in the Northwestern Mediterranean. *Scientia Marina*. 69.
- Payan, P., Edeyer, A., De Pontual, H., Borelli, G., Boeuf, G., and Mayer-Gostan, N. 1999. Chemical composition of saccular endolymph and otolith in fish inner ear: lack of spatial uniformity. *American Journal of Physiology-Regulatory Integrative and Comparative Physiology*, 46: R123-R131.

- Phelps, Q. E., Whitley, G. W., Tripp, S. J., Smith, K. T., Garvey, J. E., Herzog, D. P., Ostendorf, D. E., et al. 2012. Identifying river of origin for age-0 Scaphirhynchus sturgeons in the Missouri and Mississippi rivers using fin ray microchemistry. *Canadian Journal of Fisheries and Aquatic Sciences*, 69: 930-941.
- Piñeiro CG, Morgado C, Saínza M, McCurdy WJ, (Eds). (2009) Hake age estimation: state of the art and progress towards a solution. ICES Cooperative Research Report No. 294. 43 pp
- Pracheil, B., George, R., and Chakoumakos, B. 2019. Significance of otolith calcium carbonate crystal structure diversity to microchemistry studies. *Reviews in Fish Biology and Fisheries*.
- Quinn II TJ, Deriso RB, Ganz PD (2017) Combining the Cohen-Fishman growth increment model with a Box-Cox transformation. *Fisheries Research* 187: 11-21 doi <http://dx.doi.org/10.1016/j.fishres.2016.11.001>
- Ruf, T. 1999. The Lomb-Scargle Periodogram in Biological Rhythm Research: Analysis of Incomplete and Unequally Spaced Time-Series. *Biological Rhythm Research*, 30: 178.
- Scargle, J. 1983. Studies in astronomical time series analysis. II - Statistical aspects of spectral analysis of unevenly spaced data. *The Astrophysical Journal*, 263.
- Scholkmann, F., Boss, J., and Wolf, M. 2012. An Efficient Algorithm for Automatic Peak Detection in Noisy Periodic and Quasi-Periodic Signals. *Algorithms*, 5: 588-603.
- Seyama H, Edmonds JS, Moran MJ, Shibata Y, Soma M, Morita M (1991) Periodicity in Fish Otolith Sr, Na, and K Corresponds With Visual Banding. *Experientia* 47: 1193-1196
- Siskey MR, Lyubchich V, Liang D, Piccoli PM, Secor DH (2016) Periodicity of strontium: Calcium across annuli further validates otolith-ageing for Atlantic bluefin tuna (*Thunnus thynnus*). *Fisheries Research* 177: 13-17 doi 10.1016/j.fishres.2016.01.004
- Smith, S. W. (1997). The scientist and engineer's guide to digital signal processing.
- Smith KT, Whitley GW (2010) Fin Ray Chemistry as a Potential Natural Tag for Smallmouth Bass in Northern Illinois Rivers. *Journal of Freshwater Ecology* 25: 627-635 doi 10.1080/02705060.2010.9664412
- Staeudle T (2016) State space modelling of otolith microstructure: extracting time-varying correlation signals among young flatfish (*Pleuronectes platessa*).
- Staeudle TM, Brophy DB, Minto CM (in prep) State space modelling of increment structures: extracting time-varying correlation signals. *Ecological modelling* (expected submission date: April 2017).
- Sturgeon RE, Willie SN, Yang L, Greenberg R, Spatz RO, Chen Z, Scriver C, Clancy V, Lam JW, Thorrold S (2005) Certification of a fish otolith reference material in support of quality assurance for trace element analysis. *Journal of Analytical Atomic Spectrometry* 20: 1067-1071 doi 10.1039/B503655K
- Tomas J, Geffen AJ, Millner RS, Piñeiro CG, Tserpes G (2006) Elemental composition of otolith growth marks in three geographically separated populations of European hake (*Merluccius merluccius*). *Marine Biology* 148: 1399-1413
- VanderPlas, J. 2017. Understanding the Lomb-Scargle Periodogram. *The Astrophysical Journal Supplement Series*, 236.
- Velasco F, Landa J, Barrado J, Blanco M (2008) Distribution, abundance, and growth of anglerfish (*Lophius piscatorius*) on the Porcupine Bank (west of Ireland). *Ices Journal of Marine Science* 65: 1316-1325 doi 10.1093/icesjms/fsn130
- Vigliola, L. (1997), Validation of daily increment formation in otoliths for three Diplodus species in the Mediterranean sea. *Journal of Fish Biology*, 51: 349-360. doi:10.1111/j.1095-8649.1997.tb01671.x
- Woodroffe DA, Wright PJ, Gordon JDM (2003) Verification of annual increment formation in the white anglerfish, *Lophius piscatorius* using the illicia and sagitta otoliths. *Fisheries Research* 60: 345-356 doi 10.1016/s0165-7836(02)00174-1
- Wright PJ, Woodroffe DA, Gibb FM, Gordon JDM (2002) Verification of first annulus formation in the illicia and otoliths of white anglerfish, *Lophius piscatorius* using

otolith microstructure. *Ices Journal of Marine Science* 59: 587-593 doi
10.1006/mjsc.2002.1179

Yoshinaga J, Nakama A, Morita M, Edmonds JS (2000) Fish otolith reference material
for quality assurance of chemical analyses. *Marine Chemistry* 69: 91-97 doi
[http://dx.doi.org/10.1016/S0304-4203\(99\)00098-5](http://dx.doi.org/10.1016/S0304-4203(99)00098-5)

HOW TO OBTAIN EU PUBLICATIONS

Free publications:

- one copy:
via EU Bookshop (<http://bookshop.europa.eu>);
- more than one copy or posters/maps:
from the European Union's representations (http://ec.europa.eu/represent_en.htm);
from the delegations in non-EU countries
(http://eeas.europa.eu/delegations/index_en.htm);
by contacting the Europe Direct service (http://europa.eu/europedirect/index_en.htm)
or calling 00 800 6 7 8 9 10 11 (freephone number from anywhere in the EU) (*).

(*) The information given is free, as are most calls (though some operators, phone boxes or hotels may charge you).

Priced publications:

- via EU Bookshop (<http://bookshop.europa.eu>).

Priced subscriptions:

- via one of the sales agents of the Publications Office of the European Union
(http://publications.europa.eu/others/agents/index_en.htm).



Publications Office
of the European Union

doi: 10.2826/748632